



## RESEARCH SCHOLARS PROGRAM 2011

THIS PROGRAM IS SPONSORED IN PART  
BY THE NATIONAL SCIENCE FOUNDATION



*“The program has no set time limits. Research is a lifelong learning experience, and we hope to remain a resource to our students long after ‘graduation’.”*

The Garcia Center for Polymers at Engineered Interfaces is a collaboration of eleven academic, industrial, and government laboratories. The Center was founded in 1996 and is named after the late Queens College professor, Narciso Garcia, a pioneer in the integration of education and research. The Garcia Center is funded by the **National Science Foundation as part of its Materials Research Science and Engineering Center (MRSEC)** program. The goal of the MRSEC is to combine the instrumentation and expertise of the participating institutions into a coordinated research program on polymer interface science. The principal focus areas include thin films, coatings, nano composites, self assembled structures, biomaterials, and tissue engineering.

These areas address both the fundamental and applied aspects that are relevant to the development of cutting-edge technologies in both engineering and medicine. In the community, the mission of the center is to serve as a valuable resource, providing easy access for technological assistance to educational and industrial institutions. For information on the numerous programs that are available, please see our web site at:

<http://polymer.matscieng.sunysb.edu>

The Research Scholar Program offers the opportunity for high school teachers and students to perform research on the forefronts of polymer science and technology together with the Garcia faculty and staff. Students work as part of focused research teams and are taught to make original contributions of interest to the scientific community. In addition to entering national competitions, the students are encouraged to publish in revered scientific journals and present their results at national conferences.

**Our goal** is to convey to the students the excitement we enjoy daily in research. The program has no set time limits. Research is a lifelong learning experience, and we hope to remain a resource to our students long after “graduation”.



**Jonathan  
Sokolov**



**Miriam  
Rafailovich**

**Miriam Rafailovich**  
Professor, Garcia MRSEC

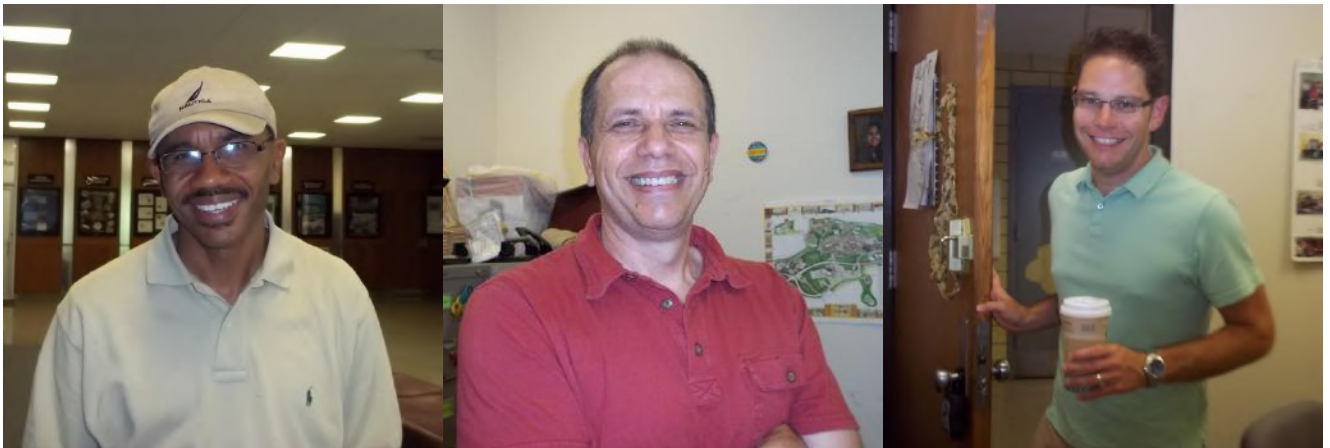
**Jonathan Sokolov**  
Professor, Garcia MRSEC

# Research Experience for Teachers



Joanne  
Figueiredo

Shardha  
Sambasivan



John  
Jerome

Vladimir  
Jurukovski

Robert  
Bolen

# Guest Faculty



**Rebecca Grella**



**Cindy Lee**



**Steven Walker**



**Michael Gouzman**



**Anil Bhardwani**



**Marcia Simon**



**Richard Clark**



**Dennis Galanakis**

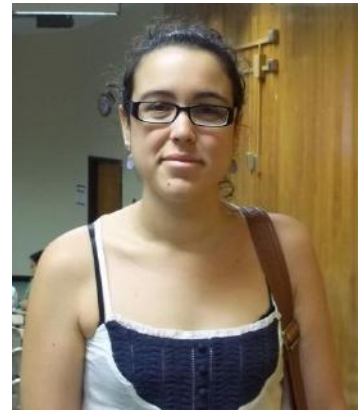
# Research Experience For Undergrads



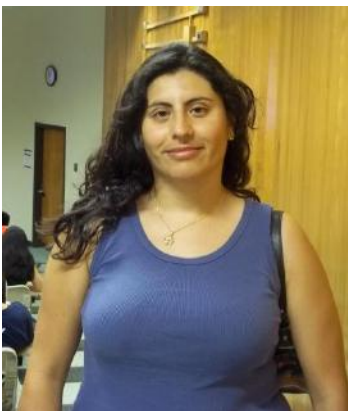
Aaron Akhavan



Alfred Francis



Claire Beaulieu



Clara Cuervo



Beatris Jimenez



Chani Stern



Coralie Beaulieu



Alan Czemerinski



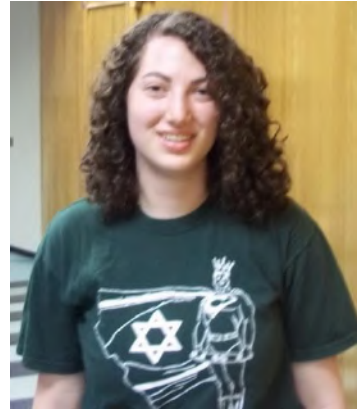
Adam Ossip



Katelyn Ireland



Jovanna Linnen



Dalia Leibowitz



Debby Greenstein



Marion Beckaert



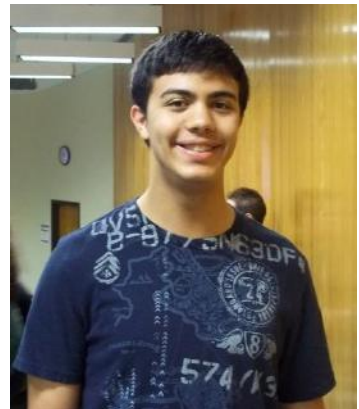
Julia Budassi



Karan Sikka



Lauren Herrera



Maxwell Plaut



Zohar Bachiry



Sherri-Ann Francis



Miriah Geritano



Nazac Saleh



Neha Kinariwalla



Nikhil Mehandru



Neil Muir  
REU of the Year



Sally Lin



Penina Safier

# Grads



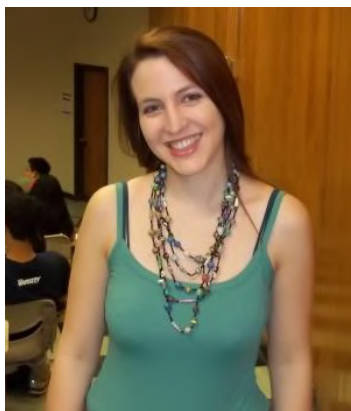
Liudi Zhang



Suphanee  
Pongkitwitoon



Harry Shan He



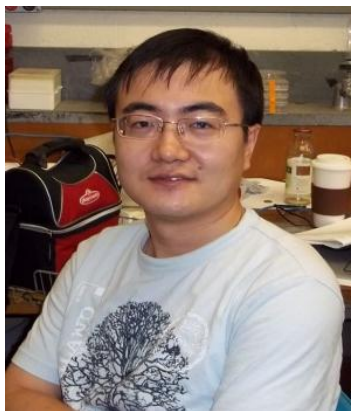
Giulia Suarato



Manideep Chavali



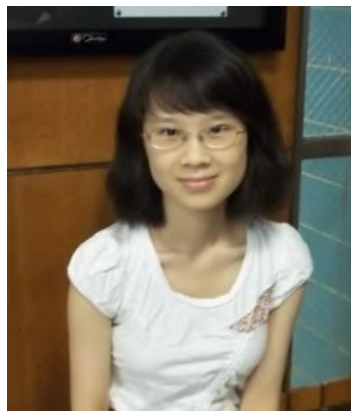
Chung Chueh  
Chang



Cheng Pan



Kai Yang



Sisi Qin

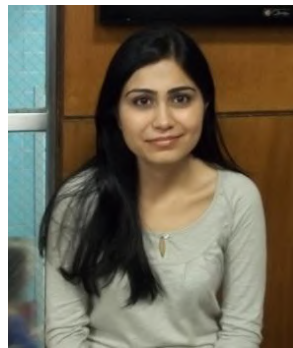




Liudi Zhang



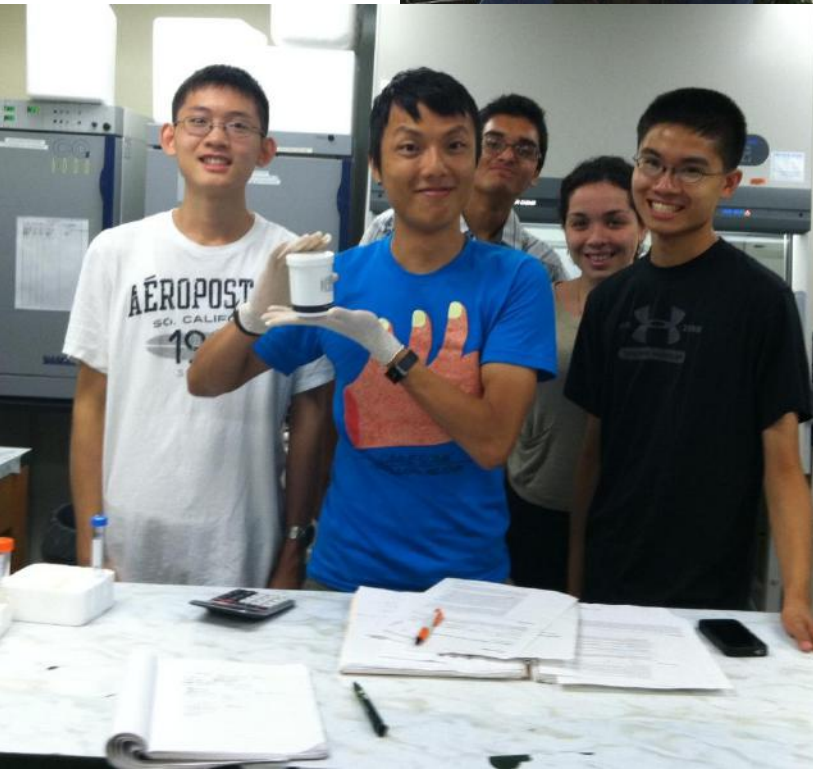
Chien-Hsiu Lin



Divya Bhatnagar



Tatsiana Mironava



# Staff



**Elana  
Levy**



**Lamiya  
Allahverdiyeva**



**Veronica Collazo**



**Lourdes Collazo**



**Lauren Collazo**



**David Pirraglia**

# Students



Aniruod Pochiraju



Alexa Aseel-Fine



Alex Lee



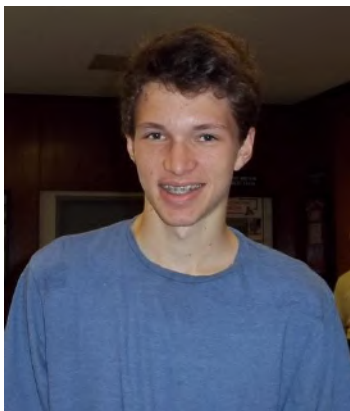
Amy Sullivan



Alissa Zhang



Andrew Chen



Andrew O'Neil



Alina Ranjbaran



Alexandra Tse



Bradley Kaptur



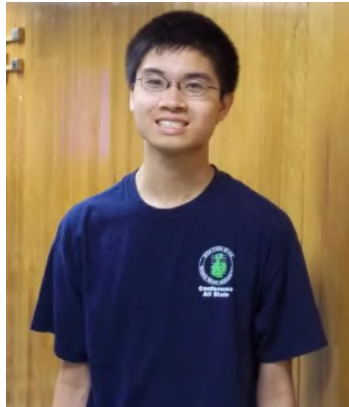
Arvind Viswanathan



Austin Wild



Daniel Moskowitz



Brian Lei



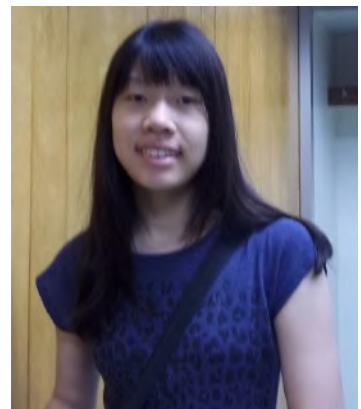
Carl Gao



Aniruod Sailesh



Ashley Crespo



Caroline Juang



Emily Shea



Eve Byington



Drew Owen



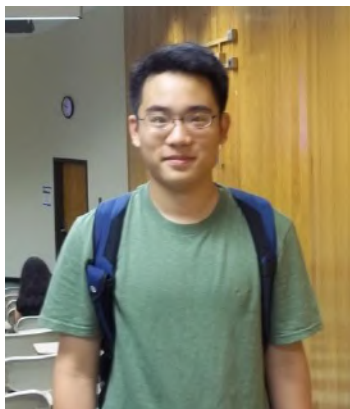
George Mo



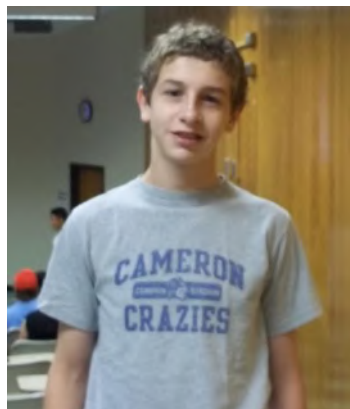
Eric Metodiev



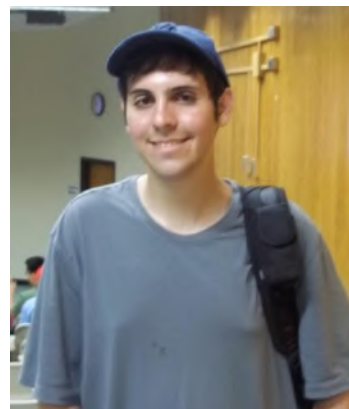
David Nam



Elliot Tan



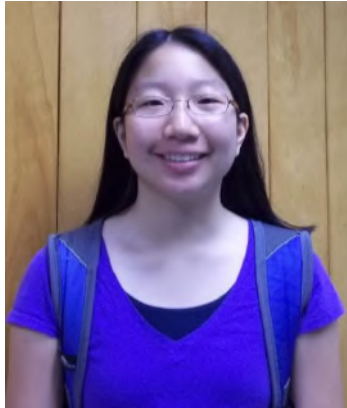
Evan Schneider



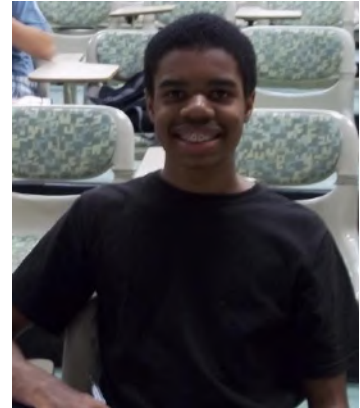
Eric Hirsch



Hansen Qian



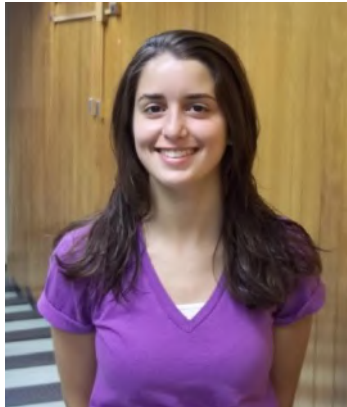
Jessica Lam



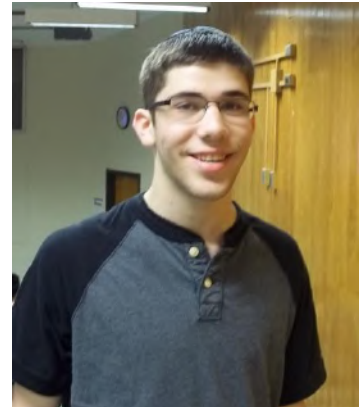
Joshua Millings



Holly Flores



Ilana Teicher



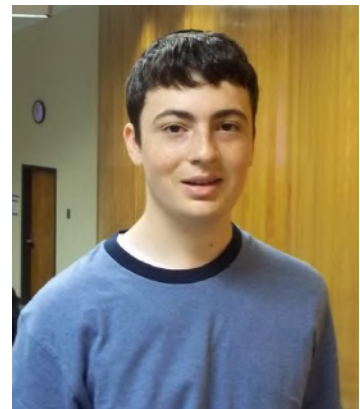
Jonathan Rosenberg



Japbani Nanda



Jason Kuan



Jonathan Zolty



Merry Mou



Mohit Batra



Julia Landsberg



Matthew Rudin



Kathy Benhamou



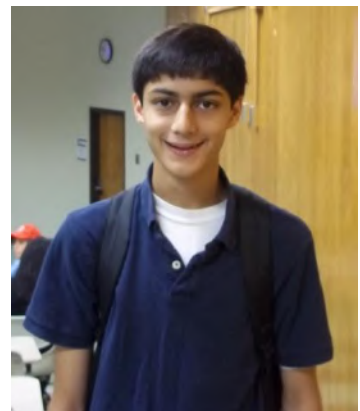
Leah Slaten



Manita Singh



Jun Hwan Ryu



Kunal Sangani



Noman Hamlani



Rachel Davis



Ray Weng



Nicholas Suss



Monika Batra



Reyna Guzman



Ryan Lindeborg



Robin Mehta



Rebecca Somach





Shoshana Javitt



Sean Ballinger



Sneha Chittabathini



Scott Zhou



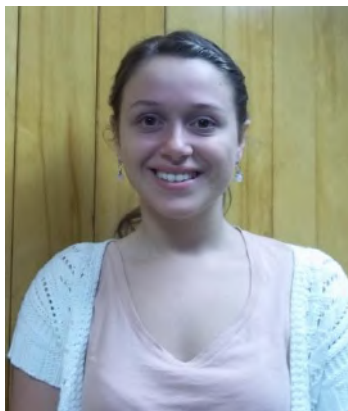
Snehashish Sridhar



Sneha Subramaniam



Suduti Sood



Sarah Cacciabauda



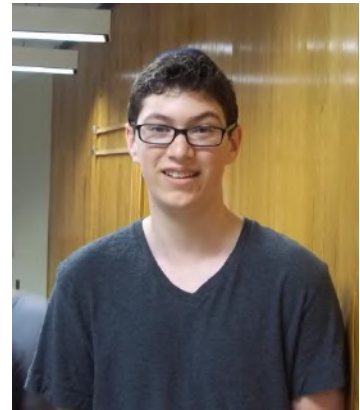
Suri Bandler



Tyler Lawrence



Victoria Petrova



Wade Miller



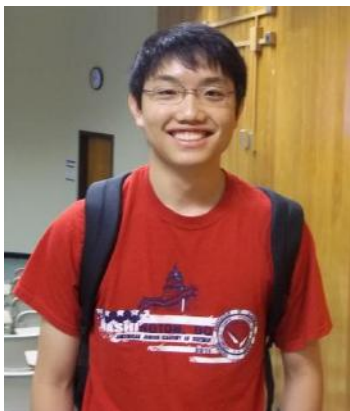
Tom Wang



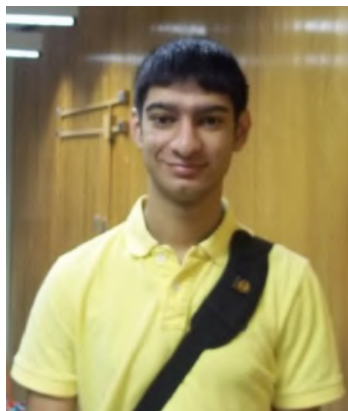
Thomas Yurek



Yicheng Sun



Yan Jang



Zohaib Shaikh

# Summer Fun

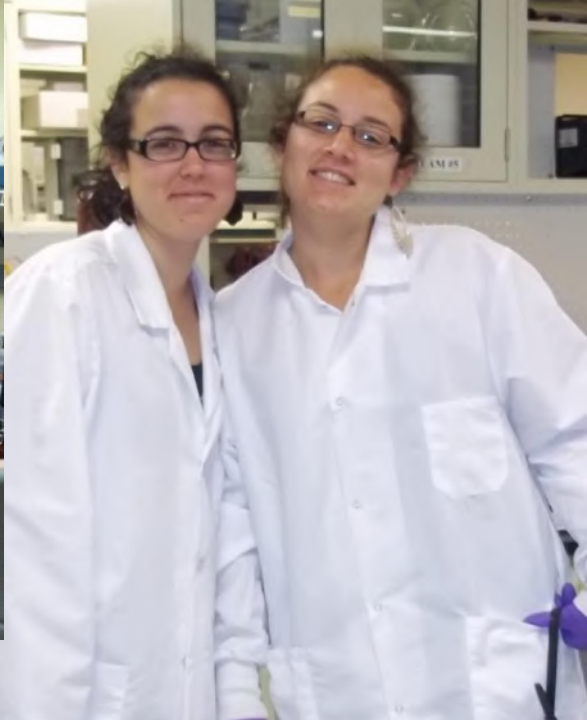
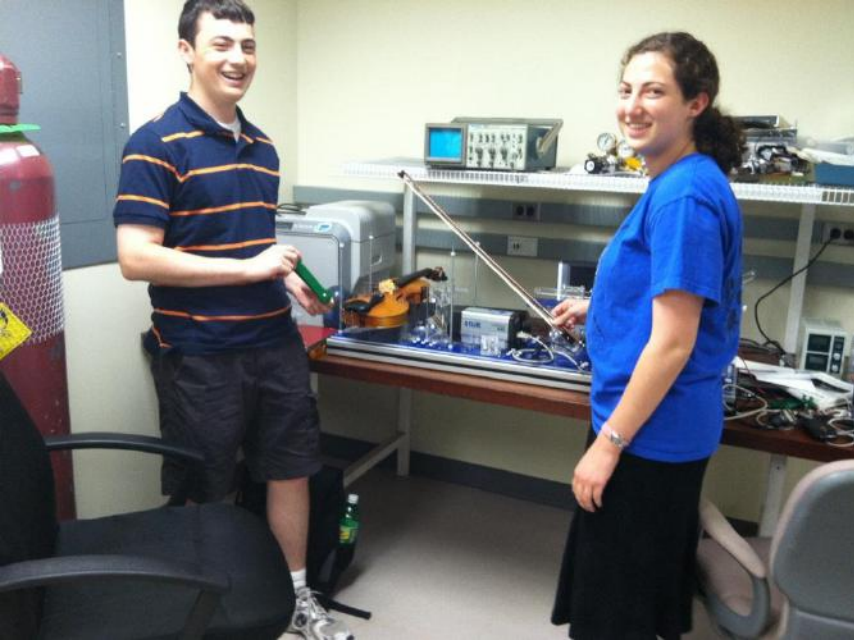


# Learning



# Lab Life





# Atlantis Trip



# Canoe Trip





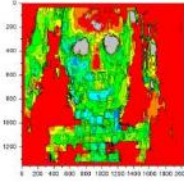




**Please Join Us For the  
Garcia MRSEC Summer Scholar Research Luncheon  
which will take place on *Friday, August 12<sup>th</sup>, 2011*  
in the SAC Ballroom A, from 10:00 - 1:00 pm.**

- **Oral research presentation by the students**
- **Original musical arrangement performed by the GARCIA MRSEC student orchestra.**

# 2011 Summer Research Symposium



10:00-10:05

Welcome Remarks

10:05-10:15

String Quartet Performance by Garcia Students

## ***Session I: Dental Pulp Stem Cells***

***Graduate Student Mentors: Aneel Bherwani, Tatsiana Mironava, Chung-Chueh Chang, Chien-Hsiu Lin, Giulia Suarato, Divia Bhatnagar, Sisi Qin***

10:15-10:22

### **a) Flat Surfaces**

*Chair: Dr. Vladimir Jurukovski, Suffolk Community College, NY*

**The Effects of Magnetic Fields on the Bio-mineralization and Differentiation of Dental Pulp Stem Cells**

Holly Flores and Austin Wild

**The Effect of Graphene and Graphene Oxide on the Growth, Differentiation and Biomineralization of Dental Pulp Stem Cells**

Eric Hirsch and Wade Miller

10:25-10:33

### **b) Patterned Surfaces**

*Chair: Max Plaut, Massachusetts Institute of Technology, MA*

**The Effects of Mechanical Nanopatterns on the Differentiation of Dental Pulp Stem Cells**

Sarah Cacciabauda and Robin Mehta

**A Study on the Effects of Biocompatible Nanopatterned Titanium Surfaces on Human Dental Pulp Stem Cell Growth and Biomineralization**

Scott Zhou and Suditi Sood

**The Effect of Chemical Nanopatterning on the Differentiation of Human Dental Pulp Stem Cells** Brad Kaptur, Joshua Millings

**10:35-10:41**

**c) Electrospun Surfaces**

Chair: **Aaron Akhavan**, Yeshiva University, NY

**Effects of the Mechanical Properties of Polycaprolactone and UV Plasma Treated Poly (Methyl Methacrylate) 3D Electrospun Scaffolds on Dental Pulp Stem Cell Differentiation and Biomineralization**

Manita Singh and Nicholas Suss

**The Effect of Surface Modification of PMMA Scaffolds through Plasma Etching and Different Media on the Proliferation and Migration of Fibroblasts**

Ryan Lindeborg

**10:45-10:51**

**d) Hydrogel Surfaces**

Chair: **Nikhil Mehandru**, Harvard University, MA

**Quantitative Analysis of Novel Thermoreversible Pluronic F127, Gelatin, and Hyaluronic Acid Composite Hydrogels for the Creation of Cellular Substrates with Application in Regenerative Medicine**

Yicheng Sun and Japbani Nanda

**A Study of the Biomineralization of Human Dental Pulp Stem Cells on Crosslinked Gelatin Hydrogels**

Sneha Subramaniam and Elliot Tan

***Session II: Nanoparticle Toxicity***

***Graduate Mentors: Tatsiana Mironava, Chien-Hsiu Lin***

**10: 55-11:05**

**a) Au and Pt Nanoparticles**

Chair: **Zohar Bachiry**, Macaulay Honors Program, Queens College, NY

**Differently sized charged gold nanoparticles alter HeLa cell membrane properties**

Merry Mou

**The Effect of Platinum-Folate Coated Nanoparticles on Dental Pulp Stem Cells as a Function of Proliferation and Differentiation**

Alexa Aseel-Fine

**Platinum Folate Nanoparticles: A Novel Instrument for Receptor Targeted Cancer Treatment**

Evan Schneider

**Cytotoxicity and Differentiation of Dental Pulp Stem Cells: Effects of Gold Nanoparticle Size**

Alissa Zhang and Tyler Lawrence

**11:10-11:18**

**b) TiO<sub>2</sub> and ZnO Nanoparticles**

Chair : *Channi Stern*, Stern College for Women

**The Effect of Titanium Dioxide and Zinc Oxide Nanoparticles on Pseudorabies Virus**

Arvind Viswanathan

**Effects of TiO<sub>2</sub> and ZnO Nanoparticles on Healthy and Infected Macrophages with Leishmania tropica and Staphylococcus aureus In Vitro**

Brian Lei, Alexander Lee and Anirudh Pochiraju

***Session III: Sensing Biomolecules on Surfaces***

**Graduate Student Mentors: Yingjie Yu, Suphanee Pongkitwitoon**

**11:21-11:35**

Chair: *Alan Czemerinski*, Columbia University, NY

**Developing a Biosensor Utilizing Self-Assembled Monolayers to Detect Bacteria**

Zohaib Shaikh, Kathy Benhamou and Mohit Batra

**Towards the Expansion of Biosensor Applications and Characterization of Thiol-based Self-Assembled Monolayers**

Tom Wang, David Nam and Alina Ranjbaran

**Blood Clotting on a Hydrophobic Surface**

Anirudh Sailesh

**Computational Modeling of Fibrin Polymerization and Adsorption on Hydrophobic Substrates**

Carl Gao

***Session IV: Device Engineering***

***Graduate Student Mentor: Divia Bhatnagar***

**11: 37-11:45**

Chair: *Dalia Leibowitz*, Massachusetts Institute of Technology, MA

**Using Digital Image Speckle Correlation Photographic Analysis to Detect Response to Olfactory or Audio Stimuli**

Leah Slaten and Andrew O'Neil

**Using Digital Image Speckle Correlation to Diagnose Facial Paralysis and Track the Recovery of Facial Paralysis**

Rebecca Somach and Julia Landsberg

**The Modification of a Bowing Machine to Analyze the Effects of Different Types of Rosin on the Temperature of a Violin's Strings and the Sound Produced**

Jonathan Zolty

***Session V: Nanocomposites***

**Graduate student mentors: Harry Shan He, Kai Yang, Liudi Zhang**

**11: 47-11:55**

*Chair: Neil Muir, Cooper Union, NY*

**Creating a Non-Flammable and Strong Material for Insulating Electrical Cable: Using Ethylene-Vinyl Acetate (EVA) with Flame Retardant Additives**

Shoshana Javitt

**A Non-Corrosive Biodegradable Polymer**

Claire Beaulieu

**Flame Retardant Biodegradable Polymers: Blending polylactic acid (PLA) and Ecoflex (PBAT) with various additives to improve thermal, mechanical, and degradation properties**

Rachel Davis and Caroline Juang

***Session VI: Renewable Energy Sources***

**Graduate student advisor: Cheng Pan, Yingjie Yu**

**12:00 – 12:15**

*Chair: Sherri-Ann Francis, Suffolk Community College, NY  
Karan Sikka, Carnegie Mellon, PA*

**Using Gold and Palladium Alloy Nanoparticle Co-catalysts as a Novel Means to Improve the Power Output Efficiency and Lower the Cost of Hydrogen Fuel Cells**

Victoria Petrova and Ilana Teicher

**The Effect of Gold-Dodecanethiolate Core-Shell Nanoparticles on a Hydrogen PEM Fuel Cell Stack**

Sean Ballinger

**Investigating Au/Pd Catalyst Mechanisms via PEM Fuel Cell Power Output Enhancements**

Hansen Qian, Daniel Jang and Matthew Rudin

**The Effect of Au Nanorods on the Power Output of PEM Hydrogen Fuel Cells**

Daniel Moskowitz

**Nanoscale Morphology of the Self-Assembled Ordered Bulk Heterojunction in the PS:P3HT:PCBM Active Layer of Polymer:Fullerene Photovoltaic Cells**

Eric Metodiev

**Incorporation of Graphene Oxide and Graphene into Layers of Organic Polymer Solar Cells**

Andrew Chen, Sneha Chittabathini and Alexandra Tse

***Session VII: Green Imprinting Technologies***

***Graduate student advisors: Giulia Suarato***

**12: 17- 12:23**

*Chair: Mariah Geritano, SUNY Stony Brook, NY*

*Debby Greenstein, University of Pennsylvania, PA*

**Formation of Superhydrophobic Nanopatterned Silidon Substrates by the Sputtering of Phase-Segregated Polymer Blends**

Ray Weng and Thomas Yurek

**Assessing the Enzyme Kinetics of *Candida antarctica* lipase B to Control the Degradation of Poly- $\epsilon$ -caprolactone Surfaces**

George Mo, Jessica Lam, Monika Batra and Eve Byington

***Session VIII: DNA Molecules on Surfaces***

**Graduate student advisor: Ke Zhu**

**12: 25- 12:35**

*Chair : Julia Budassi, SUNY Stony Brook, NY*

**Polarization and Angle Dependence of Fluorescence from Aligned DNA**

Ashish Sridhar and Suri Bandler

**Using Microcontact Printing as a Novel Method for Dyeing and Cutting DNA**

Emily Shea

**Electric-field Assisted Deposition of DNA on Polymer Surfaces**

Jun Hwan Ryu

**Stretching DNA Molecules on a Polymer Surface**

Jonathan Rosenberg

***Session IX: Environmental Remediation***

**Advisors: Rebecca Grella, Joanne Figueiredo**

**12: 40-12: 52**

*Chair: Lauren Herrera, Suffolk Community College, NY*

*Katelyn Ireland, University of Miami, FL*

**A study on the Geological and Environmental Implications of Hydraulic Fracturing in Upstate New York**

Kunal Sangani

**Analyzing the Role of Marine Gels in a Negative Feedback Loop for Ocean Acidification**

Jason Kuan

**Toxicity of Different Clay Nanoparticles**

Coralie Beaulieu

**Encapsulation of a Herbicide: A Model System for Fabrication and Assessment of Effectiveness**

Amy Sullivan, Ashley Crespo and Reyna Guzman

**The Effect of Crude Oil on Byssal Thread Formation and Structure in *Mytilus edulis*, Blue Mussel**

Alexander Harwood, Noman Hamlani, Michael Emerson

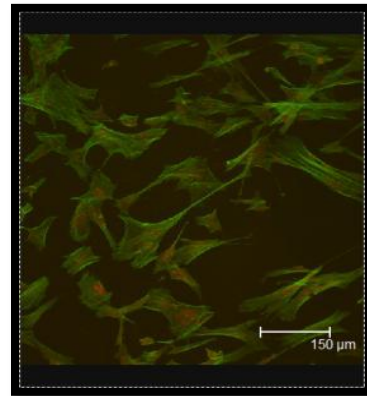
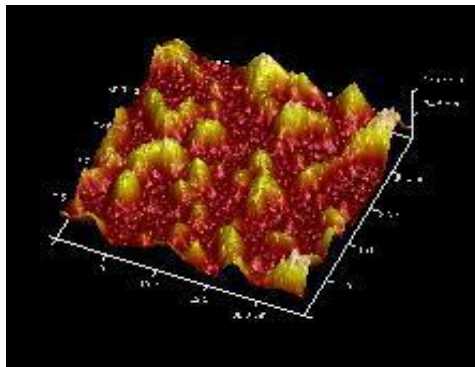


**Luncheon Catered by Wing Wan of West Hempstead**



# Dental Pulp Stem Cells

## SESSION 1



**Chairs: Vladimir Jurukovski, Max Plaut,  
Aaron Akhavan, Nikhil Mehandru**

**Graduate Advisors: *Aneel Bherwani,  
Tatsiana Mironava, Chung-Chueh Chang,  
Chien-Hsiu Lin, Giulia Suarato, Divia  
Bhatnagar, Sisi Qin***

## The Effects of Magnetic Fields on the Bio-mineralization and Differentiation of Dental Pulp Stem Cells

Holly Flores, Huntington High School, Austin Wild, South Side High School

Jovanna Linnen, City College of New York (Sophie Davis)

Vladimir Jurukovski, Suffolk County Community College

ChungChueh Chang, Lourdes Collazo, Miriam Rafailovich, Dept. of Materials Sciences, Stony Brook University

Dental Pulp Stem Cells [DPSCs], are a type of pluripotent stem cells with the ability to differentiate into mainly osteoblastic or odontoblastic lineages, and have shown great promise in regenerative medicine. Research has shown that the extracellular matrix [ECM] is a critical component in regulating the cell function and behavior, and that the morphology of the ECM varies with different types of tissue. This has many applications in engineering and differentiating stem cells. Sulfonated polystyrene [SPS] was the chosen substrate because of its negative charge, allowing the slightly positive proteins of the extracellular matrix to be imaged using the Atomic Force Microscope [AFM]. Prior research shows a tendency for the cells to differentiate on SPS<sup>1</sup>. A magnetic field was introduced because studies have shown that magnets affect the orientation, differentiation, and growth of the cells.

The purpose of this experiment was to analyze the effects of SPS and magnetic fields on the differentiation and bio-mineralization of DPSCs. This was done by creating a thin film of the SPS polymer and conducting various experiments and tests on the cells plated, with or without presence of a magnetic field.

First, a sulfonated polystyrene solution was spuncast onto a thoroughly cleaned silicon wafer and annealed. Afterwards, the cells were plated onto said silicon wafers. Half of the plated samples were put into a magnetic field created by two sets of strong magnets and the other samples were without magnets. The samples were then studied on days 3, 5, 7, 14, and 21 in order to run accurate tests on the extracellular matrix [ECM] formation and quality (by AFM), and bio-mineralization (by SEM-EDAX). Confocal microscope was used to visualize the overall structure of the cells and their cytoskeleton in the presence or absence of the magnetic field (Fig.1). Preliminary results show that the magnetic field appears to have an effect on the organization of the cells which align better when the field is present.

Further experiments will include study the ECM collagen fibers and RT-PCR for gene expression of differentiation cell markers such as osteocalcin and osteonectin<sup>2</sup>.

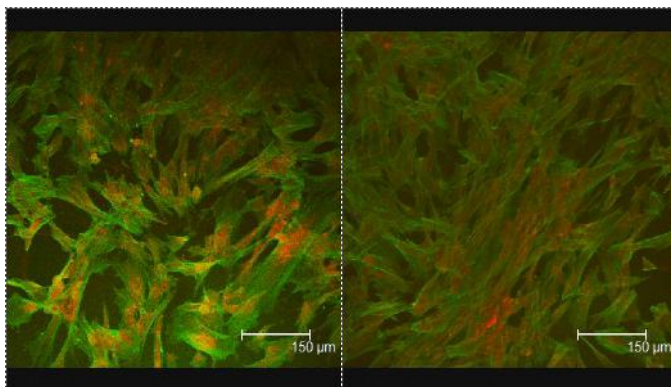


(Figure 1.) On the left is a confocal-microscopy image of Dental Pulp Stem Cells on Sulfonate Polystyrene without magnets. The image on the right has the same conditions except has an increased magnetic field.

1. Zhang, W., X. Frankwalboomers, T. Vankuppevelt, W. Daamen, Z. Bian, and J. Jansen. "The Performance of Human Dental Pulp Stem Cells on Different Three-dimensional Scaffold Materials." *Biomaterials* 27.33 (2006): 5658-668.
2. Eastell, R. *Bone Markers: Biochemical and Clinical Perspectives*. London: Martin Dunitz, 2001.

# The Effect of Graphene and Graphene Oxide on the Growth, Differentiation and Biomineralization of Dental Pulp Stem Cells

**Eric Hirsch and Wade Miller**, Hebrew Academy of the Five Towns and Rockaway Cedarhurst NY  
**Rebecca Isseroff**, Chemistry Department, Lawrence High School, Lawrence NY; **Vladimir Jurukovski and Miriam Rafailovich**, Department of Materials Science & Engineering, Stony Brook University

The capacity of dental pulp stem cells (DPSCs) for osteogenesis suggests a potential application in reparative and constructive therapies associated with bone tissue. Significant growth and osteogenesis has been observed in DPSCs treated with the corticosteroid dexamethazone. However, dexamethazone may have irritating effect on the tissues, and an alternative method for inducing proliferation and osteogenesis is required to make a number of DPSC-based treatments clinically viable. One approach is to develop mechanical scaffolds that optimize growth and differentiation. Our study looks at the effects of scaffolds composed of graphene, graphene oxide, and graphene and graphene oxide incorporated into poly-4-vinylpyridine (P4VP) on DPSC growth and differentiation. Graphene is a single layer of SP-2 bonded carbon atoms that was first isolated in 2004. The unique mechanical and electrical properties of graphene, which include the highest known Young's modulus and lowest known resistivity, have made it the subject of extensive research in electronic applications. Research on the biological applications of graphene has not been as significant, although preliminary work suggests that DPSCs can survive on graphene scaffolds. Our experiment will be the first to measure the potential of graphene and graphene oxide in P4VP scaffolds to induce growth and osteogenesis in DPSCs.

Scaffolds were created by spin-casting thin-films onto cleaved silicon wafers. Solutions contained dimethylformimide and , depending on the construct, 5.0 mg/ml graphene, 5mg/ml graphene and 3mg/ml P4VP, 2.5 mg/ml graphene and 3mg/ml P4VP , and 1.5mg/ml graphene oxide and 3mg/ml P4VP. Samples were spun at 2500rpm for 30 seconds, and then annealed for 18-24 hours at 160°C. Some samples were imaged with an atomic force microscope (AFM) (Fig. 1) in order to determine the uniformity of the scaffolds. After the samples were established as sufficiently uniform, 400 DPSCs were plated on each of the scaffolds. Half of the samples were then treated with dexamethazone. Cell growth was calculated with a hemocytometer on the second, fourth and seventh days after plating. The growth curve (Fig. 2) showed that the 5mg/ml graphene in P4VP and the 1.5mg/ml graphene oxide in P4VP proved to be the best scaffolds for cell.

We intend to analyze cell differentiation on various scaffolds with confocal microscopy and EDAX at the eighth and twenty-first days after plating, to determine cell morphology, differentiation and biomineralization on the different scaffolds. We also plan to conduct a further study on the growth and differentiation of DPSCs on graphene oxide and graphene oxide/ P4VP thin film scaffolds. Finally, we will attempt to electrospin P4VP fibers with various concentrations of graphene and graphene oxide, in order to create novel scaffolds for DPSC growth and differentiation.

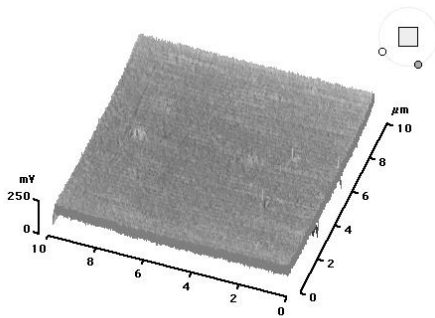


**Fig. 1-** AFM image of 2.5mg/ml graphene and 3mg/ml P4VP spun onto a silicon wafer

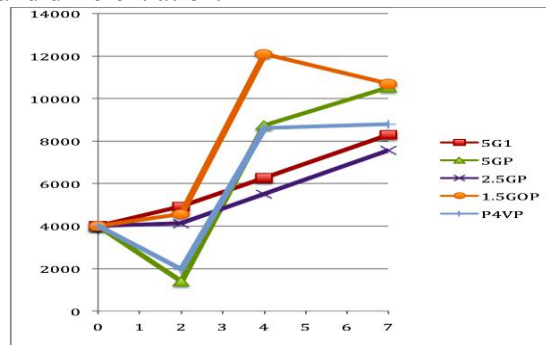


**Fig. 2-** Growth curve of the DPSCs on various scaffolds

## **The Effects of Mechanical Nanopatterns on the Differentiation of Dental Pulp Stem Cells**

**Sarah Cacciabaudo<sup>1</sup> and Robin Mehta<sup>2</sup>**, Miriam Rafailovich<sup>3</sup>, John Jerome<sup>4</sup>, Vladimir Jurukovski<sup>4</sup>, Zohar Bachiry<sup>5</sup>, Clara Cuervo<sup>4</sup>, Debby Greenstein<sup>6</sup>, Maxwell Plaut<sup>7</sup>, [1]Smithtown High School West, Smithtown,NY;[2]Paul D. Schreiber High School, Port Washington, NY[3] Department of Material Science and Engineering, Stony Brook University; [4]Suffolk County Community College, Brentwood, NY; [5]Macaulay Honors at Queens College, Queens, NY; [6]University of Pennsylvania, Philadelphia, PA; [7]Massachusetts Institute of Technology, Cambridge, MA

Stem cell research is currently a leading topic of study due to its prospective regenerative capabilities. Because embryonic stem cell research is often restrictive due to ethical constraints, the pluripotent human dental pulp stem cells (DPSCs) are now a preferred topic of research due to the potential in treatment of disorders such as osteonecrosis, dental carries, and stroke.<sup>1</sup> DPSCs have the ability to differentiate into osteoblasts, melanocytes, neurons, and glial cells<sup>2</sup>. Because DPSCs react to hard and soft surfaces differently, this study dealt with finding the polymer blends to create the most biocompatible surfaces for their differentiation. Creating nanopatterns in vitro to mimic the stiffness of various internal human tissues, which can affect stem cell differentiation. In this study, DPSCs were plated on silicon surfaces with mechanically etched nanopatterns to analyze the cellular proliferation and understand the process of differentiation, which will enable the control of differentiation when necessary.

Nanopatterns were created by spin-casting a variety of polymer blends in a 1:1 ratio including Polystyrene (PS) and Ethylene-vinyl Acetate (EVA); Poly(lactic Acid (PLA) and Poly (Methyl Methacrylate) (PMMA); PMMA and EVA; and PS and PLA. The phase segregation of these immiscible blends resulted in the formation of nanopatterns as shown by the Atomic Force Microscope (Figure 1).

The ion mill was used to sputter the pattern into the surface of the silicon followed by high temperature evaporation of the polymer, which leaves just the etched silicon wafer. Polybutadiene (PB) was spin-casted upon all etched samples, to create a hydrophilic surface. Cells were then plated on each sample, and future research includes analyzing if the different nanopatterns will induce differentiation of the DPSC along the osteoblastic lineage. This will be achieved by analyzing the cell growth, actin fibers distribution, and biomineralization of each sample at three, fourteen, and twenty-one day intervals. Currently, after three days, the samples have been analyzed (Figure 2). Under both AFM and Confocal Microscopy, cell development looks prosperous. The actin fibers seem numerous and are spread uniformly throughout the sample. Our future research includes continued analysis for the fourteen and twenty-one day period.

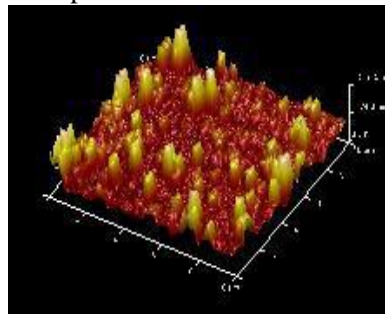


Figure 1: AFM analysis of PS: PLA 1:1 blend after 15minute sputtered interval

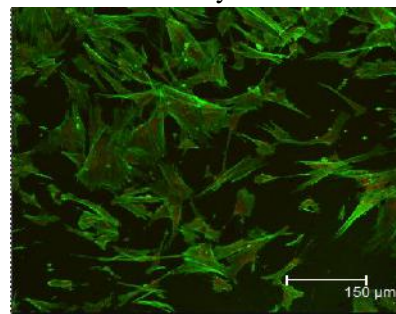


Figure 2: Confocal Microscopy Analysis after 3 day of growth for the PS: PLA 1:1 blend

<sup>1</sup> Misako Nakashima, Koichiro Iohara, Masahiko Sugiyama, Human dental pulp stem cells with highly angiogenic and neurogenic potential for possible use in pulp regeneration, Cytokine & Growth Factor Reviews, Volume 20, Issues 5-6, Bone Morphogenetic Proteins, Stem Cells and Regenerative Medicine, October-December 2009, Pages 435-440, ISSN 1359-6101, DOI: 10.1016/j.cytogfr.2009.10.012.

<sup>2</sup> Tirino, V, F Paino, R d'Aquino, V Desiderio, and Athanasios De Rosa. "Methods for the Identification, Characterization and Banking of Human DPSCs: Current Strategies and Perspectives." *Stem Cell Reviews and Reports* 7.3 (2011): 608-615.

# A Study on the Effects of Biocompatible Nanopatterned Titanium Surfaces on Human Dental Pulp Stem Cell Growth and Biomineralization

Scott Zhou and Suditi Sood

Dobyns Bennett High School and Herricks High School

Yingjie Yu, Miriam Rafailovich, John Jerome, Maxwell Plaut

Massachusetts Institute of Technology

Currently, titania is the bone and dental implant material of choice because of its biocompatibility, osseointegration, and tensile modulus similar to bone. However, many implants still fail because of loosening at the titania-bone interface due to repeated load application inherent at the implant location.<sup>[2]</sup> There has been previous research on osteoblast activity on titania, but almost none on the growth of dental pulp stem cells (DPSCs) on such a surface. These pluripotent stem cells are easily obtained and ethically uncontroversial, but have been shown to differentiate into osteoblasts and generate bone matrix.<sup>[1]</sup> Thus, we studied the effects of a nanopatterned titania substrate on human DPSC growth and differentiation with the hope of finding a method of both inducing DPSCs to differentiate into osteoblasts and creating a better interface for titania-bone adhesion.

We created a titania surface on top of a silicon substrate using physical vapor deposition (PVD), and then spuncast 1:3 ratio blends of PS:PMMA dissolved in toluene in 10, 20, and 30 mg/ml concentrations onto the titania. The samples were then annealed to allow for phase separation, where the polymers separate from each other to naturally form structures on the nanoscale. Afterwards, they were sputtered using an ion mill to etch the nanopattern formed by annealing into the titania and after sterilization plated human DPSCs isolated from third molars of a consenting adult. We also plated cells onto glass controls without nanopatterning.

The stem cells were cultured for three days in fetal bovine serum (FBS) with and without dexamethasone to induce biomineralization, and were then fixed with formaldehyde. Using confocal microscope it was observed that the cells on titania nanopattern grew as well or better than they did on the glass controls, and that the cells on the 10 mg/ml concentration nanopattern grew extremely well, as shown by Figure 1 (left panel).

Further work includes analyzing cell growth at 7, 14, and 21 days to characterize their differentiation and biomineralization.

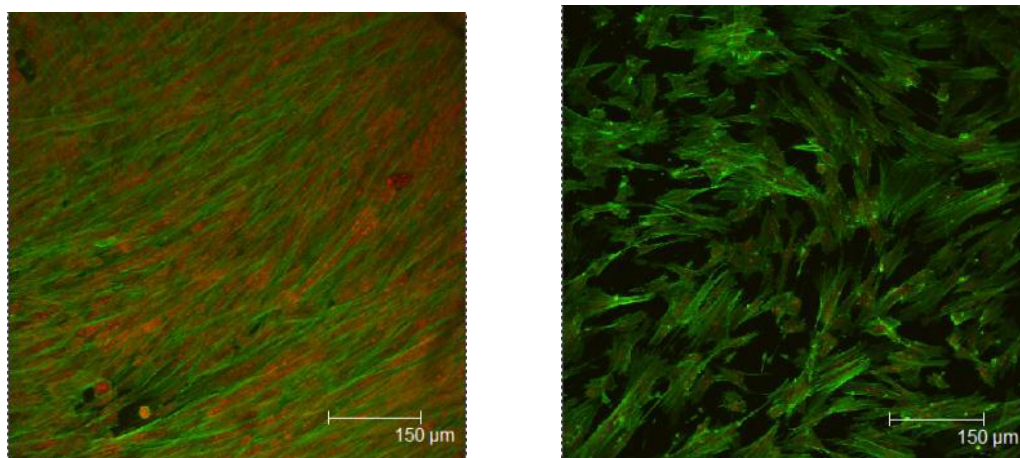


Fig. 1 – The image on the left shows the cells grown with dexamethasone on the sputtered titanium nanopattern from the 10mg/ml concentration solution, while the one on the right shows the cells grown on the glass control. The cells grew much more quickly on the titanium, which is almost completely covered in a layer of cells.

<sup>[1]</sup> d'Aquino, Riccardo, Gianpaolo Papaccio, Gregorio Laino, and Antonio Graziano. "Dental Pulp Stem Cells: A Promising Tool for Bone Regeneration." *Stem Cell Reviews* 4.1 (2008): 21-26. *Web of Science*. Web. 1 Aug. 2011.

<sup>[2]</sup> Riedel, Nicholas A., John D. Williams, and Ketul C. Popat. "Ion beam etching titanium for enhanced osteoblast response." *Journal of Materials Science* 46.18 Sept. (2011): 6087-95. *Web of Science*. Web. 1 Aug. 2011.

## The Effect of Chemical Nanopatterning on the Differentiation of Human Dental Pulp Stem Cells

Brad Kaptur, Joshua Millings

Maxwell Plaut, Debby Greenstein, Zohar Backiry, Dr. John Jerome, Dr. Vladimir Jurukovski, Dr. Miriam Rafailovich

---

Stem Cells are a promising source in a wide range of medical fields, including bone tissue regeneration<sup>1</sup> and nerve regeneration. Human Dental Pulp Stem Cells (hDPSCs) have self-renewing and multipotent qualities which have applications in regenerative medicine and tissue engineering. In this experiment, hDPSC proliferation and characteristics were observed as a function of their environment, which was controlled by chemical nanopatterning. Spincoating and chemical etching were used to create the chemical nanopatterns on copper-coated silicon wafers, utilizing the phase separation properties of immiscible polymers within a polymer-blend solution. Solutions of polystyrene (PS), poly(methyl methacrylate) (PMMA), or polycaprolactone (PCL) were blended with polybutadiene (PB) in ratios of 1:1, 1:3, and 3:1 (polymer : polybutadiene). PS and PMMA were removed from the surface via chemical etching, while PCL was removed via enzyme etching leaving a pattern of PB and copper. Atomic Force Microscopy (AFM) was used to obtain images and elastic modulus of the patterns (Figure 1). hDPSCs were then plated on the nanopatterns in both non-inducing and inducing media with appropriate controls. After 7 and 14 days the modulus of the hDPSCs (AFM) and cells' proliferation and structure (confocal microscopy) will be observed. The same characterization will be performed 21 days in addition to an enzyme-linked immunosorbent assay (ELISA) for osteocalcin, a marker of cell differentiation, to confirm cells' differentiation in osteoblast like cells capable of biomineralization. This experiment will aid the scientific community by highlighting hDPSC's sensitivity to the mechanical characteristics and chemical composition of their environment.

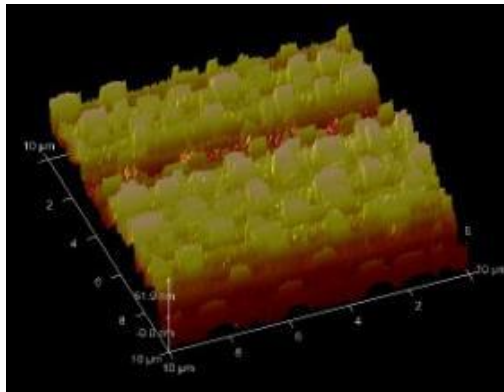


Figure 1. AFM image of a nanopattern after chemical etching

---

<sup>1</sup>Giorgini, Elisabetta, et al. "FT-IR microscopic analysis on Human Dental Pulp Stem Cells." *Vibrational Spectroscopy* (2011).

# Effects of the Mechanical Properties of Polycaprolactone and UV Plasma Treated Poly (Methyl Methacrylate) 3D Electrospun Scaffolds on Dental Pulp Stem Cell Differentiation and Biomineralization

**Manita Singh**, Canyon Crest Academy; **Nicholas Suss**, South Side High School

**Aaron Akhavan**, Yeshiva University

**Dr. Miriam Rafailovich<sup>1</sup>, Dr. Vladimir Jurukovski<sup>1,2</sup>, Dr. Marcia Simon<sup>2</sup>, Aneel Bherwani<sup>2,2</sup>, Chung-Chueh Chang<sup>1,3</sup>, Sisi Qin<sup>1,4</sup>**

1. Materials Science Department, Stony Brook University, 2. School of Dental Medicine, Stony Brook University

The use of polymers to construct 3D biomimetic scaffolds resembling the extracellular matrix (ECM) possesses great potential in the field of tissue engineering. Dental pulp stem cells (DPSCs), multipotent stem cells extracted from the third molar of humans, can be plated onto engineered scaffolds and induced to differentiate into different cell types including odontoblasts and osteoblasts. The effects of two FDA approved polymers, Poly (methyl methacrylate) (PMMA) and Polycaprolactone (PCL) are assessed to determine the potential that these polymers have in terms of tissue engineering applications. Previously, the chemical manipulation of the surfaces of scaffolds to enhance the differentiation of the DPSCs along desired pathways has been shown to be effective; however, there may be unforeseen consequences when chemical inducers are used in the body. Therefore, the mechanical properties of 3D scaffolds and their effects on DPSC differentiation are being investigated.

Electrospinning is a process that generates fibers from a polymer solution. Previous studies have shown that the hydrophobic properties of electrospun PMMA fibers form a non-adhesive scaffold for DPSCs. UV Ozone Plasma treatment is a process often used to make surfaces more hydrophilic. A portion of this study investigates the effect of UV Plasma treated PMMA substrates on DPSC differentiation and biomineralization. Scaffolds of PCL were also created as the polymer's biodegradable properties make it ideal for safe implantation into the body. DPSCs were plated onto unmodified electrospun scaffolds and thin films of PCL in order to analyze its potential for mechanically inducing DPSC differentiation.

Glass coverslips were either spun cast with a solution of 30 mg/ml of PMMA in toluene or a solution of 5% PCL in toluene. These samples were then electrospun with solutions varying in concentrations of PMMA or PCL and their respective solvents to form fibers of various diameters<sup>1</sup>. PMMA and PCL fibers of random orientation were constructed. In addition, parallel fibers of PCL were created. Glass coverslips spun cast with 25 mg/ml of PMMA in toluene or 2.5% PCL in toluene served as thin film controls. The PMMA samples were treated with UV plasma for 10 minutes and the PCL samples were soaked in ethanol for sterilization. DPSCs were then plated on the scaffolds and grown in either non-inducing media or media containing the inducer dexamethasone.

To verify the effect of UV Ozone Plasma treatment, contact angle measurements of PMMA thin film samples were conducted. Atomic force microscopy was used to determine Young's Modulus of Day 7 and 14 samples. Mercury Lamp images of PMMA fibers show evidence of biomineralization (Figure 1), and confocal microscopy images (Figure 2) of Day 14 PMMA samples show evidence of the cells' adhesion to the fibers, collectively signifying the success of UV Ozone Plasma treatment as a method for enhancing the mechanical properties of the PMMA scaffolds. Vinculin staining will be used to analyze the focal adhesion points of the DPSCs as they grow on the fibers<sup>2</sup>.

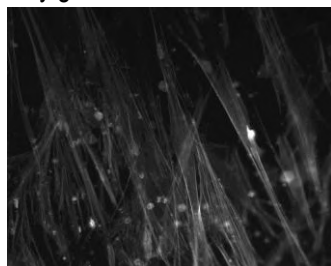


Figure 1. Mercury Lamp image of non-induced PMMA nanofibers

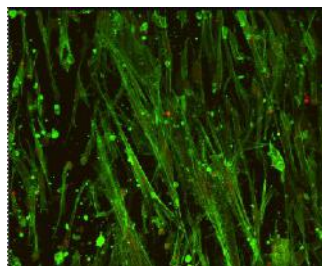


Figure 2. Confocal image of PMMA nano fibers in non-induced media.

Additional research will determine the presence of calcium phosphate crystal deposits on the scaffolds using Scanning Electron Microscopy (SEM) imaging and energy dispersive x-ray analysis (EDX). Additionally, alizarin red, osteocalcin staining and RT-PCR will be used to determine the presence of osteoblastic differentiation markers.

1. Ramakrishna, Seeram. *An Introduction to Electrospinning and Nanofibers*. Singapore: World Scientific, 2005.

2. Liu, Ying. "Effects of fiber orientation and diameter on the behavior of human dermal fibroblasts on electrospun PMMA scaffolds." *Journal of Biomedical Materials Research Part A* 90A.4 (2008): 1092.

## The Effect of Surface Modification of PMMA Scaffolds through Plasma Etching and Different Media on the Proliferation and Migration of Fibroblasts

Ryan Lindeborg<sup>1</sup>, Sisi Qin<sup>2</sup>, Miriam Rafailovich<sup>3</sup>

<sup>1</sup>Dana Hills High School, Dana Point, CA

<sup>2,3</sup>Department of Material Science and Engineering, SUNY Stony Brook, NY  
Clark Wound Healing Laboratory, Health Sciences Building  
State University of New York, Stony Brook

---

### Abstract

Wound healing requires complex interactions between multiple substrates within the extracellular matrix (ECM). The most important cell type within the ECM is the fibroblast, which is vital for granulation tissue formation and wound contraction.<sup>1</sup> Although there is a basic understanding of how fibroblasts and the ECM interact in wound healing, the specific combination of substrates that stimulate fibroblast activity maximally is still unknown.

This investigation sought to better define the interactions between fibroblasts, the various components of the ECM, and the modified polymer scaffold. As a model, fibroblasts were studied with individual components of the ECM on a poly (methyl methacrylate) (PMMA) scaffold. The first study measured fibroblast activity on a scaffold surface that had undergone plasma etching, that is exposure to UV radiation, with and without a fibronectin (FN) coating. The second study compared the effects of collagen, FN, platelet-derived growth factor (PDGF), and fetal bovine serum (FBS) on the distance and velocity of fibroblast migration.

First, a PMMA thin film was deposited onto a glass cover slip using the spincasting technique with a solution of 30mg/mL PMMA in toluene. Next, electrospinning was performed with a solution of 20% PMMA in chloroform to produce microfiber scaffolds (Figure 1). Fibroblasts were cultured, incubated with a fluorescent stain, and pipetted onto the fibers. Using a fluorescent microscope, fibroblast migration was observed and both the velocity and distance over calculated time intervals were measured. Focal adhesion (FA) sites were also measured using a vinculin staining method and a confocal microscope.

Plasma etching had a positive effect on fibroblast activity, stimulating a higher initial migration velocity, which was further improved with the addition of FN. It caused the surface to become more hydrophilic and biocompatible.<sup>2</sup> The FBS stimulated fibroblast migration much more than PDGF, but the FN and collagen were relatively equal in their effect on fibroblast migration.

Utilization of biocompatible scaffolds to provide the necessary components of the extracellular matrix holds potential in regenerative tissue engineering and future research, with the ultimate goal of facilitating accelerated wound healing.

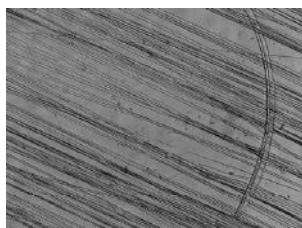


**Figure 1:** PMMA microfibers: 20% PMMA in chloroform: scaffold on which fibroblast cells will migrate.

### References:

<sup>1</sup> Clark, R. A. F. *The Molecular and Cellular Biology of Wound Repair*. New York: Plenum, 1996. Print.

<sup>2</sup> Chu, P. K., J. Y. Chen, L. P. Wang, and N. Huang. "Plasma-surface Modification of Biomaterials." *Reports: A Review Journal* 36 (2002): 143-206. Elsevier Science. Web. 1 Aug. 2011.



# Quantitative Analysis of Novel Thermoreversible Pluronic F127, Gelatin, and Hyaluronic Acid Composite Hydrogels for the Creation of Cellular Substrates with Application in Regenerative Medicine

Yicheng Sun<sup>1</sup>, Japbani Nanda<sup>2</sup>, Nikhil Mehandru<sup>3</sup>, Divya Bhatnagar<sup>4</sup>, Miriam Rafailovich<sup>5</sup>  
<sup>1</sup>Mission San Jose High School, Fremont, CA, <sup>2</sup>W. Tresper Clarke High School, Westbury, NY, <sup>3</sup>Harvard University, <sup>4,5</sup>SUNY Stony Brook

In recent years, the field of regenerative medicine has displayed potential to provide tremendous improvements to public health with applications in wound healing, cell therapy, and organ repair. Regenerative medicine's ultimate goal is to replace damaged tissue with tissue that is physiologically and functionally identical in order to facilitate natural body recovery. To do so, an effective targeted delivery system of the cells and proteins that comprise the given tissue is required. One particularly promising method involves the encapsulation of the cells inside the hydrogels. In this study, a novel composite hydrogel was designed to be both biocompatible and have the necessary high elastic modulus, a measure of hardness under deformation, needed for effective cell delivery.

The triblock copolymer Pluronic F127 was selected as the primary component of the hydrogel for its thermoreversible gelation properties. This is useful in that cells can be loaded or encapsulated and inserted into the body in the sol state. Once the solution enters the body, it gels, allowing it to better withstand the shear forces within the body. Despite this, previous research has shown that pure PF127 gels do not serve as an optimal medium for cell growth.<sup>1</sup> To remedy the problem, the natural polymers Hyaluronic Acid (HA) and gelatin were added to create a polymer blend. Although HA displays poor mechanical strength and rapid degradation, it is known for its biocompatibility and biodegradability. Gelatin was added for increased cell adhesion. The experiment showed that the resulting composite HA-gel-PF127 hydrogel displayed synergistic properties: high elastic modulus of up to 10K Pa more compared to pure Pluronic and increased biocompatibility for cell encapsulation.

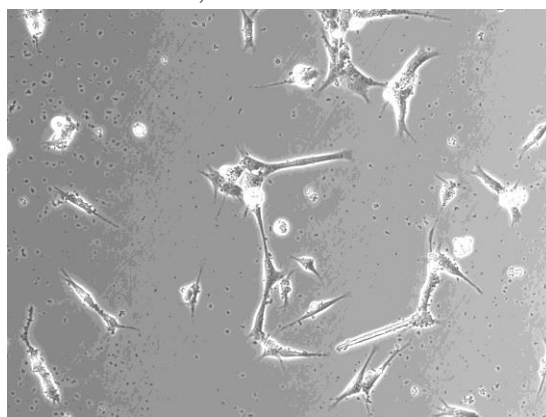


**Fig. 1:** Phase contrast image of 1:80 HA-PF127 Gel

Gels comprising of different concentrations of HA and Pluronic F127 were made and rheological analysis was performed. When running amplitude sweep tests, it was found that the gels of ratio 1:80 exhibited the highest elastic modulus ( $G'$ ). Temperature sweep tests displayed that as the concentration of HA increased, the critical solution temperature (CST) also increased. In order to model a more physiologically relevant testing medium, the gel of ratio 1:80 HA to PF127 was doped with varying levels of sodium chloride and glucose. Both additives did not significantly alter the  $G'$  of the gel, but it was found that as the concentration of each of the additives was increased, the CST decreased. Specifically, glucose doped HA-PF127 gel CST dropped from 19.1°C at 0% glucose to 12.3°C at 10.000%. For salt doped gels, the CST dropped even lower to 6.8°C. This drastic decrease in the CST was most likely due to the hygroscopic properties of each of the additives, which caused a decrease in available water molecules for interaction with the Pluronic monomers.<sup>2</sup>

Finally, to quantify the hydrogel's effect on cells, human dermal fibroblasts were cultured on sterile HA-gelatin Pluronic PF127 gels. The cells were plated on the inside of the matrix of the gel for a three-dimensional tissue culture (See Fig. 1). A growth curve will be obtained by counting the number of cells within a set time period to see how cells react to the gel.

Future research will involve analyzing the crystalline structure of the hydrogel using SAXS. Further rheological testing will be conducted on hydrogels containing both gelatin and HA in Pluronic F127 to quantify any synergistic viscoelastic properties.

<sup>1</sup> Yuhan, Lee, et. al. "Thermo-sensitive, injectable, and tissue adhesive sol-gel transition hyaluronic acid/pluronic composite hydrogels prepared from bio-inspired catechol-thiol reaction." *Soft Matter* 6.5 (2010): n. pag. 977-983. Web. 9 Aug. 2011.

<sup>2</sup> Jiang, Jun, et. al. "The effect of physiologically relevant additives on the rheological properties of concentrated Pluronic copolymer gels." *Polymer* 49.16 (2008): 3561-3567. *Web of Knowledge*. Web. 9 Aug. 2011.

## A Study of the Biomineralization of Human Dental Pulp Stem Cells on Crosslinked Gelatin Hydrogels

Sneha Subramaniam and Elliot Tan

Westborough High School and Fayetteville-Manlius High School

Divya Bhatnagar , Dr. Miriam Rafailovich, Department of Materials Science, Stony Brook University  
Dr. Aneel Bherwani , Dr. Marcia Simon, School of Dental Medicine, Stony Brook University

Human dental pulp stem cell (DPSC) differentiation and biomineralization has promising applications in bone injury repair as well as in the orthopedic and orthodontic fields. Previous studies have shown that the multipotent DPSCs can differentiate into osteoblasts that can ultimately construct adult bone tissue *in vivo*<sup>1</sup>. For such regeneration to be possible, it is essential to provide proper substrate mechanics and chemistry as well as soluble factors that enhance stem cell differentiation. In our study, we used scaffolds composed of gelatin crosslinked with microbial transglutaminase (mTG) and collagen with or without crosslinking. The influence of substrate mechanics and chemistry and of the soluble differentiation mediator dexamethasone was evaluated as a function of biomineralization. The role of soluble cell derived factors on hydrogel mineralization is also being assessed using conditioned media from DPSC grown on transglutaminase crosslinked gelatin.

To understand the mechanics and dynamics of the scaffolds, amplitude and frequency sweeps were run on mTG crosslinked gelatin gels of soft, medium and hard stiffnesses using a Bohlin rheometer. To simulate the human body environment, the hydrogels were incubated at 37°C for set time intervals. With data obtained from the rheometer, it was possible to observe differences in the change in elastic modulus for the gels with varying stiffnesses as a function of time.

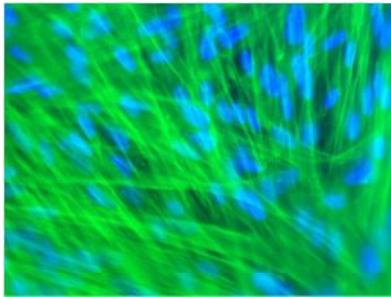


**Figure 2:** 21 day fluorescent image of actin filaments and nuclei.

Using these gels, DPSC's were also seeded and incubated at 37°C for 21 days on crosslinked gelatin and pure collagen. It was expected that both

substrates would have similar biomineralization, but that collagen would support less biomineralization than gelatin<sup>3</sup>. In order to analyze the samples, Alizarin Red staining (for calcium deposits), optical microscopy, Scanning Electron Microscopy (SEM) with EDX analysis (to analyze mineral composition), real time polymerase chain reaction (to test the presence of marker genes), and fluorescence staining will all be completed on the samples at days 14 and 21. As shown in Figure 3, the Alazarin Red Staining is a deeper red on the day 21 samples, indicating that much more biomineralization occurred between day 14 and 21. Presence of dexamethasone had no visible effect on biomineralization levels.

The 21 day samples were also sectioned, and the optical images taken (see Figure 1) showed that the cells do not enter the gels even though biomineralization occurred in the gel. Therefore, another experiment was set up to determine whether the DPSCs secreted substances into the media that induced biomineralization within the gel matrix. To do this, an acellular mTG-crosslinked gelatin gel will be fed with the media collected from a DPSC plated gel. If biomineralization takes place on the acellular gel, there will be promising future research in the creation of bone without the direct use of DPSCs.

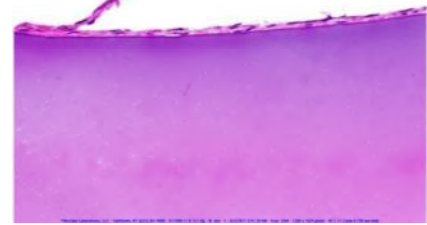


**Figure 1:** Optical Microscope Image of 21 day non-induced media. The image shows a layer of dental pulp stem cells on top of an mTG crosslinked gelatin hydrogel. The dark purple stains for the biomineralization within the gel.

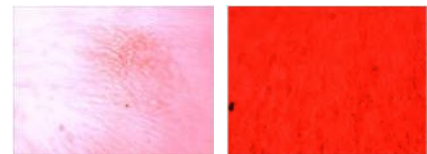


**Figure 3:** Alazarin Red Staining of Calcium Phosphate on 14 and 21 day non-dexamethasone induced samples.

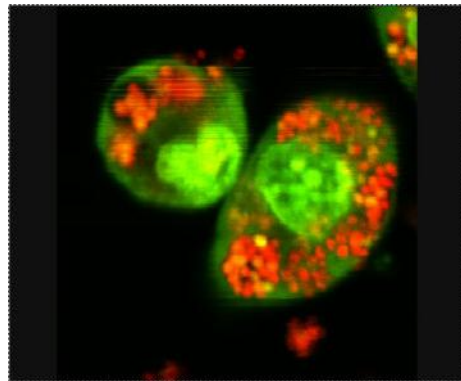
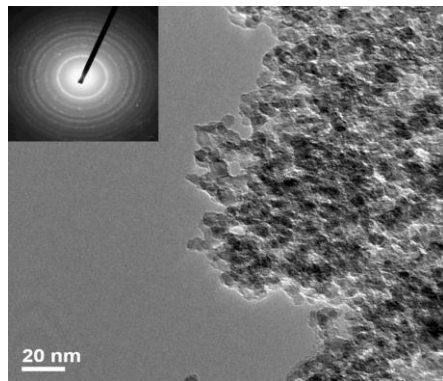
<sup>1</sup>D'Aquino, Riccardo, et al. "Human Dental Pulp Stem Cells: From Biology to Clinical Applications." *Journal of Experimental Zoology* 14 Nov. (2008).

<sup>2</sup>Yung, C.W. , et al. "Transglutaminasecrosslinked gelatin as a tissue engineering scaffold." *JOURNAL OF BIOMEDICAL MATERIALS RESEARCH PART A* 83A.421 June (2007)

<sup>3</sup>Kim, Na Ryoung, et al. "Distinct differentiation properties of human dental pulp cells on collagen, gelatin, and chitosan scaffold" *Mosb.* (2009)

# Nanoparticle Toxicity

## SESSION 2



**Chairs: Zohar Bachiry, Channi Stern**

***Graduate Mentors: Tatsiana Mironava,  
Chien-Hsiu Lin***

## Differently sized charged gold nanoparticles alter HeLa cell membrane properties

Merry Mou<sup>1</sup>, Penina Safier<sup>2</sup>, Miriam Rafailovich<sup>3</sup>, Tatsiana Mironava<sup>4</sup>

<sup>1</sup>Mission San Jose High School, Fremont, CA; <sup>2</sup>College of Staten Island, Staten Island, NY; <sup>3,4</sup>SUNY Stony Brook, Stony Brook, NY

Membrane potential, the difference in electrical charge on two sides of a membrane, has been found to play an important role in cell cycle and growth regulation<sup>1,2,3</sup>, apoptosis<sup>4</sup>, and oncogenicity<sup>5,6</sup>. Membrane potential is mostly affected by ion distribution, which is determined partly by the state of the ion channels they must pass through. Some ion channels, known as voltage-gated channels, are regulated by voltage: when the membrane experiences a change in potential, the rate of transport that the channel allows also changes.

We investigated the effects of differently sized nanoparticles on HeLa cell membranes and their membrane potential. We hypothesized that the negatively charged nanoparticles will affect the membrane by altering the membrane potential and thus opening or closing voltage-gated ion channels. These changes will be able to be detected using the whole-cell patch clamp technique, which measures total current carried by ions through the cell membrane. We also hypothesize that different sizes of particles will have different affect because they will influence the electric field and membrane potential differently.

Using the patch clamp technique, we created I-V graphs that indicate a significant difference between the average conductances of control cells

with nanoparticles (Figure 1). Specifically, significantly less current flowed through membranes with nanoparticles; additionally, less current flowed through cells exposed to 13 nm AuNPs than those to 45 nm AuNPs. Atomic force microscopy was also used to determine elastic modulus of the membrane. The and thus the stiffness, of the control cell significantly greater than that of the membranes exposed to nanoparticles.

With this preliminary data, we that nanoparticles have a significant the HeLa cell membrane. We hope to further confirmatory studies and to our investigation to include other kinds nanoparticles with different charge and properties.

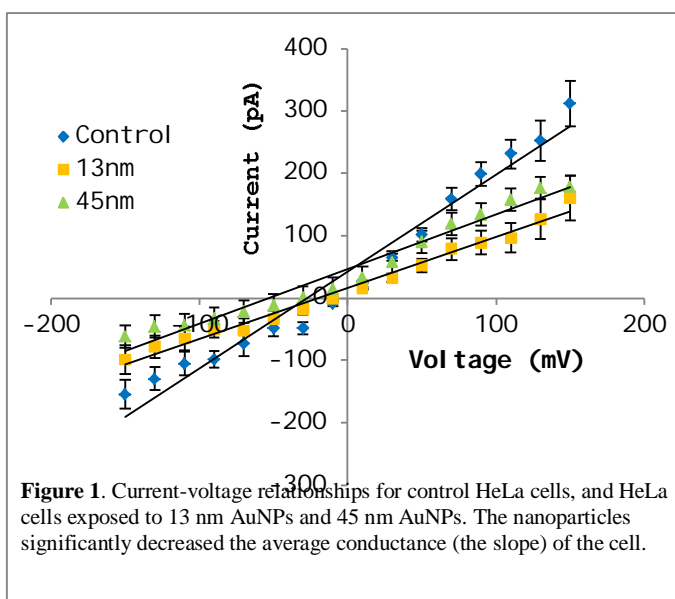


**Figure 1.** Current-voltage relationships for control HeLa cells, and HeLa cells exposed to 13 nm AuNPs and 45 nm AuNPs. The nanoparticles significantly decreased the average conductance (the slope) of the cell.

<sup>1</sup>Blackiston DJ, McLaughlin KA, Levin M. 2009. Bioelectric controls of cell proliferation: ion channels, membrane voltage and the cell cycle. *Cell Cycle* 8(21):3519-3528.

<sup>2</sup>Binggeli R, Weinstein RC. 1986. Membrane potentials and sodium channels: hypotheses for growth regulation and cancer formation. *J Theor Biol* 123:377-401.

<sup>3</sup>Pardo LA. 2004. Voltage-Gated Potassium Channels in Cell Proliferation. *Physiology* 19:285-292.

<sup>4</sup>Mann CL, Cidlowski JA. 2001. Glucocorticoids Regulate Plasma Membrane Potential During Rat Thymocyte Apoptosis in Vivo and in Vitro. *Endocrinology* 142(1):421-429.

<sup>5</sup>Pardo LA, Camino D, Sanchez A, et al. 1999. Oncogenic potential of EAG K<sup>+</sup> channels. *The EMBO Journal* 18(20):5540-5547.

<sup>6</sup>Zs.-Nagy I, Lustyik G, Nagy V, et al. 1981. Intracellular Na<sup>+</sup>/K<sup>+</sup> Ratios in Human Cancer Cells as Revealed by Energy Dispersive X-Ray Microanalysis. *J Cell Biol* 90:769-777.

and cells

flowed

cells  
exposed

the  
modulus,  
was

can infer  
effect on  
conduct  
expand  
of  
size

## The Effect of Platinum-Folate Coated Nanoparticles on Dental Pulp Stem Cells as a Function of Proliferation and Differentiation

Alexa Aseel-Fine, Jericho High School, Jericho, NY

Tatsiana Mironava, Stony Brook University, Department of Materials Science and Engineering

Vladimir Jurukovski, Suffolk County Community College, Department of Biology

Recently, there has been much evidence supporting the idea that nanoscale materials can facilitate stem cell therapy<sup>3</sup>. Dental Pulp Stem Cells (DPSCs) are characterized as multipotent cells, which give rise to a number of cell lineages including: osteogenic, chondrogenic, miogenic, cardiac, and adipogenic. Additionally, platinum is a noble metal and a catalyst in chemical reactions such as hydration, hydrogenation, and oxidation. Because Pt is a relatively stable and unreactive metal, it is hypothesized to aid in early differentiation of DPSCs<sup>1</sup>. Although aiding in the differentiation process, nanoparticles may be toxic to the cells<sup>2</sup>. Likewise, folic acid is part of the cell metabolic process therefore it is not cytotoxic to cells. Thus, covering Pt with folate, it will allow for solely the platinum to be detected. At the same time, the interactions between noble metals and DPSCs have not been studied in detail and little is known about their effect on differentiation<sup>3</sup>.

This study tested the toxicity as a function of proliferation and differentiation of folate-covered platinum nanoparticles and their effect on DPSCs as well as the effect of folate alone. In order to characterize the nanoparticles, the zeta potential, FT-IR spectroscopy, and UV-Vis were all recorded. An MTS assay of the nanoparticles was then taken and it was determined that the 3% and 6% concentration were the least harmful to the cells. However, because the experiments were planned for 14 and 21 days, the concentrations of Pt were decided to be kept as 2% and 4%. In order to properly assess the effect of the nanoparticles on the cells, the cells were tested for proliferation with and without nanoparticles on days 0, 3, 5, and 7 (**Figure 1**). As expected, the 2% concentration was less harmful to the cells than the 4% concentration of platinum. Moreover, an ELISA assay will be used to analyze the osteocalcin production by normalizing the amount of osteocalcin produced as compared to the total amount of proteins in the cells. Furthermore, confocal microscopy will be used to check for changes in morphology of the cells in the presence of the nanoparticles.

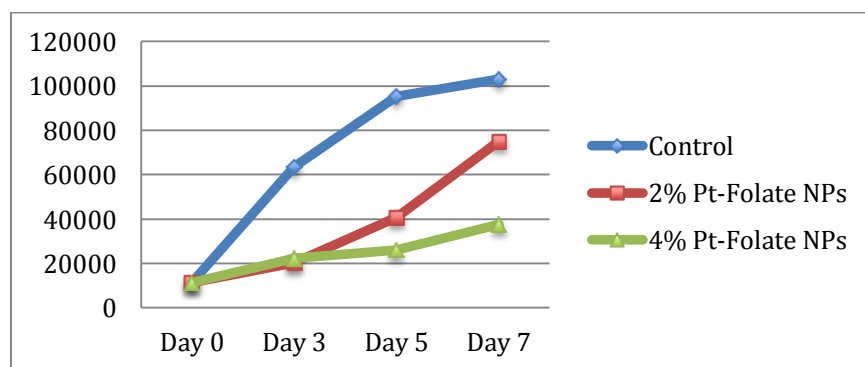


**Figure 1:** 7 Day growth curve of 2% Pt-Folate NPs and 4% Pt-Folate NPs

### References

- [1] Gehrke, H., Pelka, J., Blank, H., Bleimund, F., Schneider, R., Gerthsen, D., . . . Hartinger, C. G. (2011). Platinum nanoparticles and their cellular uptake and DNA platination at non-cytotoxic concentrations. *Arch Toxicol*, 85, 799-812.
- [2] Mironava, T., Hadjiargyrou, M., Simon, M., Jurukovski, V., & Rafailovich, M. H. (2010, March). Gold nanoparticles cellular toxicity and recovery: Effect of size, concentration and exposure time. *Nanotoxicology*, 4(1), 120-137.
- [3] Yi, C., Liu, D., Fong, C.-C., Zhang, J., & Yang, M. (2010). Gold nanoparticles promote osteogenic differentiation of mesenchymal stem cells through p38 MAPK pathway. *American Chemical Society Nano*, 4(11), 6439-6448.

## Platinum Folate Nanoparticles: A Novel Instrument for Receptor Targeted Cancer Treatment

**Evan Schneider**, Roslyn High School, Roslyn Heights, NY  
**Lourdes Collazo**, Department of Materials Science and Engineering  
**Miriam Rafailovich**, Department of Materials Science and Engineering

The field of science known as *nanotechnology* is currently transforming nearly every aspect of society. This transformation can be widely credited to the increasing use of nanoparticles. The applications of nanoparticles vary from their use as preservatives in food packaging and disinfectants in swimming pools to their use in the medical world.

While nanoparticles can be found in almost any product, their medical application is perhaps what makes these miniscule particles so beneficial. One study showed that the combination of folate-coated gold nanoparticles and intense pulsed light was shown to be an effective mechanism for killing two cancerous cell lines, HeLa and MCF7<sup>1</sup>. Additionally, nanoparticles have been used as a drug delivery mechanism (that reduces side effects) for cancer treatments<sup>2</sup>.

One particular aspect of nanoparticles that hasn't been extensively studied is the effect that the *nanoparticle coating* has on cell targeting. In this research, the fact that cancerous cells are known to express over 500 times as many folate receptors as non-cancerous cells was used as a basis for coating nanoparticles in folate<sup>1</sup>. Additionally, platinum nanoparticles were used as platinum in a known cancer therapy and is known to be extremely toxic to cells (once inside the membrane). One novel aspect of this research is that a control, pure platinum nanoparticles (uncoated), will be used to prove that the folate coating is truly what makes the platinum nanoparticles *enter* and *kill* the cancer cells to a higher degree. With this fact established, nanoparticle coatings can be developed in unique ways to specifically target cancerous cells (in different parts of the body) while leaving non-cancerous cells relatively unharmed.

Growth curves will be used to show the relative rates of growth of both the cancerous cells (ROS 18/2.8) and non-cancerous cells (MC-3T3-E1) when exposed to both pure platinum and folate-coated platinum nanoparticles. Additionally, confocal microscopy will be used to show the actin fiber alignment (indicative of cell health) of the cells after exposure to nanoparticles. Finally, the Transmission Electron Microscope (TEM) will be used to observe the nanoparticles' localization inside the cells. These TEM images will then be used to determine if the *folate coating* is what facilitates the nanoparticles' entrance inside the cancerous cells. Future work also will seek to determine if other coatings (aside from folate) will also allow nanoparticles to specifically target specific cancer cell lines.

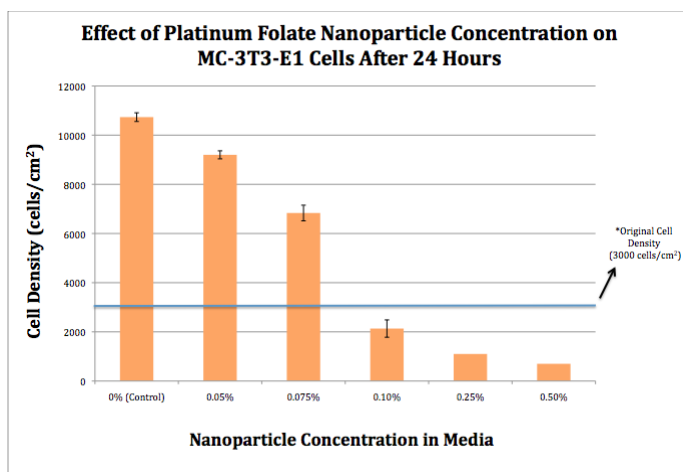


Figure 1: Dose Response Graph – Indicating which concentrations of platinum nanoparticles have a limited toxic effect on non-cancerous cells

<sup>1</sup> Shakeri-Zadeh, Ali, G. Ali Mansoori, A. Reza Hashemian, Hossein Eshghi, Ameneh Saizgarnia, and A. Reza Montazerabadi. "Cancerous Cells Targeting and Destruction Using Folate Conjugated Gold Nanoparticles." *Global Science Books* (2010): 1-11. Print.

<sup>2</sup> De Jong, Wim Howard, and Paul JA Borm. "Drug Delivery and Nanoparticles: Applications and Hazards." *International Journal of Nanomedicine* (2008): 133-36. Print

## Cytotoxicity and Differentiation of Dental Pulp Stem Cells: Effects of Gold Nanoparticle Size

Alissa Zhang<sup>1</sup>, Tyler Lawrence<sup>2</sup>, Beatris Jiminez<sup>3</sup>,  
Tatsiana Mironava<sup>4</sup>, Vladimir Jurukovski<sup>3,4</sup>, Miriam Rafailovich<sup>4</sup>

<sup>1</sup>Saratoga High, <sup>2</sup>Smithtown High West, <sup>3</sup>Suffolk Community College, <sup>4</sup>SUNY Stony Brook

Stem cells are an important repair system for the body due to their ability for self renewal and differentiation. Dental pulp stem cells (DPSCs) are of particular interest because they are multipotent and can easily be isolated from teeth and tooth buds. They are capable of producing bone and may be used in regenerative medicine.<sup>1</sup> A safe, noninvasive long-term imaging technique is necessary to monitor DPSCs during wound healing. Gold nanoparticles are an optimal choice due to their ability to be easily imaged, ease of cell penetration, and relative biocompatibility.<sup>2</sup> However, there is insufficient research on the cytotoxicity of gold nanoparticles with respect to cell type and size.

Gold nanoparticles of different sizes have been shown to significantly affect dermal fibroblasts, with larger nanoparticles being more toxic.<sup>3</sup> Our experiment examines the effects of different sizes of gold nanoparticles on DPSCs using citrate-capped gold nanoparticles with diameters of 13 and 45 nm. We hypothesize that higher concentrations and longer exposure times will be more toxic. We also expect that gold nanoparticles will not affect stem cell differentiation.<sup>2</sup>

To test this hypothesis, we synthesized nanoparticles with diameters of 13 and 45 nm and characterized them using Fourier transform infrared spectroscopy (FTIR), ultraviolet-visible spectroscopy (UV-Vis), transmission electron microscopy (TEM), and zeta potential. We added gold nanoparticles at two concentrations to dental pulp stem cells and monitored cell growth over eight days to determine cytotoxicity. **Figure 1** shows that higher concentrations and longer exposure times to nanoparticles are more toxic. Also, the 13 nm nanoparticles were slightly more toxic than the 45 nm ones. To measure nanoparticle allocation, we will take TEM images of the cells after incubating them for three days with nanoparticles. For stem cell differentiation, we added the nanoparticles to cells in both non-inducing and osteogenesis-inducing media and will measure the production of osteocalcin using the ELISA assay after fourteen and twenty-one days. We will normalize the amount of osteocalcin to amount of protein overall in the cells to determine the degree of biomineralization. We also will use confocal microscopy to characterize the morphology of the cells and observe the alignment of their actin fibers, which may be disrupted by nanoparticle uptake and allocation.<sup>3</sup>

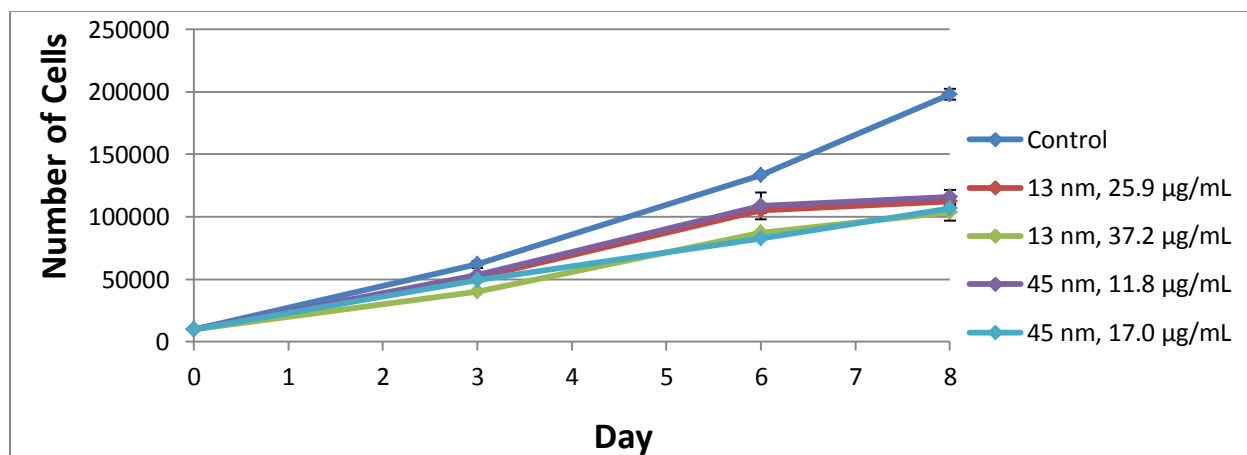


**Figure 1.** Cell proliferation with different sizes and concentrations of gold nanoparticles over a period of 8 days.

<sup>1</sup>D'Aquino, R., et al. "Human Dental Pulp Stem Cells: From Biology to Clinical Applications." *Journal of Experimental Zoology* 5 (2008): 408-415.

<sup>2</sup>Ricles, L.M., et al. "Function of Mesenchymal Stem Cells Following Loading of Gold Nanotracers." *International Journal of Nanomedicine* 6 (2011): 407-416.

<sup>3</sup>Mironava, T., et al. "Gold Nanoparticles Cellular Toxicity and Recovery: Effect of Size, Concentration and Exposure Time." *Nanotoxicology* 4 (2010): 120-137.

# The Effect of Titanium Dioxide and Zinc Oxide Nanoparticles on Pseudorabies Virus

Arvind Viswanathan, *Herricks High School*

Sarah Gross, *SUNY Farmingdale*

Chien-Hsiu Lin and Miriam Rafailovich, *Department of Materials Science & Engineering, Stony Brook University*

Aujeszky's Disease, caused by the Pseudorabies Virus (PRV), is often fatal to the animals it afflicts. The virus is naturally found in swine but can infect many other wild and domestic species.<sup>1</sup> In recent studies, nanoparticles, a relatively young technological trend, have shown promising antiviral abilities. Titanium Dioxide (TiO<sub>2</sub>) nanoparticles and Zinc Oxide (ZnO) nanoparticles are known to create reactive oxygen species (ROS), free radicals which could possess inhibitory effects in the spread of infection, and both metallic oxides are therefore potentially potent antiviral agents.<sup>2,3</sup> ROS are, however, damaging to living cells above certain concentration thresholds; therefore, TiO<sub>2</sub> and ZnO nanoparticles are only practical in antiviral capacities at low concentrations. The purpose of this experiment is to determine the effect of TiO<sub>2</sub> and ZnO nanoparticles on PRV.

For this experiment, rabbit kidney (RK13) cells were cultured to serve as the host for PRV. Free radical generation by the metallic oxide nanoparticles was confirmed by reacting nanoparticle solutions with Red 28 dye and measuring the change in dye color through UV-Vis spectrophotometry (Figure 1). Solutions containing ZnO and TiO<sub>2</sub> (rutile and anatase forms of TiO<sub>2</sub> were regarded as two separate species) nanoparticles at concentrations of 0.1

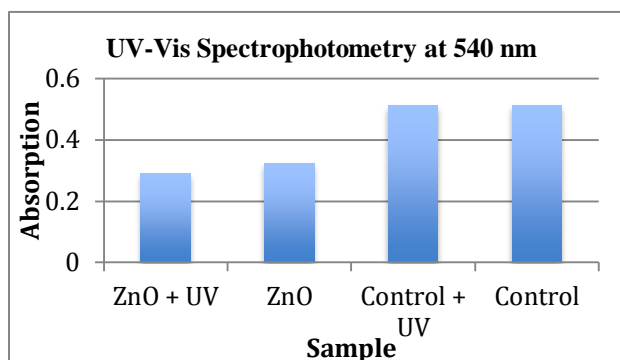


Figure 1: Red 28 dye peak absorbance. Lower absorption values signify greater free radical generation.

mg/mL and 1.0 mg/mL were created. The viruses will be pre-incubated with the nanoparticles to test inactivation. After PRV has been incubated with nanoparticles, it will be used to infect RK13 cells. The remaining PRV in the medium after the infection process will be harvested and used to run a plaque assay. For the plaque assay, ten-fold serial dilutions of the harvested virus from 10<sup>-2</sup> to 10<sup>-9</sup> will be used. The purpose of the plaque assay is to determine the plaque forming units (PFU) of the virus samples as well as their relative infectivity after treating them with nanoparticles. The nanoparticles will be deemed effective at inactivating PRV if the plaques are fewer in number than the control of untreated PRV or if the plaques are significantly smaller than the control.

A follow-up study on the effect of nanoparticles and free radicals on the entry of PRV into cells could also be crucial to determine the exact effects of nanoparticles on viral activity. Nanoparticles could potentially inhibit viral entry into cells by preventing the fusion step of the viral process, potentially rendering the virus benign.

<sup>1</sup> Thawley, David G., Donald P. Gustafson, and Robert R. Ormiston. *Pseudorabies (Aujeszky's Disease)*. West Lafayette: Purdue University Cooperative Extension Service, n.d. 1-2. Web. 8 Aug. 2011.

<sup>2</sup> Brunet, Léna, Delina Y. Lyon, Ernest M. Hotze, Pedro J. Alvarez, and Mark R. Wiesner. "Comparative Photoactivity and Antibacterial Properties of C60 Fullerenes and Titanium Dioxide Nanoparticles." *Environmental Science & Technology* 43.1214 May (2009): 4355-56. Web. 8 Aug. 2011.

<sup>3</sup> Skulachev, V P. "Possible Role of Reactive Oxygen Species in Antiviral Defense." *Biokhimiya* 63.129 Sept. (1998): 1-2. Web. 9 Aug. 2011.



## Effects of TiO<sub>2</sub> and ZnO Nanoparticles on Healthy and Infected Macrophages with *Leishmania tropica* and *Staphylococcus aureus* In Vitro

Brian Lei<sup>1</sup>, Alexander Lee<sup>2</sup>, Anirudh Pochiraju<sup>3</sup>, Chien-Hsiu Lin<sup>4</sup>, Adil Allahverdiyev<sup>5</sup>, Yury Yakubchyk<sup>4</sup>, Wilson A. Lee<sup>6</sup>, Stephen Walker<sup>4</sup>, Chana Stern<sup>7</sup> and Miriam H. Rafailovich<sup>4</sup>

<sup>1</sup>Arlington High School, LaGrangeville, NY, <sup>2</sup>Hauppauge High School, Hauppauge, NY, <sup>3</sup>Irvine High School, Irvine, CA, <sup>4</sup>Stony Brook University, Stony Brook, NY, <sup>5</sup>Department of Bioengineering, Yildiz Technical University, Istanbul, Turkey, <sup>6</sup>Research and Development, Estée Lauder Inc., <sup>7</sup>Stern College for Women, Yeshiva University, NY

Spread by the bite of certain species of sand fly, the disease leishmaniasis causes widespread skin lesions and ulcers, damages tissue (cutaneous), and can be fatal if left untreated (visceral).<sup>1</sup> Nanotechnology, a rapidly expanding field of engineering, provides us with a new hope of combating infectious diseases, including leishmaniasis. This is particularly important due to the development of drug resistant diseases.<sup>2</sup> Titanium dioxide (TiO<sub>2</sub>) and zinc oxide (ZnO) nanoparticles have been found to be toxic to cells through free radical generation, to which *Leishmania* is very sensitive. Therefore, the goal of our study was to examine the effects of TiO<sub>2</sub> and ZnO on *Leishmania* parasites and their hosts.

In our experiments, we used cultures of *Leishmania* parasites, J774A.1 macrophage-like cells, and for infection of macrophages, *Staphylococcus aureus* bacteria. We used different concentrations of TiO<sub>2</sub> (two crystalline structures - rutile and anatase, 0.1 – 0.4 mg/mL) and ZnO (0.05 – 0.1 mg/mL) nanoparticles. Our results show that the higher concentrations of ZnO had the most toxic effects on the macrophages, making them too lethal to use as they would destroy healthy cells in addition to the parasite. In order to minimize damage to healthy cells, we have studied minimal concentrations of nanoparticles (< 0.4 mg/mL TiO<sub>2</sub> and < 0.05 mg/mL ZnO). Results show that in these concentrations there is no significant impairment of macrophage growth.

As a subsequent step, we studied the effects of low concentrations of nanoparticles on macrophages that were infected with *S. aureus* in a 10 : 1 ratio of bacteria to macrophages. Confocal microscopy of the macrophages without nanoparticles (Figure 1) did not show a difference in cell death as compared to cells with nanoparticles (Figure 2). We therefore increased the concentration of bacteria to be performed with a 1000 : 1 bacteria to macrophage ratio, and further microscopy with TEM is planned.

To study the mechanism of action of nanoparticles, we placed them in Red No. 28 dye and exposed to UVC light, which catalyzes free-radical generation causing the dye to degrade. Measuring the degradation of the dye with a UV-VIS spectrophotometer, we found that an increased concentration in nanoparticles and an increased exposure to UV light resulted in greater free radical generation; furthermore, ZnO emitted more free radicals than TiO<sub>2</sub>, demonstrating its greater potency. We also studied the effect of nanoparticles in λ-DNA. Gel electrophoresis results showed that the nanoparticles damaged DNA, causing a lower mean intensity of the DNA bands in the gel. Zinc oxide was more powerful than TiO<sub>2</sub> and nanoparticle concentration varied directly with potency. This experiment was previously performed but used only pure and coated TiO<sub>2</sub> nanoparticles.<sup>3</sup>

Currently, our results show that TiO<sub>2</sub> and ZnO nanoparticles readily generate free radicals. Depending on nanoparticle concentration, this affects bacteria-infected macrophage function with varying severity. Because of their anti-microbial properties, these nanoparticles are potential candidates for the development of new drugs against infectious diseases, such as *Leishmania*, in the future.

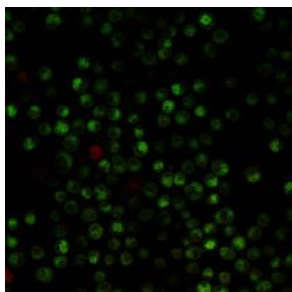


Figure 1: Macrophage-like cells infected with bacteria

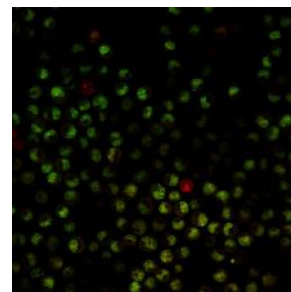


Figure 2: *S. aureus* infected cells exposed to ZnO nanoparticles

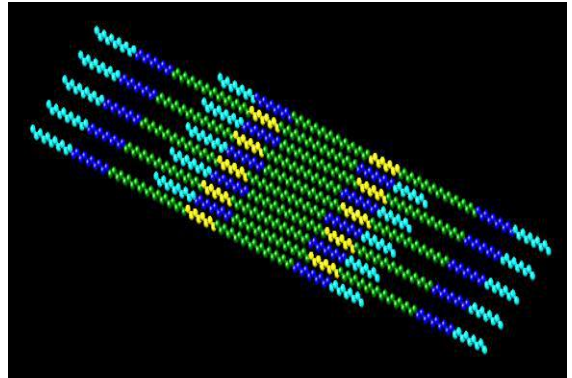
<sup>1</sup>Allahverdiyev, Adil M., Rabia C. Koc, Sezen C. Ates, Malahat Bagirova, Serhat Elcicek, and Olga N. Oztel. "Leishmania Tropica: The Effect of Darkness and Light on Biological Activities in Vitro." Elsevier (2011).

<sup>2</sup>Allahverdiyev, Adil M., Emrah S. Abamor, Malahat Bagirova, and Miriam Rafailovich. "Antimicrobial Effects of TiO<sub>2</sub> and Ag<sub>2</sub>O Nanoparticles against Drug-resistant Bacteria and Leishmania Parasites." Future Microbiology (2011). (in press)

<sup>3</sup>Lee, Wilson A., Nadine Pernodet, Bingquan Li, Chien H. Lin, Eli Hatchwell, and Miriam H. Rafailovich. "Multicomponent Polymer Coating to Block Photocatalytic Activity of TiO<sub>2</sub> Nanoparticles." ChemComm (2007): 4815-817.

# Sensing Biomolecules on Surfaces

## SESSION 3



**Chair: Alan Czemerinski**

**Graduate Student Mentors: Yingjie Yu,  
Suphannee Pongkitwitoon**

## Developing a Biosensor Utilizing Self-Assembled Monolayers to Detect Bacteria

**Zohaib Shaikh**, The Wheatley School, Old Westbury, NY

**Kathy Benhamou**, Yeshiva University High School for Girls, Holliswood, NY

**Mohit Batra**, Valley Stream North High School, Franklin Square, NY

**Nikhil Mehandru**, Harvard University; **Alan Czemerinski**, Columbia University

**Yingjie Yu**, Department of Materials Science & Engineering, Stony Brook University

**Miriam Rafailovich**, Department of Materials Science & Engineering, Stony Brook University

Considering the ubiquity of certain bacterial infections, and especially the emergence of antibiotic-resistant strains, the development of an efficient and inexpensive method of early detection is imperative. The aim of this experiment is to engineer a potentiometric biosensor utilizing molecular imprinting (MI) that would fulfill this goal.

Molecular imprinting has been successfully used for the detection of a wide range of substances. Self-assembled monolayers (SAM) have proven efficient in the detection of small molecules, especially proteins.<sup>1</sup> However, limited research has been done to apply this technique to imprint larger molecules, let alone entire organisms.<sup>2</sup>

In this experiment, we construct biosensors capable of detecting *Staphylococcus aureus* and *Bacillus cereus*. We introduce a gold-plated silicon wafer into a blend solution consisting of thiol (11-mercapto-1-undecanol), dimethyl sulfoxide, Dulbecco's phosphate buffered saline (DPBS), and the bacteria, which acts as the template molecule. Over the two hour incubation period, the bacteria become imprinted in a SAM matrix as the thiol molecules bind to the gold. After incubation, the wafer is rinsed with de-ionized water, which is hypothesized to cause the bacterial cells to be washed off and leave cavities complimentary in size and shape.

The imprinted chip is then connected to the potentiometer and submerged in a beaker filled with 10 mL DPBS. Bacteria from the stock solution were re-introduced into the system, and as cells fell into their complimentary cavities, a jump in potential was observed, indicating successful detection (Fig. 1).

Future work includes optimizing the sensor by manipulating the concentration of bacteria and thiol used and by utilizing nanopatterning to form more favorable cavities to imprint the cells. Atomic Force Microscopy will also be used to image the imprinted monolayer in comparison to an unimprinted monolayer.

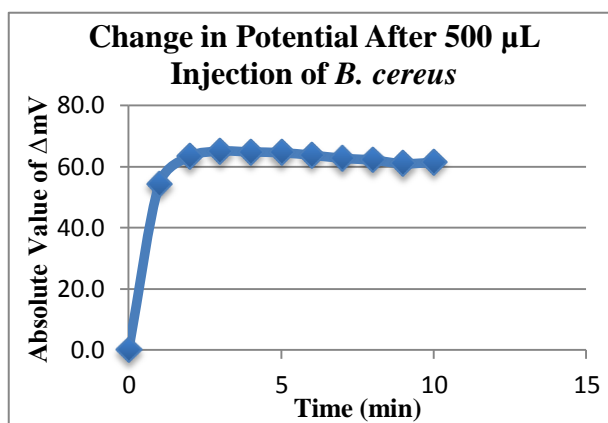


Figure 1. 500  $\mu\text{L}$  bacteria injected at 0 minutes

<sup>1</sup>Wang, Y., Zhou, Y., Sokolov, J., Rigas, B., Levon, K., and Rafailovich, M. "A Potentiometric Protein Sensor Built with Surface Molecular Imprinting Method." *Biosensors & Bioelectronics* 24 (2008): 162-66.

<sup>2</sup>Wang, Y., et al. "Potentiometric Sensors Based on Surface Molecular Imprinting: Detection of Cancer Biomarkers and Viruses." *Sensors and Actuators B: Chemical* 146 (2010): 381-87.

# Towards the Expansion of Biosensor Applications and Characterization of Thiol-based Self-Assembled Monolayers

Tom Wang<sup>1</sup>, David Nam<sup>2</sup>, Alina Ranjbaran<sup>3</sup>

Nikhil Mehandru<sup>4</sup>, Alan Czemerinski<sup>5</sup>, Yingjie Yu<sup>6</sup>, Dr. Miriam Rafailovich<sup>6</sup>

<sup>1</sup>The Wheatley School, Old Westbury, NY, <sup>2</sup>Monta Vista High School, Cupertino, CA

<sup>3</sup>Garden City High School, Garden City, NY, <sup>4</sup>Harvard University, Cambridge, MA

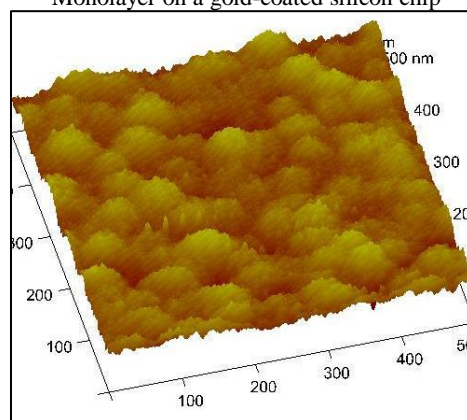
<sup>5</sup>Columbia University, New York, NY, <sup>6</sup>Stony Brook University, Stony Brook, NY

In the area of medicinal and biomedical devices, one of the key aims of ongoing research is the low-cost and efficient diagnosis of diseases. One way to detect such clinical conditions quickly is the biosensor. Potentiometric biosensors are devices that integrate a biological detection element with a transducer that emits an electrical signal. The magnitude of this electrical signal is related to the amount of a substance in a sample and thus can determine the concentration of that analyte.<sup>1</sup>

In an attempt to expand applications of biosensor detection, we sought to imprint a molecule called Lipophosphoglycan (LPG), a glycoconjugate on the surface of the protozoan parasite *Leishmania donovani*.<sup>2</sup> The genus *Leishmania* is comprised of pathogens that cause Leishmaniasis, a “neglected” disease that poses a serious problem to countries with tropical climates.<sup>3</sup> Previous research involving SAM biosensors has been limited only to various proteins and protein capsids, with limited applications towards detection of glycoconjugate molecules.

To detect the LPG, incremental injections of LPG

Figure 1: AFM Scan of a Thiol Monolayer on a gold-coated silicon chip



detection solution were inserted into a beaker

containing a reference electrode and the wafer imprinted with LPG. The readings from a potentiometer were subsequently used to determine the relationship between LPG concentration and the voltage output. Next, to characterize the thiol monolayer, atomic force microscopy (AFM) scans were taken of gold substrates and computer simulations were run to

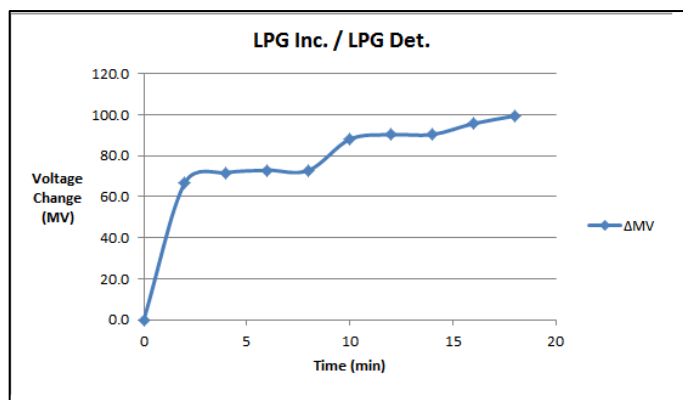


Figure 2: Voltage response of standard LPG detection test

confirm the geometric complementarity of the biosensor with hemoglobin, a reliable detection molecule.

The LPG imprints proved to successfully detect the glycoconjugate, as the voltage curve corresponded properly with examples found in literature. The subsequent AFM scans on the SAMs also showed the thiol monolayer to be relatively hilly compared with the rest of the gold-plated silicon wafer, which confirms our current theory of quasi-three-dimensional molecular imprinting. Further research is needed to confirm our biosensor’s specificity to LPG by using various control detection solutions and other similarly-structured molecules.

<sup>1</sup> Wang, Yantian et al. "A Potentiometric Protein Sensor Built with Surface Molecular Imprinting Method." *Biosensors and Bioelectronics* 24.1 (2008): 162-66. Print.

<sup>2</sup> McConville, Malcolm J et al. "Structure of the Lipophosphoglycan from *Leishmania Major*." *The Journal of Biological Chemistry* 265.32 (1990): 19611-9623. Print.

<sup>3</sup> Perinoto, Ângelo C et al. "Biosensors for Efficient Diagnosis of Leishmaniasis: Innovations in Bioanalytics for a Neglected Disease." *Analytical Chemistry* 82.3 (2010): 9763-768. Print.

## Blood Clotting on a Hydrophobic Surface

Anirudh Sailesh<sup>1</sup>, Suphanee Pongkitwitoon<sup>2</sup> and Dr. Miriam Rafailovich<sup>2</sup>

<sup>1</sup> Neuqua Valley High School, <sup>2</sup> Material Science Engineering at Stony Brook University

Wound healing has always been an important part of medical research. Even if major injuries do not occur minor cuts occur all the time. Although the body is able to naturally heal most wounds, in certain cases the pathways associated with wound healing have a difficult time forming clots. The process of blood clotting has been known for over 60 years. In this process, prothrombinase converts prothrombin into thrombin. After, thrombin transforms fibrinogen, a protein created in the liver into fibrin<sup>1</sup>. The fibrin is what holds the platelets together ensuring that the bleeding reduces and eventually stops.

In this study, fibrinogen will be converted into fibrin by forming fibers without the prothrombinase or thrombin. By controlling the surface properties, hydrophobicity is found necessary in order for the fibrinogen to connect and form fibers. In this experiment, hydrophobic surfaces of polymethyl methacrylate (PMMA – MW: 120,000) are used. PMMA dissolved in toluene will create a hydrophobic surface which will allow the fibrinogen to open up alpha C domains and form fibers by interacting with the other fibrinogen molecules. Within the body, alpha C domains form large fibers through lateral aggregations<sup>2</sup>. Different concentrations of PMMA solutions are used to study whether the thickness of the thin PMMA film can provide different amounts of the formed fiber. The PMMA solution is spin-casted onto a silicon wafer (1 cm x 1 cm) after the surface is treated with hydrofluoric acid to modify it into a hydrophobic surface. The PMMA coated wafer is then annealed (i.e. the surface is completely cross-linked) before fibrinogen (4 mg/mL) is plated on the surface. The results of this experiment show that at 20 mg/mL of a PMMA solution, fibrinogen clots the best compared with 8 mg/mL. On 20 mg/mL PMMA (which spin-casted film is ~ 2000-3000 Å thick), fibrinogen is able to form fibers that are clearly visible through optical microscopy.

In order to understand the effect of hydrophobicity, ozonization of the PMMA film compared with PMMA rheology cup and pin is studied. The PMMA cup and pin is used in the medical field in order to see how well a patient's blood can clot. If the patient is unable to clot properly, the patient will need a blood transfusion. By UV oxidation, the surface hydrophilicity directly increases with the time of ozonization. When the surface undergoes longer ozonization, the surface becomes more hydrophilic, resulting in lower contact angles. From the results, the issue with the surface ozonization becomes crucial in correctly diagnosing blood clotting deficiencies. Currently, manufacturers use UV ozonization to clean the cups and pins with no standard regulations. When the cup and pin is ozonized for 1 minute, there is a 56.51% decline in the resistance, and after 5 minutes, the resistance declined by 87.71% from the original zero minute ozonization. From the results, the time of ozonization is directly related to the resistance where the blood becomes less viscous with longer ozonizing times.

In conclusion, the PMMA with 20 mg/mL shows prominently formed fibrins on hydrophobic surfaces. For future experiments, different types of hydrophobic, biodegradable polymers should be studied to investigate which polymers provide the best surface to form fibrins. Additionally, the effect of UV oxidation should be further studied in order to standardize the UV plasma process.

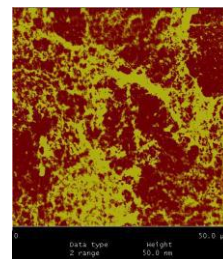


Figure 1: Fibrinogen formed fibers (lighter color) on 20mg/ml PMMA

<sup>1</sup> Seegers, Walter H. "Multiple Protein Interactions as Exhibited by the Blood-Clotting Mechanism." *The Journal of Physical and Colloid Chemistry* 51.1 (1947): 198-206. ACS Publications. American Cancer Society. Web. 8 Aug. 2011.

<sup>2</sup> Weisel, John W., and Leonid Medwed. "The Structure and Function of the Alpha C Domains of Fibrinogen." *Annals of the New York Academy of Sciences* 936.1 (2001): 312-27. Wiley Online Library. John Wiley & Sons, 25 Jan. 2006. Web. 8 Aug. 2011.

# Computational Modeling of Fibrin Polymerization and Adsorption on Hydrophobic Substrates

Carl Gao, Harvard University

Dilip Gersappe and Miriam Rafailovich, Department of Materials Science & Engineering,  
Stony Brook University

Fibrin, a fibrous protein, plays a critical role in the formation of blood clots which stem from blood loss from wounds, via the coagulation cascade of hemostasis. Abnormal fibrin behavior can lead to excessive hemorrhaging from insufficient clotting, or thrombosis in the case of unwanted clotting within undamaged blood vessels. Thus, in order to fully understand and manipulate the action of fibrin in natural biological systems, it is important to isolate and scrutinize the mechanisms by which fibrin forms its characteristic mesh networks, especially while adsorbed upon hydrophobic surfaces such as wounds and atheromatous plaques. This study aims to examine the conformation of fibrin polymers on a generic hydrophobic surface in a theoretically ideal environment.

The molecular dynamics simulator LAMMPS was used to create and compute interactions between scaled fibrin monomers. The fibrin molecules' globular domains, alpha chains, and interconnecting coils were represented by hard-core bead-spring particles interacting via Lennard-Jones potentials and FENE bonds. In lieu of directly simulating the biological process by which thrombin converts soluble fibrinogen into insoluble fibrin in clot formation, the inter-monomer attraction and hydrophobic surface were added after a certain time period, during which the fibrin monomers were allowed to equilibrate. As per experimental evidence, attractive interactions were set between D and E globules (Fig. 1), represented respectively by the blue and yellow segments in the model (Fig. 2). Running the simulation, the fibrin monomers were found to assemble into micellar clusters during equilibration, after which limited formation of an ordered network occurred.

More research will be done on characterizing the specific molecular dynamics mechanisms behind this behavior. Further work will be to quantitatively analyze and optimize the growth rate and size of the fibrin mesh network as polymerization progresses, and to correlate its adsorption tendencies with the hydrophobicity of the surface.

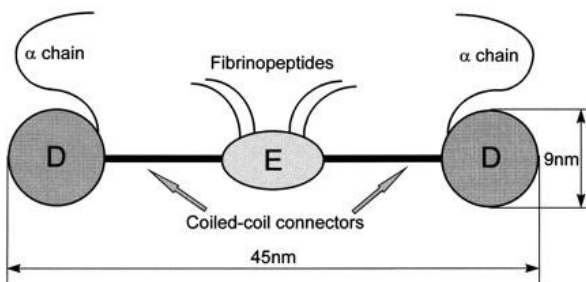


Fig. 1: Schematic model of a fibrin monomer.  
Hemmerlé (1999)

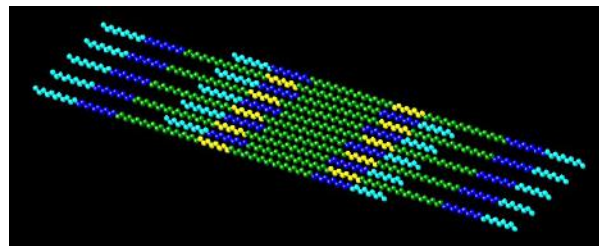


Fig. 2: Sample arrangement of fibrin in the simulation system

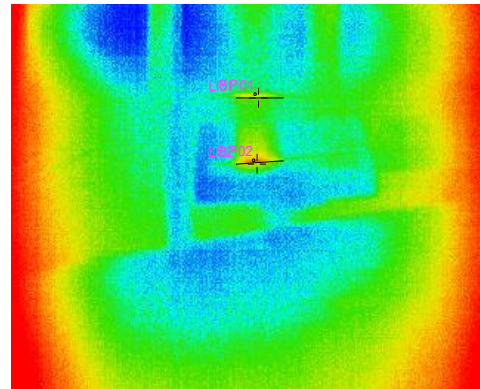
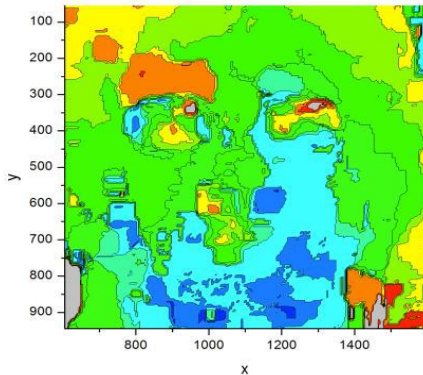
Berg, Jeremy Mark., John L. Tymoczko, and Lubert Stryer. "Fibrinogen Is Converted by Thrombin into a Fibrin Clot." *Biochemistry*. New York: W.H. Freeman, 2002. Web.

J. Hemmerlé, S. M. Altmann, M. Maaloum, J. K. H. Hörber, L. Heinrich, J.-C. Voegel, and P. Schaaf. "Direct Observation of the Anchoring Process during the Adsorption of Fibrinogen on a Solid Surface by Force-spectroscopy Mode Atomic Force Microscopy." *Proceedings of the National Academy of Sciences of the United States of America* 96.12 (1999): 6705-710. Print.

Mosesson, M. W. "Fibrinogen and Fibrin Structure and Functions." *Journal of Thrombosis and Haemostasis* 3.8 (2005): 1894-904. Print.

# Device Engineering

## SESSION 4



**Chair: Dalia Leibowitz**

***Graduate Student Mentor:***

***Divia Bhatnagar***

## Using Digital Image Speckle Correlation Photographic Analysis to Detect Response to Olfactory or Audio Stimuli

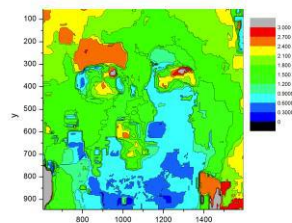
Leah Slaten<sup>1</sup>, Andrew O'neil<sup>2</sup>, Adam Ossip<sup>3</sup>, Divya Bhatnagar<sup>4</sup>, Miriam Rafailovich<sup>4</sup>

1. SAR High School, Riverdale, NY
2. South Side High School, Rockville Centre, NY
3. Brandeis University, Waltham, MA
4. SUNY Stony Brook

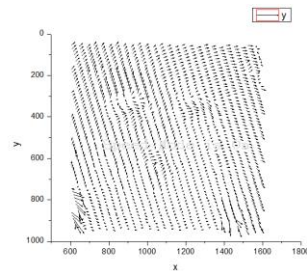
Devising a method of tracking involuntary underlying facial motion could have numerous applications in the fields of lie detection and communication with the mentally impaired. Being able to correlate involuntary facial motion and emotion could be used to devise a more accurate lie detector and understand whether autistic, Alzheimer's, and Parkinson's patients express themselves in similar ways to healthy patients. Unfortunately, current methods of detecting facial motion are inaccurate. For instance, techniques such as the Facial Action Coding System rely on the subjective testimonies of researchers and detect visible motion only. More objective methods such as video analysis are only capable of comparing live feeds to preset data, so they cannot detect abnormalities.<sup>1</sup> Furthermore, these methods cannot detect underlying muscle movement. It is therefore imperative to devise a more accurate and objective method of detecting subtle facial motion.

Digital Image Speckle Correlation has shown great promise at tracking facial motion. In this study, the facial motion of subjects while a stimulus was applied was measured by taking photographs of the subjects before, during, and after application of the stimulus. Both olfactory and auditory stimuli were used. The auditory stimulus was a set of two songs: a disturbing song and a relaxing song. The olfactory stimulus was a set of two smells: curdled milk as a bitter smell and vanilla as a pleasant smell. Using OriginPro 8, the motion of the subjects' faces was graphed in order to recognize patterns in motion for each different stimulus applied. Statistics were then extracted from the graphs to find the average motion and angle of motion of the subjects' faces.

The data revealed clear distinctions between pictures taken under control settings and pictures taken under experimental conditions. Higher levels of motion were observed during the beginning of the disturbing music than at any other stage of music, suggesting a strong initial response with gradual acclimation. Similar results were observed when the subjects were exposed to the milk and vanilla smells. For both smells, the motion of the subjects' faces rose in comparison to control pictures with no distinct smell passed before the subject. These findings suggest a possible correlation between involuntary facial motion and emotion.



Contour Map of Subject Listening to Disturbing Music



Vector Map of Subject Listening to Disturbing Music

<sup>1</sup> Essa, Irfan A., Trevor Darrell, and Alex Pentland. *Tracking Facial Motion*. Tech. no. 272. Cambridge, MA: Massachusetts Institute of Technology, 1994. Print.



## Using Digital Image Speckle Correlation to Diagnose Facial Paralysis and Track the Recovery of Facial Paralysis

Rebecca Somach- North Shore Hebrew Academy High School- Great Neck, NY

Julia Landsberg- Yeshiva University High School for Girls- Holliswood, NY

**REU:** Adam Ossip- Brandeis University

**Mentors:** Divya Bhatnagar, Dr. Aneel Kumar, Dr. Miriam Rafailovich- Stony Brook University

Monitoring the recovery of a patient after they have had surgery can help medical professionals prescribe future treatment and monitor the patient's health more effectively. As facial surgeries often cause temporary facial paralysis, it is helpful to track the motion of facial muscles after surgery. However, current methods such as MRI and CT scans can be expensive and time consuming for the patients and the doctors involved.<sup>1</sup> Digital Image Speckle Correlation, or DISC, is an emerging method in the medical field which is relatively inexpensive, and is not time consuming for the patients.<sup>2</sup> DISC is able to track the recovery of facial muscles in patients who have had facial surgeries, and it has the capability to examine current paralysis in patients using quantifiable methods.

We are tracking the recovery of a patient who underwent jaw reconstruction surgery. We are also examining the images of patients who have had acoustic neuroma. An acoustic neuroma is a benign tumor located on the facial nerve. To track the recovery of the jaw reconstruction surgery patient, we used a digital camera and took pictures of the subject while he placed his face on a headstand. In addition to the test subject, we took pictures of control subjects in the same age category as him. For the acoustic neuroma patients, we were provided with images taken by medical professionals. After acquiring the pictures, we used the DISC software to analyze the pictures. After analyzing the pictures, we ran the data through a graphing program called OriginPro 8. Using the graphing program, we were able to create contour maps of the faces. By analyzing the data, we were able to track the recovery of the patients who have had surgery and compare them to control subjects.

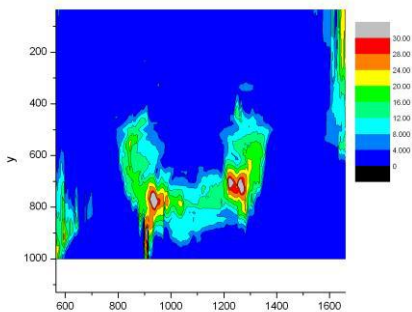


Figure 1 : Control Subject

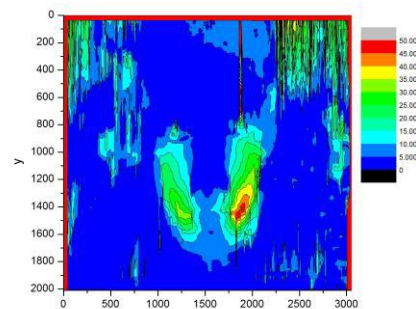


Figure 2: Test Subject

Through examination of the contour maps and images, we can determine whether a person's face has asymmetry using the DISC and graphing software. In our jaw reconstruction patient, the graphs show that the muscles on the swollen side of the patient's face did not move as much as the muscles on the other side of the face. Over time, the asymmetry seemed to lessen on the graphs. Currently, we are examining the numerical and statistical data from the graphs of the jaw reconstruction patient. We also are continuing our study of patients who have had acoustic neuroma and are examining that data graphically and statistically.

<sup>1</sup> Farrugia, M. E., G. M. Bydder, J. M. Francis, M. D. Robson. "Magnetic resonance imaging of facial muscles." *Clinical Radiology*. 62.11 (November 2007): 1078-1086. Database. Web. August 8, 2011. <<http://www.sciencedirect.com/science/article/pii/S000992600700205X>>

<sup>2</sup> Staloff, Isabelle Afriat, E. Guan, Steven Katz, Miriam Rafailovich, Aryeh Sokolov, Sara Sokolov. "An *in vivo* study of the mechanical properties of facial skin and influence of aging using digital image speckle correlation." *Skin Research and Technology*. 14.2 (May 2008): 127-134. Database. Web. August 8, 2011. <<http://onlinelibrary.wiley.com/doi/10.1111/j.1600-0846.2007.00266.x/full>>

## The Modification of a Bowing Machine to Analyze the Effects of Different Types of Rosin on the Temperature of a Violin's Strings and the Sound Produced

**Jonathan Zolty:** Yeshiva University High School for Boys, New York

**Dalia Leibowitz:** Massachusetts Institute of Technology, Cambridge, MA

**Miriam Rafailovich, John Jerome, and Michael Gouzman:** Stony Brook University, Stony Brook, NY

A bowing machine is a mechanical apparatus which simulates the playing of a violin in a controlled setting. This machine allows the researcher to test and analyze the violin and the sound it produces in controlled and repeatable conditions<sup>1</sup>. Because of the repeatability the mechanism allows for, the machine can be used to test various parameters of the violin. These analyses would help violin makers and violinists better understand their instruments<sup>2</sup>.

An old bowing machine was used for the experiment, but it first had to be redesigned to fit the project's specifications. Several pieces from the previous model were modified to add strength and stability to the bowing apparatus. A pressure system to control the vertical force on the bow was then designed. For this structure, a bridge was created to ensure that the pressure was placed directly above the point of contact between the bow and the string. Next, a counterweight was added to make the system more accurate and precise. Figure 1 depicts the pressure system. A video camera with a microphone was placed near the violin strings to analyze the sound produced and the motion of the bow, and a thermal imaging infrared camera was positioned to examine the temperature of the strings throughout the experiment. See Figure 2 for an image of the bowing machine.



Figure 1: The pressure system used to accurately measure the vertical force of the bow on the string.

Subsequently, bows with different types of rosin will be analyzed for frequency, amplitude, and temperature<sup>3</sup>. A graph comparing frequency and temperature will be generated, which can be used to assist rosin manufacturers in creating products.

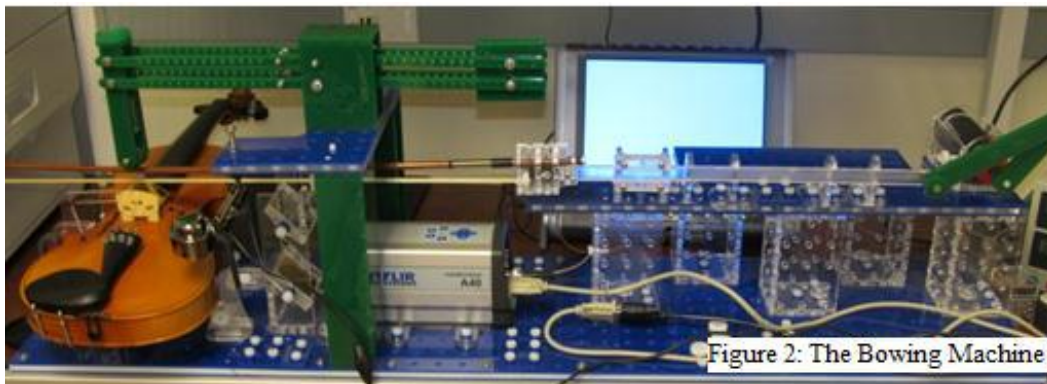


Figure 2: The Bowing Machine

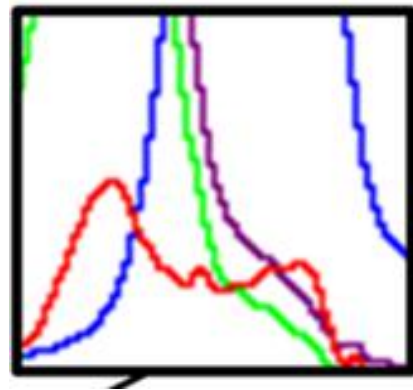
<sup>1</sup> Cronhjort, A. "A computer-controlled bowing machine (MUMS)." *STL-QPSR* 33.2-3 (1992): 061-066. <http://www.speech.kth.se>. Web. 12 July 2011.

<sup>2</sup> Pickering, Norman. "What researchers in acoustics can do to help the violin maker." *The Journal of the Violin Society of America* 6.2 (1980): 117-33. Print.

<sup>3</sup> Pickering, Norman. "A Study of Bow Hair and Rosin." *The Journal of the Violin Society of America* 7.1 (1984): 46-72. Print.

# Nanocomposites

## SESSION 5



**Chair: Neil Muir**

**Graduate student mentors: Harry Shan  
He, Kai Yang, Liudi Zhang**

## Creating a Non-Flammable and Strong Material for Insulating Electrical Cable: Using Ethylene-Vinyl Acetate (EVA) with Flame Retardant Additives

**Shoshana Javitt**, Bruriah High School, Elizabeth, NJ

**Neil Muir**, Cooper Union, NY

**Kai Yang, Harry He, and Dr. Miriam Rafailovich**,

Department of Material Science and Engineering Stony Brook University

Acknowledgment: **Dr. Shradha Sambasivan**

EVA is used to coat electrical cables because of its good tensile properties and elasticity. However, it does not have good flame retardant properties. Therefore, the research objective was to create a non-flammable polymer mixture of EVA with additives which would comply with American Standards for Testing Materials (ASTM).

The additives used were Melamine/ Cloisite 20A clay (wt% 10/10 and 15/10) and Melamine/Cloisite 20A/ATH (wt% 10/10/10). Pure EVA was also tested as a control. These mixtures were mixed in a brabender at Amco Plastics, and a heat press was used to mold the samples into the forms needed for each test. The samples were tested for flammability, tensile strength, impact toughness, bulk modulus, and thermal degradation. Fourier Transform Infrared microscopy (FT-IR) was also performed on all the materials and mixtures used.

The samples were tested for flammability by using the UL94 Vertical Flame Test. A blow torch was used to light the specimen for 10 seconds; then the blow torch was removed and the burning time was measured. A piece of cotton is also placed under the sample to measure how easily the flame spread. When the pure EVA sample was tested it burned for over 30 seconds, the specimen dripped, and the cotton caught on fire; therefore, according to the ASTM, it failed the requirements for flame retardancy. When the other samples were tested, none of them dripped and the cotton did not catch on fire; however, they all burned for over 30 seconds and therefore they also failed. After the test, it was observed that the samples with additives had formed a char on the outside which is believed to prevent the samples from dripping. It was also observed that samples with ATH burned faster than the other samples. These observations show that even though the samples made thus far are not flame retardant, the additives, without ATH, show potential for creating a flame retardant polymer.

The mechanical properties of blends are promising as well. The tensile test indicates that tensile strength (Figure 1) and impact toughness (Figure 2) for EVA does decrease as more flame retardant is added to the polymeric mixture, but not greatly. From the DMA (Dynamic Mechanical Analysis) it was determined that there was no significant change in bulk modulus between pure EVA and its blends. The Thermal gravimetric analysis, (TGA) which measures mass loss as a function of temperature, reveals that the additives cause the mixture to begin degradation at a lower temperature but the pure EVA degrades faster.

Future work will include testing melamine and Cloisite 20A clay mixed with EVA in different concentrations. Testing melamine and Cloisite 20A individually will also be helpful in determining if one of them has better flame retardant properties or if both of the materials are needed together to create the flame retardant properties. SEM and TEM can also be performed on the char created during the flame tests.

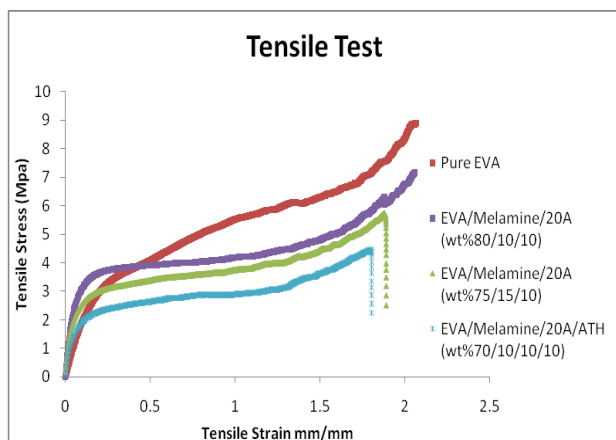


**Figure 1.** Tensile Strain vs. Stress

Samples	Average Impact	
	Toughness	Standard Deviation
Pure EVA	5.22	6.04
EVA/Melamine/Cloisite 20A (wt% 80/10/10)	4.37	5.05
EVA/Melamine/Cloisite 20A (wt% 75/15/10)	3.73	4.31
EVA/Melamine/Cloisite 20A/ATH (wt% 70/10/10/10)	2.61	3.59
EVA/Melamine (wt% 70/30)	5.22	5.38

**Figure 2.** Impact Toughness

## Flame Retardant Biodegradable Polymers: Blending polylactic acid (PLA) and Ecoflex (PBAT) with various additives to improve thermal, mechanical, and degradation properties

**Rachel Davis**, Smithtown High School East, Smithtown, NY

**Caroline Juang**, Manhasset High School, Manhasset, NY

**Neil Muir**, The Cooper Union, New York, NY

**Harry Shan He**, Stony Brook University, NY

**Kai Yang**, Stony Brook University, NY

**Sharada Sambasivan**, Suffolk Community College, NY

**Miriam Rafailovich**, Department of Materials Science & Engineering, Stony Brook University, NY

For many years, flame retardancy has been a topic of much interest in the field of materials science research. Recently, many studies have been exploring biodegradable flame retardant polymers for uses in industrial packaging, ultimately reducing damage to the environment<sup>1</sup>. Polylactic Acid (PLA) and Ecoflex (PBAT) are biodegradable polymers that have complimentary characteristics when combined<sup>2,3</sup>. However, PLA/Ecoflex blends tend to meet minimal industry standards for flame retardancy. Thus, flame retardant additives must be blended with the polymer in order to exceed the minimal flame retardant requirements of the American Standards for Testing Materials.

After PLA and Ecoflex were blended together in a 1:4 ratio, it was found that the control blend with no additives meet the standards of flame retardant test UL 94 V-2, where V-2 is the minimal industry standard for flame retardants and V-0 is the highest level of flame retardants. In order to achieve a UL 94 V-0, experimental polymer blends were created with various concentrations of Starch Melojel, resorcinol bis-diphenylphosphate (RDP), and RDP Starch (with 40% RDP). All but the 10% Starch blends were found to be V-0; the starch maintained a V-2 rating like the control, showing that flame retardancy is not inhibited by starch. Results also revealed that the control PLA/Ecoflex blend had a lower thermal stability than the pure Ecoflex, and mostly follows the degradation curve of the pure PLA. However, as Figure 1 shows, the control blend began to degrade at a slower rate than the pure PLA, showing the slight effect of the Ecoflex in the blend. These results are consistent with the Fourier Transform Infrared Spectroscopy (FT-IR) results, where the control curve almost matched perfectly with the pure PLA curve, but the peaks of the control blend were slightly broadened compared to the PLA spectra. When starch was added to the PLA/Ecoflex blend, the absorbance of Ecoflex peaks increased, as shown in Figure 2, suggesting that Starch causes phase separation between the PLA and Ecoflex in the blend. Despite this, the addition of starch increased the Young's Modulus in tensile tests and the Shear Modulus in dynamic mechanical analysis.

Future research will include adding different concentrations of starch, RDP, and RDP soaked Diatomite to the PLA/Ecoflex blend in order to improve flame retardant, mechanical, and degradation properties.

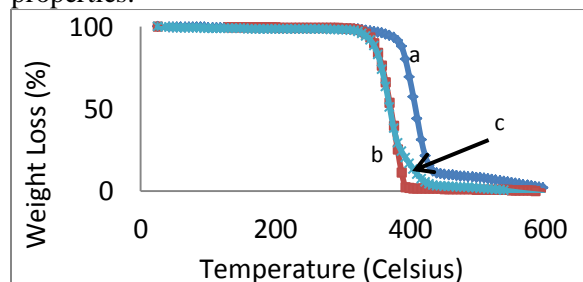


Figure 1 Shows the thermal degradation of a) Pure Ecoflex b) Pure PLA c) PLA/Ecoflex (80/20 wt%)

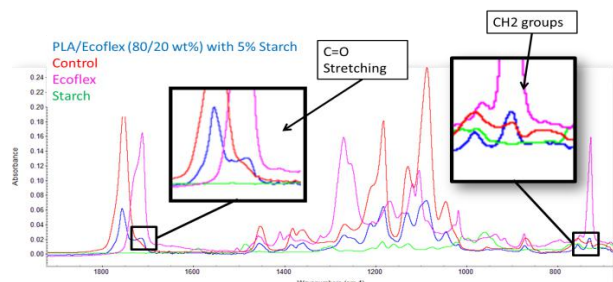


Figure 2: FT-IR spectra of the PLA/Ecoflex blend with 5% starch added

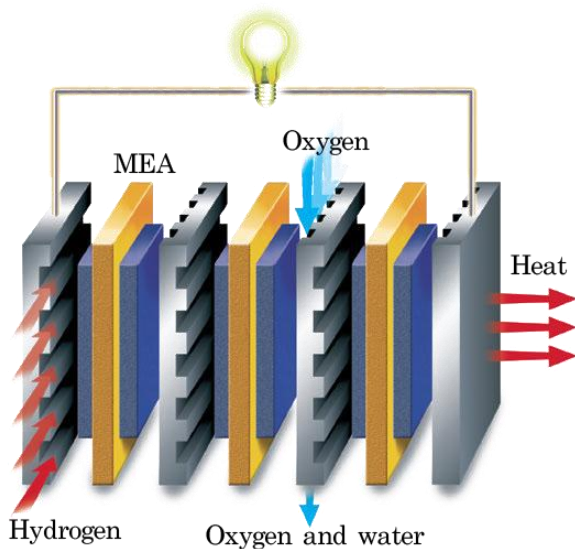
<sup>1</sup>Kumar, M.; Mohanty, S.; Nayak, S. K.; and Parvaiz, M. R. "Effect of glycidyl methacrylate (GMA) on the thermal, mechanical and morphological property of biodegradable PLA/PBAT blend and its nanocomposites." *Bioresource Technology* 101 (2010): 8406-8415.

<sup>2</sup>Pillin, I.; Montrelay, N.; and Grohens, Y. "Thermo-mechanical characterization of plasticized PLA: Is the miscibility the only significant factor?" *Polymer* 47 (2006): 4676-4682.

<sup>3</sup>Signori, F.; Coltelli, M. B.; and Beronco, S. "Thermal degradation of poly(lactic acid) (PLA) and poly(butylene adipate-co-terephthalate) (PBAT) and their blends upon melt processing." *Polymer Degradation and Stability* 94 (2009): 74-82.

# Renewable Energy Sources

## SESSION 6



**Chairs: Sherri-Ann Francis, Karan Sikka**

**Graduate student advisors: Cheng Pan,  
Yingjie Yu**

# Using Gold and Palladium Alloy Nanoparticle Co-catalysts as a Novel Means to Improve the Power Output Efficiency and Lower the Cost of Hydrogen Fuel Cells

Victoria Petrova, South Torrance High School  
Ilana Teicher, Ma'ayanot Yeshiva High School for Girls  
Karan Sikka, Carnegie Mellon University

Cheng Pan and Dr. Miriam Rafailovich, Department of Materials Science & Engineering, Stony Brook University

As the world's limited supply of fossil fuels continues to decrease, other alternative energy sources are being looked into as substitutes. Hydrogen gas has been proposed as a viable option, as it is the most abundant element on Earth, and has zero carbon emissions<sup>1</sup>. Currently, however, hydrogen fuel cells are impractical, as the essential platinum electrodes are extraordinarily expensive.

We wanted to make Proton Exchange Membrane (PEM) hydrogen fuel cells more practical by increasing their efficiency, thereby lowering the cost per watt. It has been proven that adding gold or palladium nanoparticles as co-catalysts to the platinum increases power output<sup>2</sup>, so we hypothesized that adding an alloy of gold and palladium nanoparticles to the membrane will further increase the power output of the cell.

We synthesized nanoparticles of gold, palladium, a physical mixture of gold and palladium, and an alloy of the two metals to place on the membrane and compare the results. We created them using the Brust two-phase method which uses sodium borohydride to reduce the metal salts<sup>3</sup>. As the nanoparticles were formed, thiol groups were added to the solution to act as capping agents, stopping the aggregation of the particles.

We then dissolved the nanoparticles in toluene as preparation for the coating of Nafion membranes. 200  $\mu$ L of the nanoparticle solutions were each dispersed over the water, and the barriers were compressed to spread a monolayer onto Nafion membranes at a surface pressure of three mN/m, which was determined to be optimal for the coating by an isotherm graph. We tested the membranes in an h-tec fuel cell and recorded the voltage and current as we varied the resistance. Based on the power output, we verified that the alloy produced the highest results (Table 1). In addition, a graduate student performed a TEM scan to confirm that our nanoparticles were indeed alloys and found that the average size of them was approximately 2.1 nm (Figure 1).

Next, we decided to further optimize the alloy membrane by finding the ideal Langmuir Blodgett surface pressure for coating the membranes. Therefore, we made membranes with the alloy nanoparticles at pressures of 2, 3 and 4 mN/m with the LB -trough, and tested them in the fuel cell. Although the membranes all produced extremely similar results, the one synthesized at 3 mN/m had a slightly higher efficiency.

Our last goal is to understand the catalytic reaction that the alloy nanoparticles are inducing to yield such a high power output increase. Consequently, we tested the membranes with both compressed air and pure oxygen, and saw that oxygen had a much greater power output, thereby proving that oxygen is part of the reaction. In the future, we plan on doing a cyclic voltammetry test to further understand the alloy's catalytic capabilities.

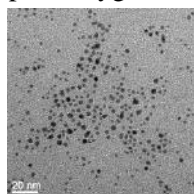


Figure 1: TEM image of AuPd nanoparticles

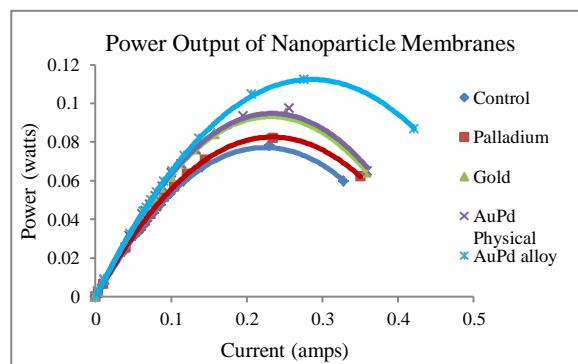


Table 1: Graph of nanoparticle membranes

<sup>1</sup> Mazumder, V., Lee, Y., & Sun, S. (2010). Recent Development of Active Nanoparticle Catalysts. *Advanced Functional Materials*, 1224–1231.

<sup>2</sup> Thomas, S., & Zalowitz, M. (2006). *Fuel Cells: Green Power*. Los Alamos National Laboratory.

<sup>3</sup> Brust, M., Walker, M., Bethell, D., Schiffrin, D. J., & Whyman, R. (1994). Synthesis of Thiol-derivatised Gold Nanoparticles in a Two-phase Liquid-Liquid. *J. Chem. Soc.*, 801-802.

# The Effect of Gold-Dodecanethiolate Core-Shell Nanoparticles on a Hydrogen PEM Fuel Cell Stack

Sean Ballinger<sup>1</sup>, Cheng Pan<sup>2</sup>, Karan Sikka<sup>3</sup>

<sup>1</sup>Phillips Academy, Andover, MA

<sup>2</sup>Department of Materials Science and Engineering, Stony Brook University, NY

<sup>3</sup>Carnegie Mellon University, Pittsburgh, PA

## Background

As the world's supply of fossil fuels declines, alternative fuels are starting to attract widespread interest. One such fuel is hydrogen, which would enable proton exchange membrane fuel cells (PEMFCs) to power the transportation vehicles of the future. PEMFCs host an oxidation-reduction reaction between hydrogen and oxygen that produces electricity, heat, and water. The reaction  $\text{H}_2 \rightarrow 2\text{H}^+ + 2\text{e}^-$  takes place at the Anode, and the Cathode contains the reaction  $\text{O}_2 + 4\text{H}^+ + 4\text{e}^- \rightarrow 2\text{H}_2\text{O}$ . In a compact fuel cell, the reactions at the Anode and Cathode occur in an electrode-catalyst material that also increases the reaction rate and provides a diffusion layer for the gases involved.

PEMFCs were found to operate with increased efficiency when using a Nafion membrane coated with a monolayer of gold nanoparticles.<sup>1</sup>

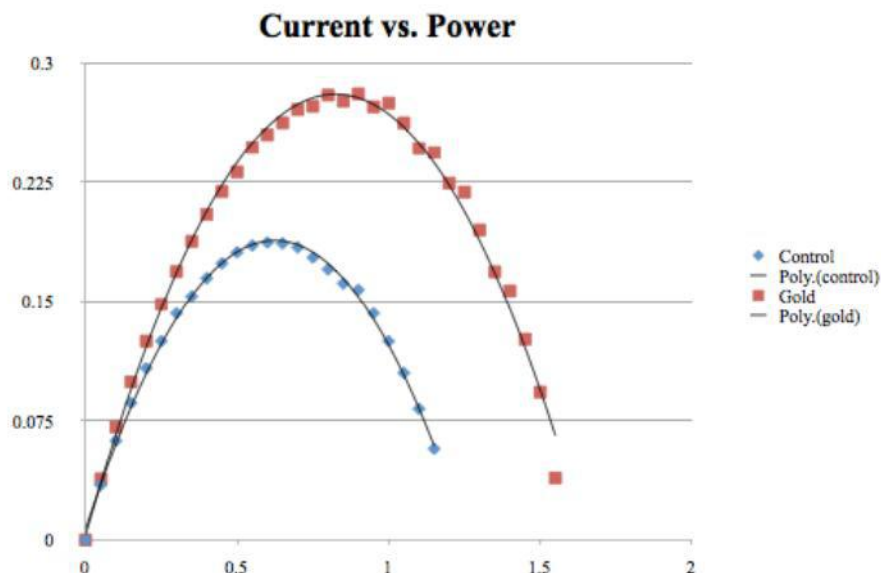
## Procedure

In this experiment, 3 Nafion membranes were coated with a monolayer of gold nanoparticles using a Langmuir-Blodgett trough. Electrode-catalyst layers were created by treating carbon paper on one side with a solution of liquid Nafion containing platinum. MEAs were created by heat-pressing each Nafion membrane in between two electrode-catalyst layers.

A PEMFC stack containing five gold nanoparticle-coated Nafion MEAs was then tested to observe whether the efficiency increase would be further enhanced by the greater current density involved in a fuel cell stack. The results will help determine whether using gold nanoparticles would significantly improve current commercial fuel cell stacks being considered for widespread use in automobiles and other vehicles.

## Results and Future Work

The comparison of the output of a single MEA coated with gold nanoparticles to an MEA without nanoparticles showed a significant boost in performance. This data supports the hypothesis that gold nanoparticles will prove very beneficial to a stack's performance.



<sup>1</sup> Cheng Pan, Kenny Kao, Sisi Qin, Miriam Rafailovich, *Gold Nanoparticle Enhancement for Polymer Electrolyte Membrane Fuel Cell (PEMFC)*.



# Investigating Au/Pd Catalyst Mechanisms via PEM Fuel Cell Power Output Enhancements

**Hansen Qian:** Saratoga High School, Saratoga, CA

**Daniel Jang:** Thomas Jefferson High School for Science and Technology, Alexandria, VA

**Matthew Rudin:** Half Hollow Hills High School West, Dix Hills, NY

**Cheng Pan and Miriam Rafailovich:** SUNY Stony Brook

**Karan Sikka:** Carnegie Mellon University

With world oil supplies set to expire in a matter of decades, developing alternatives to the petroleum-based internal combustion engine has become a crucial endeavor in the field of clean energy. The polymer electrolyte membrane (PEM) hydrogen fuel cell is promising to be a viable substitute; its design serves not only to achieve high energy conversion efficiencies (60-80%), but also to protect the ambient environment.

Despite these qualities, the PEM fuel cell remains far from practical use. The simultaneous oxidation of H<sub>2</sub> gas at the anode and reduction of O<sub>2</sub> gas at the cathode necessitate the use of expensive platinum catalysts that lead to high fuel cell costs. We hereby investigate various permutations of Au and Pd nanoparticles (NPs) and their effects on power output.

Previous research shows that the placement of an AuNP monolayer of platelets onto the membrane significantly enhances power output<sup>1</sup>. Although it is believed that the platelet structure of the AuNPs is responsible for the improvement, the full extent of this conjecture has not been determined. To affirm, we tested the following arrangements of NPs: platelets on the membrane, spheres on the membrane, and spheres inside the membrane. Furthermore, we examined the following combinations of nanoparticles: AuNPs, PdNPs, a physical mixture of both, and an alloy of both.

Nanoparticles were synthesized via the two-phase Brust method, producing spherical particles (~2-5 nm) covered in dodecanethiol chains<sup>2</sup>. As air-water interface in the LB trough used to create monolayers on the membrane creates platelets, we placed spherical nanoparticles into the membrane via recasting to compare how the differently structured affect catalysis.

Preliminary results show that the spherical nanoparticles within the membrane perform worse than a control Nafion membrane, confirming that the platelet form is required for catalysis.



**Figure 1:** Gold nanoparticles with attached thiol chains.

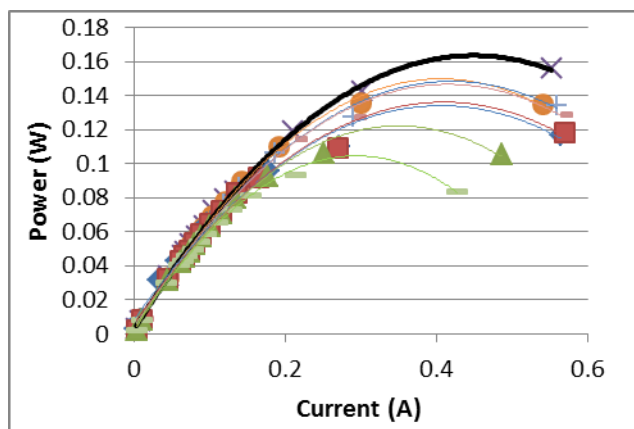


**Figure 2:** Results of nanoparticles embedded within the membrane. Bolded Line shows Control Membrane. All other tests show a lower performance than the control.

Separately, gold nanoparticles were electrospun in a solution of Nafion to create mats of nanofibers, providing AuNP with a higher surface area with which to catalyze the reaction. We hypothesize that the higher surface area may lead to great power.

Future work includes testing the membranes at higher temperatures and humidity, analyzing the effect the nanoparticles have on the Nafion membrane, and testing spherical nanoparticles placed on top of the membrane.

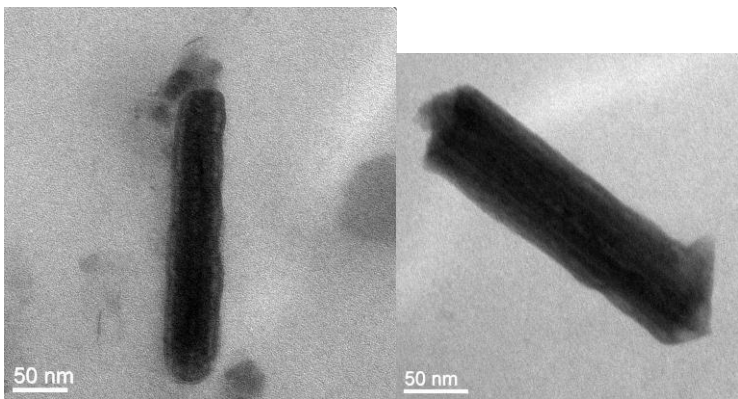
<sup>1</sup>Kao, Chun-Kai. *Nanoparticle Enhancement of Fuel Cell Power Output*. N.p., n.d. Web. 8 Aug. 2011.

<sup>2</sup>Brust, Mathias, et al. "Synthesis of Thiol-derivatised Gold Nanoparticles in a Two-phase Liquid-Liquid System." *Journal of the Chemical Society, Chemical Communications* (1994): 801-802. RSCPublishing. Web. 9 Aug. 2011. <<http://pubs.rsc.org/en/Content/ArticleLanding/1994/C3/C39940000801>>.

## **The effect of Au-Nanorods on the power output of PEM Hydrogen Fuel Cells**

Daniel Moskowitz, Sherri-Ann Francis, Suffolk Community College NY, and Karan Sikka, Carnegie Mellon, PA

In a time where traditional energy resources are running low, good alternative energy resources are very important. Hydrogen fuel cells are one of the many possible alternative energy sources. As there are attempts to use fuel cells on larger, more powerful items such as cars, the need for higher efficiency fuel cells increases. Previous research has shown that the addition of gold nanoparticles to a fuel cell assists in the reaction by acting as a catalyst, speeding up the rate of reaction at room temperature, thus increasing the power output. As shape has an effect on the ability of an object to react, the effect of the shape of the nanoparticles was tested. Nanorods have a shape with a higher surface area; therefore, Gold nanorods were synthesized by a mixture of seed solution and ascorbic acid with CTAB. The resulting nanorods (figured below) were about 150 nm and 50 nm in diameter as determined by TEM imaging.



Gold nanorods with ascorbic acid and CTAB (TEM at Brookhaven lab)

Since the ratio between the seed solution and ascorbic acid affects the size of the particles, numerous size nanorods will be synthesized by varying the ratio. The various size nanorods will be painted onto a membrane and tested for their power performance in fuel cells. Gold-Platinum nanoalloys will be synthesized and tested on the membrane of the fuel cell to test the alloy's catalytic abilities in hopes of increasing the power output as compared to a control membrane and a gold nanoparticles coated membrane.

Nanoscale Morphology of the Self-Assembled Ordered Bulk Heterojunction in the PS:P3HT:PCBM Active Layer of Polymer:Fullerene Photovoltaic Cells

Eric Metodiev<sup>1</sup>

Cheng Pan<sup>2</sup>, Hongfei Li<sup>2</sup>, Miriam Rafailovich<sup>2</sup>

West Islip High School<sup>1</sup>, Stony Brook University<sup>2</sup>

Polymer photovoltaic cells offer a novel and unique alternative to semiconductor-based solar cells due to their flexibility and cost-effectiveness. Polystyrene (PS) was explored as a means to order the bulk heterojunction of polymer:fullerene photovoltaic cells. With the addition of polystyrene, columnar formations of the electron-donor polymer Poly (3-Hexylthiophene) (P3HT) characterized the morphology of the surface and the interior of the thin film. It was found that the electron-acceptor nanoparticles of Phenyl-C61-butyric acid methyl ester (PCBM) nanoparticles migrated to the PS:P3HT polymer interface, forming channels in the PS. The formation of ordered electron-acceptor channels allows for the controlled structuring of the active layer of polymer:fullerene solar cells. The heterojunction active layer of conventional organic solar cells relies solely on randomly phase-separated regions of the P3HT and PCBM. This leads to many inefficiencies associated with random dispersal, such as lack of pathway to the electrode and dead zones in the active layer. The ordering of the active layer significantly reduces the dead zones and inefficiencies that plague the standard bulk heterojunction active layers and allow for the further increasing of efficiency of organic solar cells.

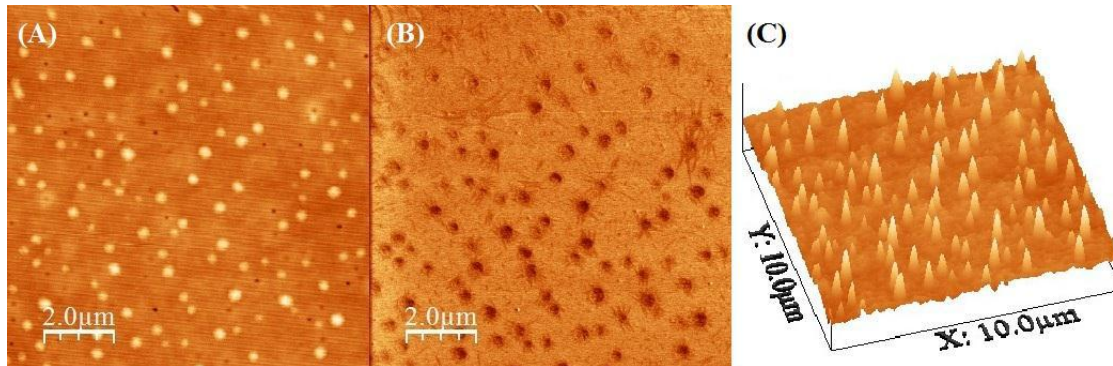


Figure 1: Atomic Force Microscope images of (A) Height and (B) Friction of the 14:1 PS:P3HT surface. In the rendering of the surface in (C), the columnar structures of P3HT can be seen more clearly.

1. Zhang, Xu, Zi Li, and Gang Lu. “*First-Principles Study of Exciton Diffusion and Dissociation in Organic Solar Cells.*” Department of Physics & Astronomy. California State University Northridge. Web. <[http://temple.birs.ca/~11w5121/Gang\\_Lu.pdf](http://temple.birs.ca/~11w5121/Gang_Lu.pdf)>.

2. Nelson, Jenny. *The Physics of Solar Cells*. London: Imperial College, 2003. Print.

# Incorporation of Graphene Oxide and Graphene into the Layers of Organic Polymer Solar Cells

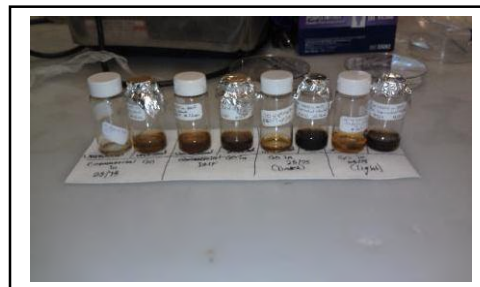
Authors: Andrew Chen, Sneha Chittabathini, and Alexandra Tse

Advisors: Nathan Akhavan, Benjamin Goldman, Rebecca Isseroff, and Cheng Pan

An organic polymer solar cell is a type of photovoltaic cell that uses conductive organic polymers or organic molecules for light absorption and charge transport.<sup>1</sup> The main disadvantages associated with organic photovoltaic cells are low efficiency, low stability and low strength compared to inorganic photovoltaic cells.<sup>2</sup> The purpose of our experiment is to incorporate both graphene and graphene oxide (GO) into the organic polymers of a solar cell, [6,6] Phenyl C-61 Butyric Acid Methyl Ester (PCBM), Poly (3-hexylthiophene-2, 5-diyl) (P3HT), and Poly(3,4-ethylenedioxythiophene) polystyrenesulfonate (PEDOT:PSS), in order to increase conductivity and thereby increase efficiency. However, the method of synthesizing graphene involves suspending it in a solution of 75:25 H<sub>2</sub>O/ETOH, resulting in the problem of blending a hydrophilic solution into a hydrophobic one. Four solar cells were created: the control; a layer of PEDOT:PSS with GO; a layer of P3HT:PCBM with graphene; and a cell with both GO and graphene in the layers above.

GO was able to be integrated into the PEDOT:PSS layer, which increased the efficiency by **52%** over the control cell; however, overall efficiency was still low. The solar cell with the graphene did not show any response to light, presumably because the graphene simply precipitated out and blocked the flow of electrons. A source of error may be the GO we used to synthesize the graphene. After analyzing the samples with FTIR spectroscopy, we found that the GO we used demonstrated only one of the several significant peaks exhibited in literature. Fig. 1 is the FTIR spectroscopy of the GO used to synthesize graphene in comparison to a sample of commercially synthesized GO. Many of the peaks that GO portrays were not exhibited in the GO we used, giving suspicion as to whether what was created was actually graphene. Fig. 2 demonstrates the exact peaks of graphene oxide, with significant peaks at 2900, 2800, 1700, 1600, and 1200. Conductivity tests were also performed, but the results are inconclusive.

In the future, it is necessary to develop a method of incorporating graphene into the active layer (P3HT:PCBM) of the solar cell, such as using a copolymer or surfactants to reduce the surface tension between the two interfaces and thereby create a blend which could then be spun cast onto a solar cell.



Vials of our graphene oxide next to their reduced graphene counterparts

<sup>1</sup> <http://user.chem.tue.nl/janssen/SolarCells/Polymer%20solar%20cells.pdf>

<sup>2</sup> <http://www.faculty.iu-bremen.de/dknipp/c300442/rd%20organic%20solar%20cells.pdf>

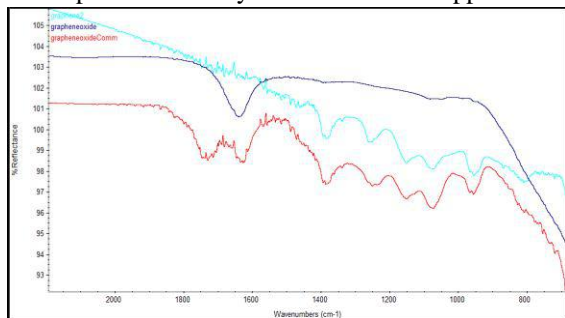


Fig. 1 FTIR of graphene oxide samples  
Dark Blue- Graphene Oxide used to synthesize Graphene  
Red- Graphene Oxide Sample  
Light Blue- Commercial Graphene Sample

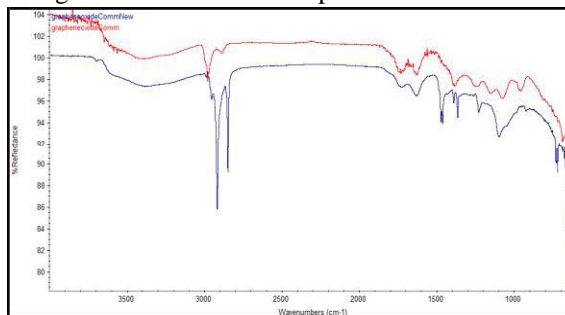
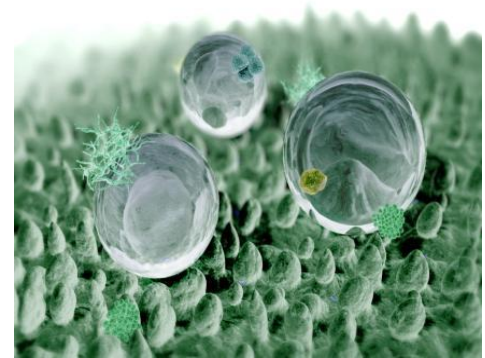
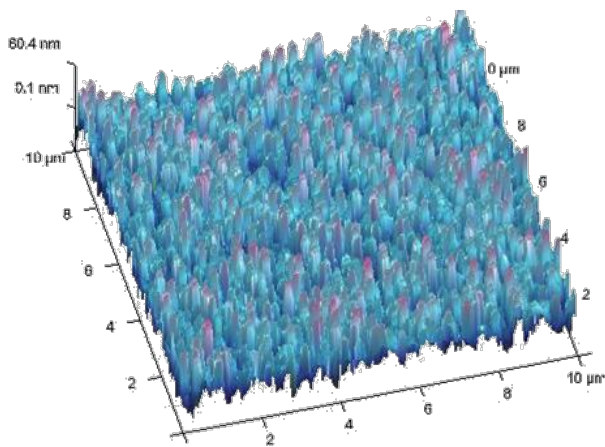


Fig. 2 FTIR of graphene oxide  
Both lines demonstrate the proper peaks of graphene oxide. However, the dark blue line demonstrates another peak at ~1200 that should be found in graphene oxide.

# Green Imprinting

## SESSION 7



**Chairs: Mariah Geritano, Debby Greenstein**

***Graduate student advisors: Giulia Suarato***

## Formation of Superhydrophobic Nanopatterned Silicon Substrates by the Sputtering of Phase-Segregated Polymer Blends

Ray Weng, Morris Hills High School, Rockaway, NJ 07856

Thomas Yurek, Munster High School, Munster, IN 46321

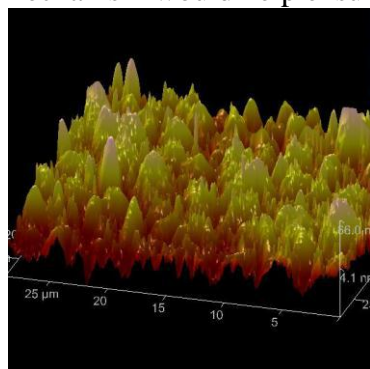
Maxwell Plaut, Massachusetts Institute of Technology, Debby Greenstein, University of Pennsylvania, Zohar Bachiry Queens College

Dr. John Jerome, Dept of Mathematics, Suffolk County Community College

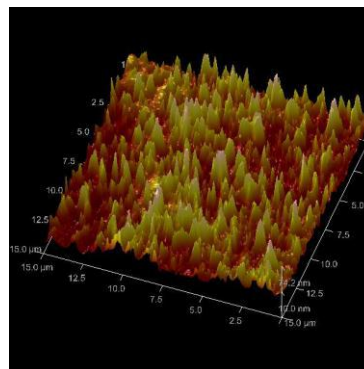
Dr. Miriam Rafailovich, Department of Materials Science and Engineering, SUNY Stony Brook

This paper investigates a method for achieving a superhydrophobic effect on silicon substrates through nanopatterning. It is desirable to give silicon more properties to increase its versatility. Superhydrophobic silicon surfaces can exhibit self-cleaning and antimicrobial properties, which would be ideal for electronics and biomedical applications<sup>1</sup>. In order to achieve superhydrophobicity, the surface energy of silicon must be lower than the surface energy of water. Since silicon oxide is naturally hydrophilic, the goal of this project was to utilize capillary forces on a hydrophobic material to expel water and increase the roughness of the surface to counteract this hydrophilicity as was shown by Suk et al<sup>2</sup>. Various common polymers - Polystyrene, Polylactic Acid, and Poly(methyl methacrylate) - were dissolved in chloroform and then spun-cast onto silicon substrates. After annealing, the polymer phase separated and self-assembled into a specific structure based on the respective interfacial tension in each blend. An Ion Mill was used to sputter the nanopattern into the silicon substrate. The remaining polymer was vaporized in a high temperature oven, leaving behind the imprinted nanopattern in the silicon. The silicon was then treated with hydrofluoric acid to make the surface of the silicon hydrophobic, which allowed the nanopatterns to function as capillary tubes that force the expulsion of water and become a superhydrophobic surface. Using the goniometer it was found that for some of the patterns the sputtered silicon had a significantly higher contact angle of the water droplet than that of untreated silicon.

A superhydrophobic silicon surface has many potential applications in the future. It can be used for improved energy conservation by manipulating the silicon's affinity between superhydrophilic and superhydrophobic. Since silicon is used in many electronics today, from LCD screens to computer chips where it is not easy to maintain its cleanliness, a self-cleaning mechanism would help ensure peak functionality.



Ideal nanopatterns contain repeating rough patterns as shown in PS:PLA 1:1 (left) and PMMA:PLA 1:1 (right). The bumps function as capillary tubes to reject water on the hydrophobic surface.



1. Li, Xue-Mei, David Reinhoudt, and Mercedes Crego-Calama. "What Do We Need for a Superhydrophobic Surface? A Review on the Recent Progress in the Preparation of Superhydrophobic Surfaces." *Chemical Society Reviews* 26 (2007): 1350-368. Web.

2. Suk, Ji Won, and Jun-Hyeong Cho. "Capillary Flow Control Using Hydrophobic Patterns." *Journal Of Micromechanics And Microengineering* 17.4 (2007): N11-15. Web.

# Assessing the Enzyme Kinetics of *Candida antarctica* lipase B to Control the Degradation of Poly- $\epsilon$ -caprolactone Surfaces

George Mo, Manhasset High School, Manhasset, NY

Jessica Lam, Scarsdale High School, Scarsdale, NY

Monika Batra, Valley Stream North High School, Valley Stream, NY

Eve Byington, West Islip High School, West Islip, NY

Mariah Geritano, Giulia Suarato, and Miriam Rafailovich, Stony Brook University, NY

Polymeric drug delivery systems have been at the forefront of pharmaceutical research. These systems must not only withstand harsh conditions found in the human body, but also release the encapsulated drugs in a controlled manner. Current researches focus on finding polymer blends suitable for sustained drug release<sup>1</sup>. A novel method to regulate the drug release is based on the enzymatic degradation of polymers<sup>2</sup>. In fact, by knowing the effect of an enzyme exposure on a certain polymer matrix, the diffusion kinetics of an embedded drug can be tailored.

*Candida antarctica* lipase B (CalB) was used to degrade polycaprolactone (PCL), a biodegradable and biocompatible polyester. This study investigated the effects of CalB on different PCL-based substrates: flat films, PCL-PEO

(polyethylene oxide) layered films, PCL-PS (polystyrene) blend films, and PCL electrospun fibers. Changes in the morphology and mechanical properties of PCL were analyzed. Atomic force microscopy images show that both crystalline and amorphous regions of PCL are greatly affected when left in CalB (10mg/ml), reaching an almost complete degradation after 1 day (Fig. 1). Similar conclusions have been obtained from the electrospun fibers analysis. Another set of experiments revealed that CalB is not active

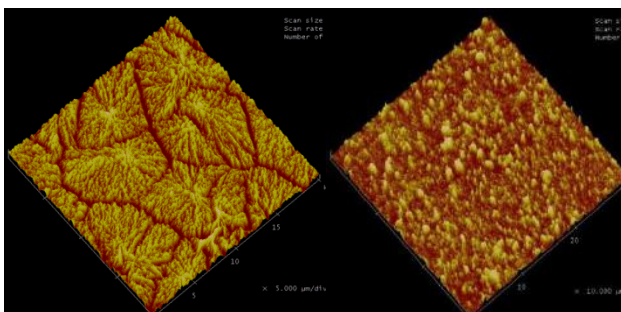


Figure 1. AFM images of semi-crystalline PCL film (Left); PCL after being soaked in CalB 10 mg/mL for 1 hour (Right)

when simply embedded in PEO and that the presence of water plays a crucial role (Fig. 2). Therefore, embedding CalB in a second polymeric system seems to constitute a method for retarding PCL degradation. From a systematic study on the polymer blends, uniformly porous films (9:1 PS-PCL) have been obtained that can be used to quantify the degradation rate. Results suggest that these CalB-PCL systems can be employed in drug delivery applications as well as nano-imprinting.

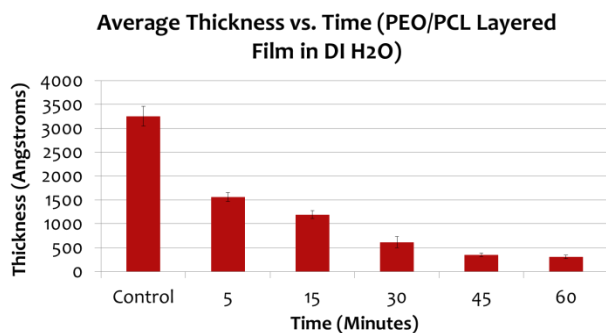


Figure 2. Effect of embedded CalB on PCL film thickness

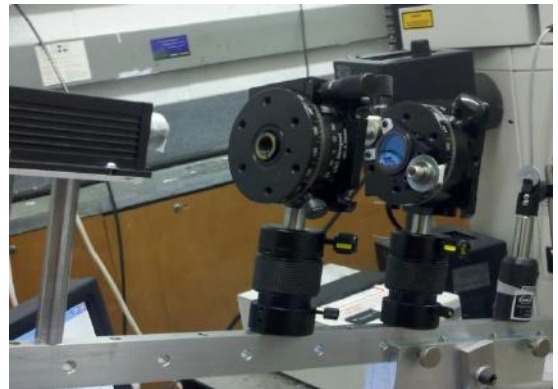
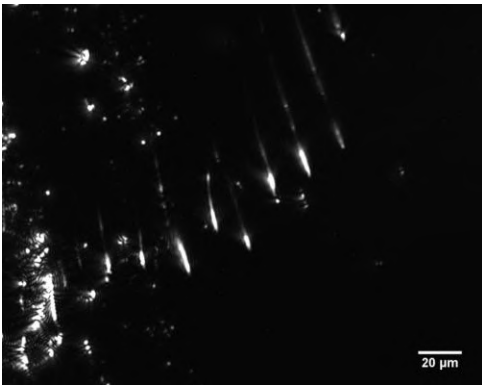
Since our main goal is to create core-shell nanofibers that would be used as a multi-drug delivery system, future experiments on drug release from PCL electrospun fibers will be conducted.

1 - Kenawy, El-Refaie, et al. "Processing of Polymer Nanofibers through Electrospinning as Drug Delivery Systems." *Materials Chemistry and Physics* 113 (2009): 296-302.

2 - Gross, Richard A., Rachna Dave, and Arthur Martin. Embedded Enzymes in Polymers to Regulate Their Degradation Rate. Patent 20090162337. 25 June 2009.

# DNA Molecules on Surfaces

## SESSION 8



**Chair: Julia Budassi**

**Graduate student advisor: Ke Zhu**



## Polarization and Angle Dependence of Fluorescence from Aligned DNA

Ashish Sridhar<sup>1</sup>, Suri Bandler<sup>2</sup>, Julia Budassi<sup>3</sup>, Jonathan Sokolov<sup>3</sup>

<sup>1</sup>Brophy College Preparatory, <sup>2</sup>Ramaz Upper School, <sup>3</sup>Dept. of Materials Science, Stony Brook University

Lauren Taylor<sup>4</sup>, Martin Cohen<sup>5</sup>, John Noé<sup>5</sup>

<sup>4</sup>Juniata College, <sup>5</sup>Laser Teaching Center at Stony Brook University

DNA molecules may be deposited and aligned on various surfaces and may be imaged by confocal microscopy when labeled with fluorescent dyes<sup>1</sup>. Such fluorescent DNA markers have been found to possess differing dependencies on polarization and angle of light<sup>2</sup>. One such marker, SyBr Gold dye, is known to possess a high angle and polarization dependence. When imaged using the typical method of confocal microscopy, in which mercury light is applied perpendicularly to samples, samples dyed with this marker fluoresce weakly. Using a blue solid-state diode laser at oblique incidence, however, we have found that samples can be observed to fluoresce strongly at different intensities due to the applied polarization of the light.

Samples were created by means of dipping PMMA-coated silicon wafers into dyed DNA solutions in a DC electric field setup. Due to DNA's slightly negative nature, the field enhanced transfer of the DNA onto the wafer. Drops of DNA solutions placed onto surfaces and left to evaporate were also used to deposit DNA. The DNA-SyBr Gold solution (Invitrogen S-11494) was diluted in concentrations ranging between 2000x and 5000x of stock, but greatest variability of DNA visibility and intensity was found between 2000x and 2500x.

The blue laser was mounted on an optical rail with a polarizer, rotatable half wave plate (to enable rotation of the incident polarization relative to the DNA molecular orientation) and beam defining aperture. The fluorescent images were taken using a Leica Confocal Microscope (Figure 1), and were analyzed using ImageJ.

When applied to samples dyed using SyBr Gold, imaged DNA strands were shown to display differing intensities through a range of input angles. The angle dependence was also compared between horizontal, vertical, and oblique strands to determine if the dye molecules fluoresce differently based upon its orientation of attachment to the DNA strand.

By varying the angle at which the input laser was placed, a clear change in the intensity was observed (Figure 2). Images were found to possess sharper contrast as well as a general increase in fluorescence intensity. We have shown that it is possible to optimize the conditions in which aligned DNA is imaged using confocal microscopy by varying the polarization and angle of incidence of laser light on the sample. Observing these trends will be used to improve the quality in which dyed DNA is imaged through laser confocal microscopy.

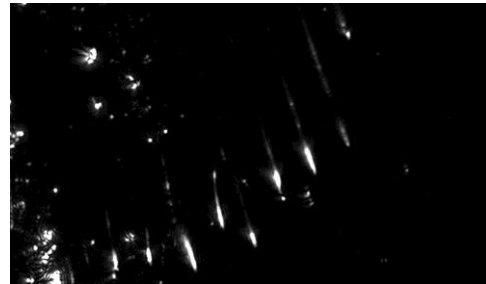


**Figure 1:** Several strands of dyed DNA imaged through confocal microscopy. This image is one in a series of many we analyzed to see the variance in fluorescence of DNA.

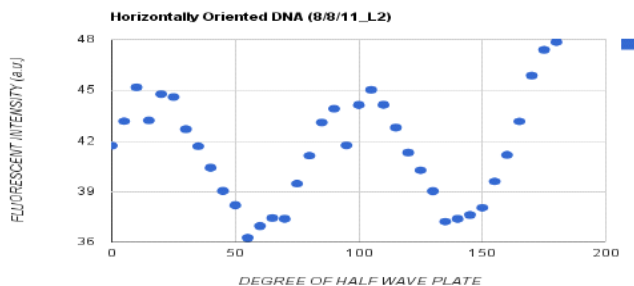


**Figure 2:** A range of data collected from a series of confocal images. A clear maximum and minimum angle can be observed.

1- Suzuki, Seichi, et al. "Quantitative Analysis of DNA Orientation in Stationary AC Electric Field Using Fluorescence." *Annual Meeting, IAS '95., Conference Record of the 1995 IEEE 2* (1995): 1274 – 1382. *IEEE Explore*. Web. 7 July '01.

2- Uy, Jeanne L., et al. "The Polarization of Fluorescence of DNA Stains Depends on the Incorporation Density of the I Library." Web. 8 July 2011.

## Using Microcontact Printing as a Novel Method for Dyeing and Cutting DNA

Emily Shea, Smithtown High School East

Julia Budassi, Stony Brook University

Dr. Jonathan Sokolov, Stony Brook University

Microcontact printing (MCP) is a method of creating patterns on a substrate using a polydimethylsiloxane (PDMS) stamp that has been altered to have a pattern of variable topography<sup>1</sup>. MCP has many applications in patterning of both biological molecules and non-biological molecules. Our goal was to use MCP for the dyeing and cutting of DNA. Being able to dye DNA with a stamp in specific places would allow for DNA solutions used for adsorption to substrates to not include dye, avoiding the complications associated with adsorbing dye-modified DNA. Enzymatic soft lithography has been used to create nano-patterns as well by digesting specific substrate layers<sup>2</sup>. Depositing non-specific nucleases on the substrate would allow DNA to be cut into fragments of a pre-set length. Furthermore, both dyeing and cutting DNA for specific lengths would aid in the effort to sequence DNA. Our hypothesis in the experiment is that a PDMS stamp will be able to deposit dye and enzymes on the substrate in order to produce the desired effects on the DNA. The control in this experiment is a number of samples that are imaged before stamping, therefore the after-stamping images can be compared to these for analysis.

Substrates for DNA adsorption are made using clean silicon wafers, cut to 1 square cm. Next, a layer of PMMA is spun-cast onto the silicon surface to act as an absorbing surface. DNA solutions of varying concentrations are prepared using lambda DNA and 6:50 buffer (made up of 6 parts 0.1 M NaOH and 50 parts 20 mM MES). These solutions are used for dipping the silicon wafers into and/or for placing drops of DNA onto the silicon wafers. At the same time, a PDMS stamp is created by mixing a 10:1 solution of Sylgard 184 base and curing agent, vacuuming out bubbles, and pouring it onto a silicon wafer with pre-made gratings. Once the wafers have DNA placed on them, the newly created PDMS stamp is saturated with Sybr Gold dye and placed on it in order to dye the DNA. Using a Leica confocal microscope, data is collected on how well this stamping procedure worked.

DNA molecules were successfully dyed with the grating in both directions parallel and perpendicular to the molecules' orientation (Figures 1 and 2). In order to view the molecules that were dyed in the perpendicular direction, it was necessary to use a sample with a known density of DNA that had been previously stained with Yoyo dye (Figure 2). However, certain conditions that have been partially optimized but can be further improved include: compression force, length of time under compression force, method of depositing dye on stamp, and method of removing excess dye from the stamp. Additionally, attaching enzymes to the PDMS stamp and achieving a new method of cutting DNA is a future aspect of this work that we hope to complete.



Figure 1: An image, of DNA stained with Sybr Gold dye using a PDMS stamp with gratings in the parallel direction.

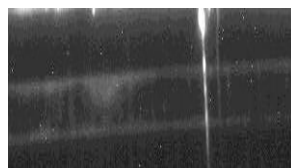


Figure 2: An image of DNA previously stained with Yoyo dye and then dyed in the perpendicular direction with a Sybr Gold stamp.

<sup>1</sup> Weibel, Douglas B., DiLuzio, Willow R., and George M. Whitesides. "Microfabrication Meets Microbiology." *Nature Reviews: Microbiology*. 5.3 (2007): 209-18.

<sup>2</sup> Guyomard-Lack, Aurélie, et al. "Site-Selective Surface Modification Using Enzymatic Soft Lithography." *Langmuir*. 27 (2011): 7629-34.

## Electric-field Assisted Deposition of DNA on Polymer Surfaces

JunHwan Ryu, Loomis Chaffee School, Windsor, CT

Ke Zhu, Julia Budassi and Dr. Jonathon Sokolov, Department of Materials Science & Engineering, Stony Brook University, Stony Brook, NY

Recently, the interaction of DNA with surfaces has been widely studied for its range of applications, including mapping, sequencing and analyzing DNAs. Adsorbing the DNA molecules in a controlled manner is critical in these applications.<sup>1</sup> In our experiment, we have established a new method, using electric field and molecular combing, to control the density and possibly the lengths of the DNA on surface.

DNA combing is a technique that extends the DNA on the polymer surface as it is pulled into the air from the DNA solution and deposits the attached DNA on the polymer surface. Previous studies show that best results yielded on polymethylmetacrylate (PMMA) surfaces and that the adsorption had strong dependence on the pH of the DNA solution.<sup>2,3</sup> Experimentally, we found that 0.1M NaOH and 20mM MES mixture at 6:50 volume ratio (6:50 solution) produced the best results.

The fact that the DNA molecules are negatively charged in solution has been used for different purposes such as electrophoresis, but not in DNA combing. In this study, the molecules were aligned in 6:50 NaOH/MES buffer solution with different electric fields and deposited onto PMMA surfaces by dipping and retracting PMMA coated silicon wafers into the solution. The electric field was set up with platinum wire and gold plated Si wafer as electrodes. The DNA strands were dyed with YoYo-1 and observed using a fluorescence microscope.

As the electric field became larger, the density went up as well (*fig.1 and fig.2*). Results showed that using 125ng/ml DNA solution with electric field of 10.64 V/cm for deposition yields similar density on the polymer surface as using 2.5mg/ml DNA solution with no electric field, raising the efficiency of DNA deposition by about 20 times (*fig. 2*). We have also probed to reduce the effects of ion build up on the electrodes and on the polymer surface, by using an alternating current (a/c) field. Future experiments include measuring the strength of DNA-polymer interaction by reversing the electric field to remove the DNA off the surface and comparing field assisted absorption of single and double-stranded DNA.

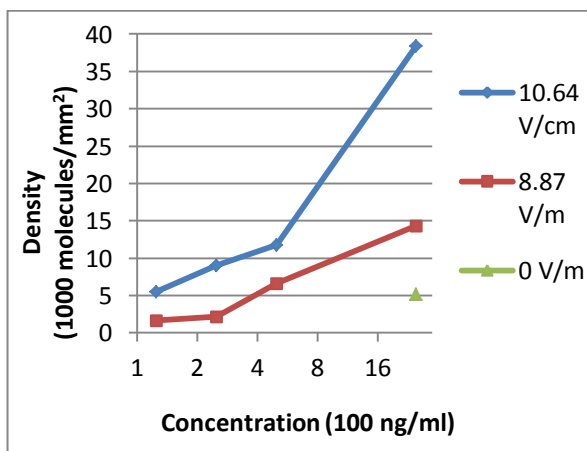
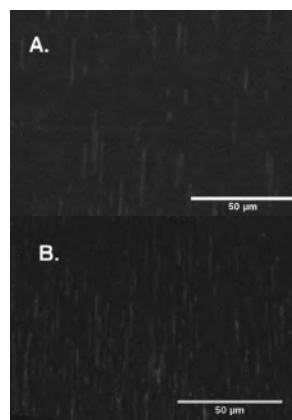


**Fig. 1 (Picture)** Strands of DNA deposited on PMMA surface with A) electric field of 0V/m and DNA conc. 2.5 mg/ml DNA. B) electric field of 8.87 V/cm and DNA conc. 2.5 mg/ml DNA. The scale bar measures 50  $\mu$ m. **Fig.2 (Graph)** Graph of DNA density vs DNA conc. at electric field of 10.64, 8.87 and 0 V/cm.

<sup>1</sup> Erdmann, M., et al. *Nature Nanotechnology* Vol. (5): pgs 154-159. (2009).

<sup>2</sup> Bensimon, A., et al. *Science* Vol (265) 2096-2098 (1994).

<sup>3</sup> Allerman, J., et al. *Biophysical Journal*. Vol. (73): pgs 2064-2070 (1997).

## Stretching DNA Molecules on a Polymer Surface

**Jonathan Rosenberg**, Torah Academy of Bergen County  
**Dr. Jonathan Sokolov, Ke Zhu** (graduate student), and **Julia Budassi** (undergraduate),  
Department of Materials Science and Engineering, Stony Brook University, NY

DNA's stretched form is one of great importance to the study of its structural characteristics and sequence. DNA has been stretched and even untwisted in solution with the use of permanent magnets acting on paramagnetic beads attached to DNA, DNA attached to a surface at one end and an AFM cantilever at another and similar manipulation methods using micropipettes, and fine glass fibers.<sup>1</sup> Another method of obtaining stretched DNA involves evaporating a drop of diluted DNA, where the DNA molecules would be deposited on a surface with the receding meniscus.<sup>2</sup>

In our experiment we studied the effects of stretching on lambda DNA, deposited onto Polydimethyl siloxane (PDMS, silicone) using the evaporating drop method. The DNA was dyed with SyBr Gold dye, or YOYO dye, which does not drastically affect the stretching properties of the DNA molecules while being deposited.<sup>2</sup> Different DNA concentrations were used, ranging from 0.025%-2% (diluted in dye and a 6:50 ratio of buffer solution of 0.1 M NaOH to 0.02 M MES solution) to optimize the density of the DNA on the surface. Once deposited, the DNA was imaged using a Leica Confocal Microscope (figure 1), for further measurements and to image stretching, in situ.

To stretch the DNA molecules after deposition onto PDMS, the PDMS sample was placed onto a modified linear stage, pinched at the ends. The DNA length was measured throughout stretching.

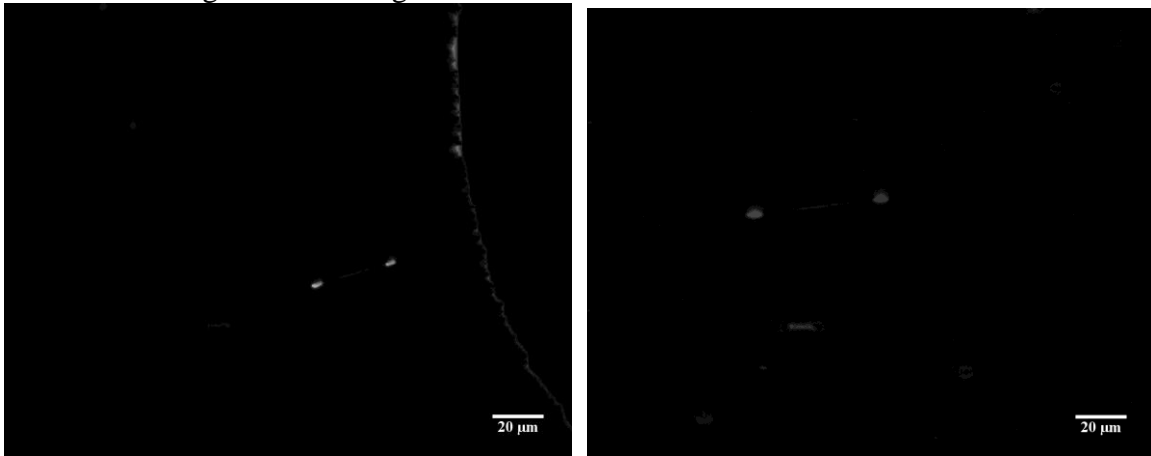


Figure 1: Deposited lambda DNA strand dyed with SyBr Gold, under 40X lens Confocal Microscope. Both images are of the same strand, but the one on the right has been stretched. The strand in the left image is 25 microns long, while the stretched one in the right image is 42 microns long.

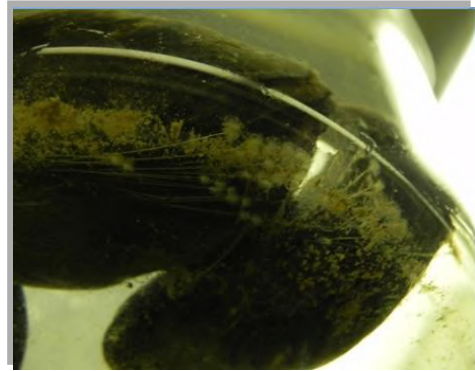
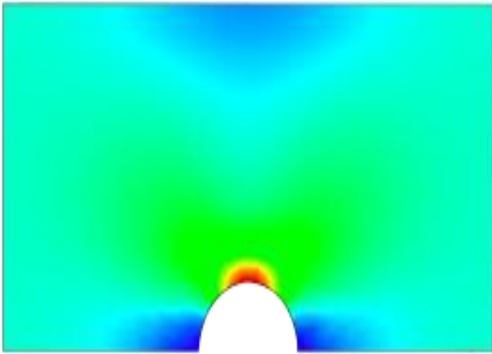
We successfully stretched DNA strands by 68% without breakage of the strands and without the strands coming off of the PDMS surface.

### References:

1. Prévost, C., Takahashi, M. and Lavery, R. (2009), Deforming DNA: From Physics to Biology. *ChemPhysChem*, 10: 1399–1404
2. Bensimon, D., Simon, A.J., Croquette, V.V., and Bensimon, A., Stretching DNA with a Receding Meniscus: Experiments and Models, *Phys. Rev. Lett.*, 1995, vol. 74, pp. 4754–4757

# Environmental Remediation

## SESSION 9



**Chairs: Lauren Herrera,**

**Katelyn Ireland**

**Advisors: Rebecca Grella, Joanne**

**Figueiredo**

# A Study on the Geological and Environmental Implications of Hydraulic Fracturing in Upstate New York

**Kunal Sangani**, Fayetteville-Manlius High School  
**Rebecca Grella**, Department of Life Sciences, Stony Brook University  
**Srivatsa Bhat, Dr. Dilip Gersappe, Dr. Miriam Rafailovich**  
Department of Materials Sciences, Stony Brook University

Given the current shortage of nonrenewable fuels, research has increasingly turned toward discovering new sources of energy. In particular, shale rock layers present an appealing source for large quantities of natural gas. Until recently, scientists believed these methane sources could not be accessed safely and efficiently. The appearance of new technologies, particularly horizontal drilling and hydraulic fracturing, has made retrieval of these fuels possible. However, some environmentalists fear that fracturing induced by these processes may facilitate the migration of chemicals upward into shallow water aquifers<sup>1</sup>. Scientists have also voiced concerns on the volume of heavily contaminated effluent produced in the process. The proposed development of the untapped Marcellus Shale has become especially controversial in Upstate New York. Thus, this study had two aims: (1) to map fracturing and permeability changes on rock surrounding the Marcellus Shale layer induced by hydraulic fracturing, and (2) to reveal the composition and assess the toxicity of produced waters on terrestrial plant and aquatic species.

In order to more completely model the induced fractures and permeability changes stemming from hydrofracking, the Abaqus Finite Element Analysis software was used. The stratigraphic column of southwestern Upstate New York was replicated through a partitioned 3D solid object. Each layer was given a distinctive material property, corresponding to the rock's modulus. In addition, the modulus was given a variable distribution within the layer-- vertically, modulus increased at lower depth; horizontally, modulus was given a randomized function based on a Gaussian distribution. The primary stresses corresponding to tectonic stresses in Upstate New York were applied to the model, and a large pressure was applied outward from a thin borehole. The Abaqus software then created initial fractures, and propagated these cracks outward in the rock. The changes in permeability of the rock were calculated using the stress at each point, and a simple percolation algorithm was run to study the ability of methane, radon, benzene, and other chemicals to migrate in the rock column.

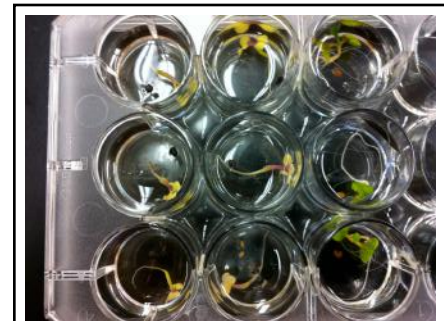


**Figure 1.** *Brassica rapa* in serial dilutions of hydrofracture effluent (6.25%, 3.125%, and 0% from left to right).

Effluent samples from hydrofracture sites in Pennsylvania were graciously donated by ProChemTech International. Several tests for composition were run on each of the three samples (FRAC-16, -17, and -18), including Total Organic Carbon Analysis and EDACS. A toxicity assessment was conducted using terrestrial plant species *Brassica rapa* and annual ryegrass, both found in Upstate New York, as well as the aquatic model organism *Hydra oligactis*<sup>2</sup>. Even at low concentrations of effluent (eg. 3.125%), seeds had delayed germination and subsequent discoloration (Figure 1), and seeds of both species were unable to germinate at any concentration greater than 6.25% effluent. Additionally, *B. rapa* seedlings were found to have significantly shorter roots at on Day 9 of growth (linear regression  $\beta_1$  test,  $P < 0.0001$ ), suggesting that contaminants in the produced water inhibited root growth and formation. Effluent was also applied to *B. rapa* plants after seven days of regular growth, mimicking the introduction of chemicals into an established ecosystem; growth curves noted stunted growth at higher concentrations of effluent, and several plants displayed morphological sublethality symptoms. *H. oligactis* were highly susceptible to even low concentrations of hydrofracture waters: lethality threshold concentrations (TC) at 72 hours were found to be 8.84%, 17.68%, and 4.42% for FRAC-16, -17, and -18 samples, respectively.

1 Osborn, Stephen G., Avner Vengosh, Nathaniel R. Warner, & Robert B. Jackson. (2011). Methane Contamination of Drinking Water Accompanying Gas-Well Drilling and Hydraulic Fracturing. Proceedings of the National Academy of Sciences of the United States of America, 108, 8172-8176.

2 Blaise, C. & T. Kusui. Acute Toxicity Assessment of Industrial Effluents with a Microplate-Based *Hydra attenuata* Assay. Environmental Toxicology and Water Quality, 12, 53-60.

# Analyzing the Role of Marine Gels in a Negative Feedback Loop for Ocean Acidification

Jason Kuan, Harker School, San Jose, CA

Cindy Lee, Department of Marine Sciences, Stony Brook University, NY

Coralie Beaulieu and Claire Beaulieu, Stony Brook University, NY

Katelyn Ireland, University of Miami

Nazac Saleh, Suffolk Community College, NY

Miriam Rafailovich, Department of Materials Science and Engineering, Stony Brook University, NY

Currently, the world's oceans are becoming more acidic due to increased carbon dioxide levels in the oceans. However, studies have shown that marine gels can cause marine organisms to aggregate, move up the size spectrum, sink to the ocean floor, and go through sedimentation before they decompose and release carbon. By doing so, carbon dioxide can be permanently removed from the atmosphere, thus leading to a reversal in ocean acidification.<sup>1</sup>

The organism focused on in this study is a coccolithophore called *Emiliana huxleyi*, which releases a gel called TEP (transparent exopolymer particle). In these experiments, the hypothesis being tested is that the ocean's surface microlayer and TEP will be able to remove enough carbon dioxide to create a negative feedback loop for ocean acidification.<sup>2</sup>

To see how TEP would respond at different pH levels, a coccolith culture was isolated and placed in different acidities after reaching the stationary phase of growth. Afterwards, rheology and viscometry tests were done with a Malvern rheometer to show how properties of TEP like shear thinning and viscosity changed at different acidities. TEP was also stained with Alcian Blue to portray how the quantities of the gel produced would change at different conditions. To study the surface microlayers, biofilms were taken from mesocosms stabilized at 3 different conditions, varying in carbon dioxide concentration and temperature. The samples were then put onto a polystyrene coated silicon wafer with a Langmuir-Blodgett trough. Once the wafers had been coated, an Atomic Force Microscope was used to examine and compare the thickness and adhesion properties of the different microlayers.

Future work should be done on quantifying TEP from viscosity. Such observations would be helpful in analyzing the gel's effects on bacteria, since staining can change the way TEP and bacteria interact. Future work could also include testing more parameters like concentrations of dissolved calcium, which is a bridging ion in TEP, to help understand how to manipulate the marine gels for the reversal of ocean acidification.

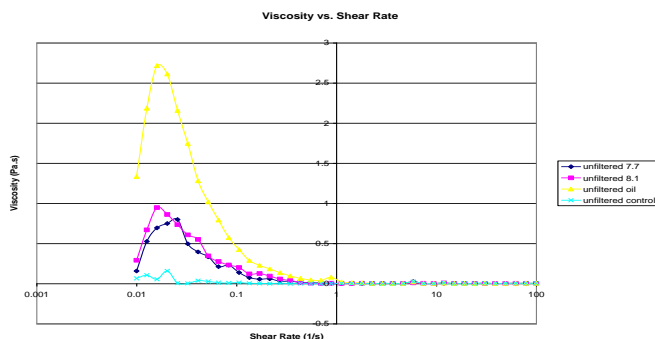


Figure 1: rheology tests done for unfiltered TEP at different pHs

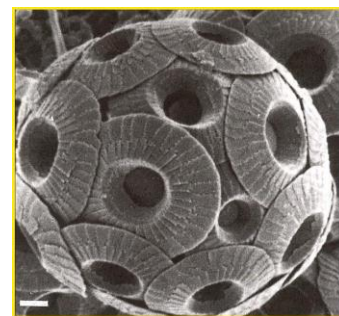


Figure 2: an image taken of a coccolith<sup>3</sup>

<sup>1</sup> Verdugo, Pedro, et al. "The oceanic gel phase: a bridge in the DOM-POM continuum." *Science Direct*: n. pag. *ScienceDirect*. Web. 26 July 2011.

<sup>2</sup> Pilson, Michael E. *An Introduction to the Chemistry of the Sea*. Upper Saddle City, New Jersey: Prentice Hall, 1998. 59. Print.

<sup>3</sup> *Rocks and the Rock Cycle*. N.p., n.d. Web. 10 Aug. 2011.  
<[http://www.geology.wisc.edu/courses/g112/rock\\_cycle.html](http://www.geology.wisc.edu/courses/g112/rock_cycle.html)>.

## Encapsulation of an Herbicide: A Model System for Fabrication and Assessment of Effectiveness

A. Sullivan, Smithtown High School, A. Crespo, Brentwood High School, R. Guzman, Brentwood High School, M. Rafailovich, MRSEC Stony Brook University, J. Figueiredo, Smithtown High School, R. Grella, Stony Brook University, L. Herrera, Suffolk County Community College

Invasive species have the potential to change the biodiversity of an environment as well as the human activities of an area<sup>1</sup>. Such species include *Centaurea nigrescence* and *Centaurea stoebe*, which have taken over viable farmland in many areas of the country, posing a problem to farmers by both reducing the crop production and livestock area. In most cases, these plants have been extremely difficult to eradicate, and widely used methods of eradication are not always ideal because of the negative environmental impacts, which include groundwater pollution as a result of run-off and damage to the atmosphere due to the release of aerosols. A novel method for reducing these negative effects is the encapsulation of an herbicide in calcium alginate beads<sup>2</sup>. This delivery system will maximize effects on invasive plants and minimize environmental contamination.

A target based delivery system is essential in regulating the amount of herbicide that is being released into the environment. This system must deliver the lowest amount of herbicide while still effectively eradicating weeds. In order to achieve this, a calcium alginate bead containing the commercial herbicide Ortho® GroundClear® was developed to apply straight into the soil. Calcium alginate beads are polymerized when dropping a mixture of sodium alginate, saline, and herbicide into a calcium chloride solution.

Our methods to test the effectiveness of the beads include a variety of chemical and biological techniques. Biologically, experiments were first conducted using *Centaurea stoebe* seeds. After observing that these seeds were very difficult to select and mature, an alternative seed, *Salvia hispanica*, was introduced to increase the pace at which data was collected. The three types of bioassays set up included a seed placed directly next to a bead to test the diffusion of the herbicide; a bull's-eye arrangement to test the area of inhibition; and soil tests to imitate a realistic scenario. Overall, our results show that the herbicide is able to diffuse out of the bead enough to only permit 9% germination (*Fig 1*); that the beads without herbicide do not harm the seeds because seeds that had a bead with no herbicide had over 80% germination; and that there is approximately a one- inch zone of inhibition with the use of four beads. Chemically, the diffusion out of the beads was tested in a time course study that lasted 24 hours. Through an analysis of the results using a UV spectrophotometer, it was evident that by two hours most of the herbicide had diffused out of the bead (*Fig 2*). Future research includes soil testing to determine the different effects of herbicide beads on the environment compared to the traditional release system. In addition, different herbicides will be utilized in the beads.

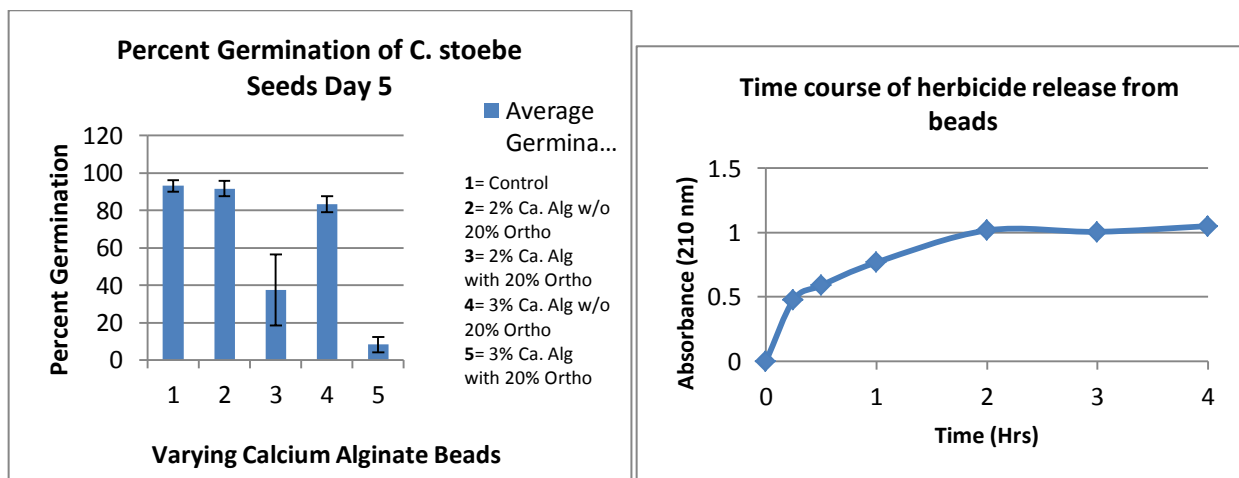


Fig 1: Percent germination rates

Fig 2: UV Spectrophotometry Results

<sup>1</sup>Williamson, M. (1996) *Biological Invasions*. Great Britain. T.J. Pres.



## The Effect of Crude Oil on Byssal Thread Formation and Structure in *Mytilus edulis*, Blue Mussel

Alexander Harwood\*, Noman Hamrani\*, Michael Emerson\*\*, Dianna Padilla Lab\*\*\*\*

\*Brentwood High School Brentwood, NY, \*\*Smithtown High School, \*\*\*Department of Ecology and Evolution Stony Brook University, Stony Brook, NY

### Abstract

*Mytilus edulis* (Blue Mussels) are a common species of marine bivalve that are of great global economic and ecologic relevance. The shellfish industry is a \$330 million industry (Fisheries Statistical Bulletin of South China Sea). Countries such as China rely greatly on their shellfish industry for exportation. Marsh ecosystems rely on this species to filter and build new habitat. Catastrophic spills such as the *Deepwater Horizon* oil spill, referred to as the BP oil spill was the largest oil spill in the oil industry history (White house.gov, White 2010, Guegel et al. 2010) over 2.604 million gallons of oil were released per day (Achenbach and Fahrenthold 2010). It still remains unclear how this spill and others effect marine bivalves. To address this question we designed a microcosm experiment in which we performed a biological assay to assess the effect of exposure to crude oil on the marine bivalve *M. edulis*. Our research addresses the effects of crude oil exposure on the development of byssal threads in *M. edulis*. Two microcosms, each with N=4 mussels were constructed. Our experimental design assesses byssal thread mechanics when mussels are reared in crude oil contaminated water over a span of two weeks. The experimental microcosm contained 1ml of crude oil per 500ml of seawater. Daily measurements included: number of byssal threads produced, and length of 4 random threads (cm). A t-test was performed to assess the differences between control and treatment group byssal length and indicates exposure to oil in a controlled setting results in a significant decrease in byssal thread length ( $P=.05$ ,  $t=2.6861$ ). Tensile strength of the thread was also recorded in Newtons (N) using the INSTRON 5542. Additional measurements include angle of attachment and rate of thread formation.

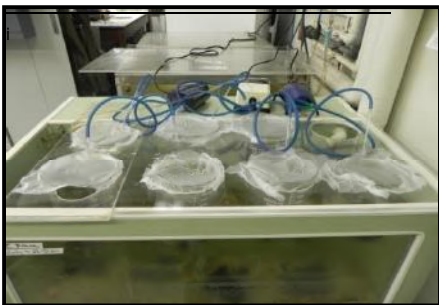


**Figure 1:** Experimental setup, N=8 microcosms, with four mussel per

### Literature Cited



The Ongoing Administration-Wide Response to the Deepwater BP Oil Spill". Whitehouse.gov. 2010-05-05. <http://www.whitehouse.gov/blog/2010/05/05/ongoing-administration-wide-response-deepwater-bp-oil-spill>. Retrieved 2010-05-08.


Fisheries Statistical Bulletin of South China Sea, Initials. Economic importance . Retrieved from <http://personal.cityu.edu.hk/~bhworm/Marine%20seafood/seafood/pages/Econindex.htm>

## SUMMER SCHOLAR PROGRAM SCHEDULE OF ACTIVITIES

**EVERY DAY STARTS WITH A GROUP MEETING**

**CHECK SCHEDULE DAILY!**

	MONDAY	TUESDAY	WEDNESDAY	THURSDAY	FRIDAY
Week of 6/27	27 10:00 AM General meeting 10:30 AM Srinivas Pentyala 11:15 AM Vladimir Jurukowski 12:00 Hyun-Joong Kim 12:30 PM Lunch 1:00 PM Jonathan Sokolov 2:00 PM ID cards and campus tour	28 10:00 AM General meeting 10:30 AM Michael Hadjiargyrou 11:30 AM Donna Tumminello 12:00 PM Rebecca Grella 12:30 PM Lunch 1:45 PM Nay Htun 2:00 PM ID cards and campus tour	29 10:00 AM General meeting 10:30 AM Steven Schwarz 11:30 PM Lunch 12:00 PM Kim Auletta 1:00 PM Jeff Carter 2:00 PM Bob Holthausen 3:00 PM Louis Mancuso	30 10:00 AM General meeting 10:30 AM "Learning Science Database", Janet Clark "Excel tutorial" Joann/Robert 12:30 PM Lunch 1:00 PM "Learning Science Database", Janet Clark Excel tutorial: Joann/Robert	1 10:00 AM General meeting 10:30 AM Facility tour 1:30 PM Pizza Lunch/ 2:00 PM Safety Quiz
Week of 7/4	4  <b>HAPPY 4<sup>TH</sup> OF JULY!</b>	5 10:00 AM General meeting 10:30 AM Tom Butcher 11:15 AM Distribution of lab boxes, lab notebooks, storage, etc. 1:00 PM Lunch 2:00 PM Ellipsometer: Jonathan Sokolov	6 10:00 AM General meeting 10:30 AM Cindy Lee 11:15 AM Dilip Gersappe 12:00 PM Lunch 1:00 PM Spinning/Journal Club 2:30 PM Journal Club/ Spinning	7 10:00 AM General meeting 10:30 AM Steve Schwarz 11:15 AM Marcia Simon 12:00 PM Lunch 12:30 PM Spinning and Journal Club	8 10:00 AM General meeting 10:30 AM Anantha Desikan 11:30 AM Allen Sachs 12:30 PM Pizza Lunch 1:30 PM Journal Club
Week of 7/11	11 10:00 AM General meeting 10:30 AM Kim Auletta 11:30 AM Richard Clark 12:30 PM Lunch 1:30 PM Project distribution/ Spinning lecture /Data Processing	12 10:00 AM General meeting 10:30 AM Kalle Levon 11:30 AM Peter Brink 12:30 PM Lunch 1:30 PM Project Distribution	13 10:00 AM General meeting 10:30 AM Allen Sachs 11:30 AM Nan-Loh Yang 12:30 PM Lunch 1:30 PM Project Distribution	15  <b>ATLANTIS MARINE WORLD AQUARIUM TRIP</b>	16 10:00 AM General meeting 10:30 AM Statistics: Miriam Rafailovich 12:00 PM Pizza Lunch 1:00 PM Journal Club
Week of 7/18	18 10:00 AM General meeting 10:30 AM TALKS 11:30 AM WORK!	19 10:00 AM General meeting 10:30 AM TALKS 11:30 AM WORK!	20 10:00 AM General meeting 10:30 AM TALKS 11:30 AM WORK!	21 10:00 AM General meeting 10:30 AM TALKS 11:30 AM WORK!	22 10:00 AM General meeting 10:30 Speakers: Spinning Group 12:00 Pizza Lunch

Week of 7/25	25 10:00 AM General meeting 10:30 AM TALKS 11:30 AM WORK	26 10:00 AM General meeting 10:30 AM TALKS 11:30 AM WORK	27 10:00 AM General meeting 10:30 AM TALKS 11:30 AM WORK	28 10:00 AM General meeting <b>CANOE TRIP!</b>  <b>&amp; BBQ</b>	29 10:00 AM General meeting 10:30 AM Student Presentations
Week of 8/1	1 10:00 AM General meeting 10:30 AM TALKS 11:30 AM WORK	2 10:00 AM General meeting 10:30 AM TALKS Student Presentations 11:30 AM WORK !!!!	3 10:00 AM General meeting 10:30 AM TALKS Student Presentations 11:30 AM WORK	4 10:00 AM General meeting 10:30 AM TALKS Student Presentations 11:30 AM WORK	5 10:00 AM Group Meeting 11:00 AM Student Presentations Pizza Lunch
Week of 8/8	8 10:00 AM General meeting 10:30 AM TALKS Student Presentations 11:30 AM WORK	9 10:00 AM General meeting 10:30 AM TALKS Student Presentations WORK	10 10:00 AM General meeting 10:30 AM TALKS Student Presentations WORK	11 10:00 AM General meeting 10:30 AM TALKS Student Presentations WORK	12 10:00 AM – 1:00 PM <b>GARCIA SYMPOSIUM</b> <b>SAC Ballroom A</b>

# ACKNOWLEDGEMENTS

Dr. Srinivas Pentyala

Dr. Charles Fortman

Mrs. Kim Auletta

Dr. Bob Holthausen

Dr. Marcia Simon

Mr. Herb Weiss

Dr. Richard Gross

Mrs. Rebecca Isseroff

Dr. Steven Schwarz

Mr. Allan Sachs

Dr. Peter Brink

Dr. Nay Htun

Dr. Dilip Gersappe

Dr. Richard Clark

Mrs. Donna Tumminello

Dr. Adil Allaverdiyev

Dr. Tom Butcher

Dr. Yury Yakubchyk

Dr. Michael Hadjiagyrou

Ms. Lamiya Allaveriyeva

Dr. Cindy Lee

Dr. Sarah Gross

Dr. Hyun Jun Kim

Miss Lauren Collazo

Dr. Michael Gouzman

**Artwork and design by David Pirraglia**

We thank the following for their support;

**The Morin Foundation**

**The National Science Foundation**

The Entenmanns Corporation

Starbucks, Stony Brook

Carl Bao  
Mia Fochsig  
Leica Tam  
ADAM M. Greenstein  
EVAN SCHWEIDER  
Kunal  
Sally Lin  
Adam Fuzums  
Ossip  
Matter  
Mudi  
Siri  
Ticky Sun  
Alex Lee  
Caroline  
Quang  
KUNAL SANGANI  
Tyler  
Lawrence  
Sapran  
Mande  
Amy  
TOM WANG  
Ashish  
Sudhak  
David Nam  
AMY  
Sullivan  
Relecom Samrah  
PENINA SAFIER  
Zoeary  
Dachery  
Kalle  
was here!  
Alphav  
Alphav  
Rosenberg  
Manda  
Sikka  
Karan  
Singer  
CLARA S. GUERZO  
LUNDA  
Greenstein  
Hana Teicher  
Kathy Penhauer  
Mohit Batora  
Chazac Sahbi  
Jason Kund  
Robin Mehta  
Sneha Subramanian  
Sneha Chittabathini  
Julia Landsberg  
Dalia Leibowitz  
Veronica Collazo  
Eve Byggh  
Tom Yurek  
Ryann Lindberg  
Shoshana Jarvitt  
Sara  
Giacca  
Aurore  
Elyse  
Holly Jones  
Wild  
Alina Ranybaran  
Aaron  
Zoeary  
Dachery  
Kalle

N	S
I	U
C	S
K	S



Mohit Batora (not me)

Sneha Subramanian  
Sneha Chittabathini

Alex Lee!  
KUNAL SANGANI  
Tyler  
Lawrence

Emily Shea  
Maxwell Platt  
Monika Batra

[SARA  
GIACCA]  
Aurore  
Elyse

Holly Jones  
Wild

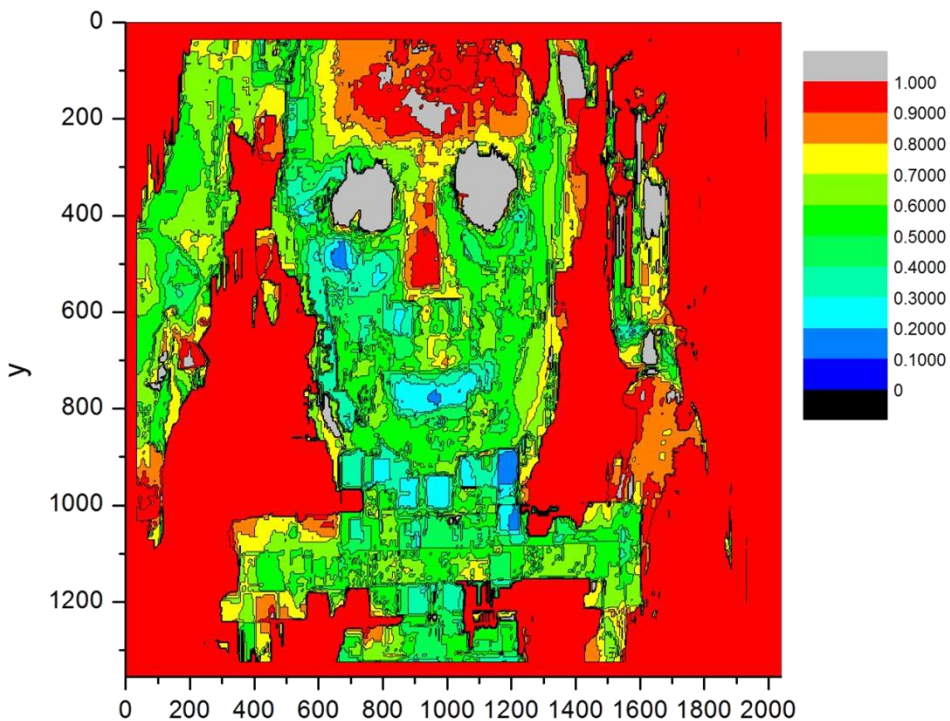
Alina Ranybaran  
Aaron

PENINA SAFIER  
Zoeary  
Dachery

AMY  
SULLIVAN  
KALLE

# Congratulations Winners

- Leah Slaten and Andrew O'Neil for the Science as Art Contest
  - Neil Muir for Best REU
- Chung Chueh Chang (Simon) for best Grad mentor
- David Nam for highest Garcia grades



Best Research Report

# Determination of the molecular weight of a packing peanut via spin casting, ellipsometry, and FTIR



Analysis of packing peanuts via solution concentration v. spun-cast thin-film thickness, FTIR spectroscopy; and silicon analysis

**Abstract:** Our group of three analyzed and determined the molecular weight of a Styrofoam® packing peanut. Prior, we also characterized a silicon wafer, which had a [1,0,0] orientation and a hydrophilic surface based on contact angle measurements. Furthermore, a hot press and FTIR were used to determine the identity of our unknown polymer. We prepared a solution of approximately 20 mg/mL of packing peanuts in toluene. A thin film of the polymer was then spun cast onto a cleaved square piece of silicon. The average thickness of the thin film, measured by ellipsometry, was found to be 127.575 nm. Extrapolating the concentration at 300 nm utilizing the regression equation for our linear plot resulted in 40.608 mg/mL. This gave us a final result of 313,000 g/mol. We concluded that the Styrofoam packing peanuts were made of materials of high molecular mass.

## **Authors:**

David Nam, Ani Pochiraju, Hansen Qian

## **Co-Authors:**

*Graduate Student:* Sisi Qin

*Undergraduates:* Julia Budassi, Alan Czemerinski,  
Sandy Guerrero, Nikhil Mehandru

*High School Students:* Japbani Nanda, Andrew O'Neil,  
Victoria Petrova, Anirudh Pochiraju, Alina  
Ranjbaran, J.J. Rosenberg, Joshua Ryu, Anirudh  
Sailesh, Evan Schneider, Zohaib Shaikh, Tom  
Wang, Alissa Zhang

7/7/2011

---

## I. INTRODUCTION

---

Molecular weight is a key intrinsic property of a compound. A polymer's molecular weight largely determines its characteristics and uses. This property stems from the individual monomers, whose shape and chemistry affect the molecular weight. Since a polymer consists of linked individual monomers, they affect the overall physical and chemical properties of the whole polymer (Gersappe).

Unique methods, such as spin casting and ellipsometry, were used to analyze the relationship between polymer concentration and thin-film thickness in order to determine the molecular weight of the polymer. Dunbar, A. D. F. et al in 2009 conducted a similar comparison by altering solution concentrations to obtain different properties of the thin-film of a polymer. However, he did not analyze the subsequent results and their application in determining the polymer's molecular weight. Schubert analyzed the possibilities of measuring molecular weight at different concentrations using thickness measurements.

This experiment aimed to analyze different concentrations of polymer solution and their thin-film thicknesses via spin casting and ellipsometry to determine the molecular weight of the original polymer.

---

### A. GOALS

---

This experiment was conducted in multiple parts, each with their own objectives. We aimed to familiarize ourselves with the process of cutting silicon wafers, creating a polymer solution, and spin casting the solution onto the silicon. After multiple trials of various concentrations, the end result was the discovery of the molecular weight of the polymer. In addition, we also sought to study the contact angles of a droplet of deionized water on different surfaces of silicon. We also aimed to understand the difference between the [1,0,0] and [1,1,1] orientations of silicon. Finally, we aimed to use a hot press and FTIR to correctly identify our polymer. In general, one of our main objectives was to practice correct safety protocols while performing the experiment.

---

## II. MATERIALS AND METHODS

---

### A. MATERIALS

---

Stony Brook University provided silicon wafers, Styrofoam® packing peanuts, unknown virgin PS beads of similar composition to packing peanuts, and nitrogen gas. We were provided with 2 mL of pre-measured toluene.

---

#### 1. MACHINES USED

---

For the spin casting and ellipsometry measurements, a Fietkau Technology AND FX-40CJ (d = 0.0001) Balance, a Headway Research Inc. PWM32 Spin-Caster, and a Rudolph Research AutoEL Ellipsometer were used. To analyze contact angle and silicon orientation, an Olympus BH2-UMA (f = 180) Optical Microscope and a KSV Instrument LTD CAM200 Optical Contact Angle Meter were used. A Fred S. Carver Inc. Model C Hot Press and a Thermo Scientific Nicolet FTIR



machine with OMNIC software were used to obtain the IR spectrum of our tested sample.

## B. METHODS

### 1. CHARACTERIZATION OF SILICON

Aside from determining the molecular weight of our unknown molecule, we also used techniques to characterize the surface of the silicon wafer itself. Images of the silicon pieces without the polymer films were taken using the optical microscope to differentiate between silicon pieces of [1,0,0] and [1,1,1] orientation.

To further characterize the silicon wafer, we determined its wettability. As shown in **Figure 1**, de-ionized water was dropped onto the front, shiny side of the silicon wafer. The contact angle for the front side of the silicon wafer was determined using the contact angle meter. The contact angle procedure was repeated for the back side of the silicon wafer and the front side of the silicon wafer treated with hydrofluoric acid.

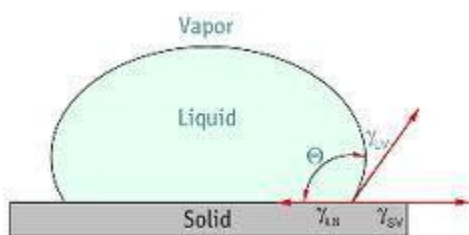


**FIGURE 1:** LIQUID ON SOLID, SHOWING MEASUREMENT  $\theta$  OF CONTACT ANGLE ("CONTACT ANGLE")

### 2. FTIR ANALYSIS

Thin films of the polymer beads were prepared using a hot press compression molder. Beads of the polymer were placed

between the two metal disks so that the compressed beads would take on the shape of a circular, thin film. The polymer beads between two metal disks were placed on the lower half of the compression molder. The temperature was set at 300 degrees Celsius, thus providing the heat for melting and cross-linking between the atoms of the polymer. Furthermore, the hydraulic press of the compression molder applied a pressure of approximately 9 psi to the polymer beads. After applying heat and pressure to the polymer beads for about 10 minutes, the disk-polymer bead assembly was left to cool down. The film created was first measured with calipers and then placed into the FTIR machine to obtain a spectrum.

### 3. PREPARATION OF SILICON AND POLYMER SOLUTION

Preparation of the silicon and solution needed for spin casting involved multiple steps. Circular silicon wafers were cleaved into approximate 1 cm x 1 cm pieces using a pair of tweezers and a diamond cutter. The front, shiny side of the cleaved silicon pieces was then cleaned with nitrogen gas. 2 silicon pieces per person were then placed in a Petri dish and sealed with Parafilm® until spin-casting.

To prepare the solution, approximately 2 mL toluene were stored in a glass vial covered first with aluminum foil then with a plastic cap to prevent the escape of toluene vapor. Aluminum foil also served as a safeguard against the dissolution of the plastic cap by the toluene vapor. 0.0404 g of the Styrofoam® packing peanuts were measured using the balance. Inside the fume hood, the 0.0404 g of packing peanuts were then dissolved in the 2 mL of toluene.

---

#### 4. SPIN CASTING AND MOLECULAR WEIGHT

---

The polymer-toluene solution was pipetted on to the cleaved silicon piece until the solution fully covered the surface of the front side of the silicon. The packing peanut polymer was spun cast on to the cleaved 1 cm x 1 cm silicon wafer at approximately 2500 rpm as shown in **Figure 2**. The spin casting procedure was repeated twice per person for a total of 6 pieces. An ellipsometer gave two measurements of thickness for each of the polymer films on the cleaved silicon substrates.

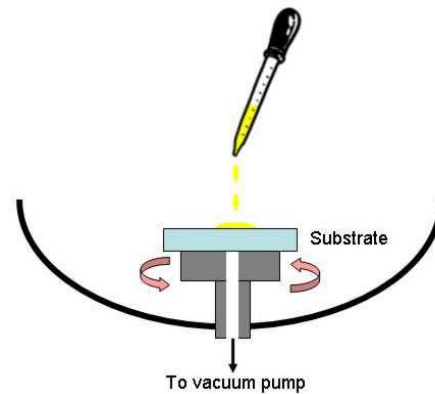


**FIGURE 2:** REPRESENTATION OF SPIN CASTING ("SPIN CASTING")

---

### III. RESULTS AND DISCUSSION

---

#### A. CHARACTERIZATION OF THE SILICON

---

Using various instruments from the Room 212 and 313 in the Engineering Building at Stony Brook University we were able to determine some basic properties of the silicon wafers prior to the coating the substrate.

We were able to determine the orientation of the crystalline structure and the contact angles of both sides of the silicon wafer.

---

##### 1. ORIENTATION

---

Because our silicon wafers were cleaved into neat rectangles, we hypothesized that they were of the [1,0,0] orientation, meaning that the crystals are arranged into cubic structures. As seen in **Figure 3** obtained by the optical microscope, the surface of silicon has protruding features

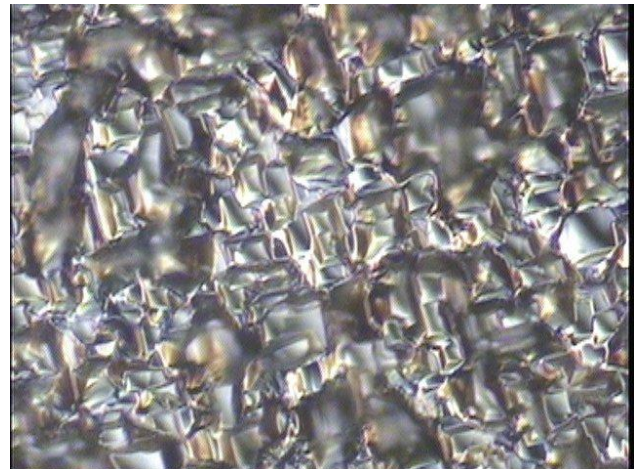


**FIGURE 3:** OPTICAL IMAGE OF [1,0,0] ORIENTATION SILICON

that are cubically oriented, proving the silicon wafer to be of the [1,0,0] orientation.

---

##### 2. CONTACT ANGLE

---

The contact angle, the angle at which the surface of the liquid meets the surface of a solid substrate, serves as a measure of the surface forces, and is thus linked to

Contact Angle:	Left(°):	Right(°):
<b>HF-treated Si (Front)</b>	88.9	88.7
	86.62	87.63
	86.21	83.7
<b>untreated Si (Front)</b>	59.89	57.65
	58.88	56.84
	46.07	46.51
<b>untreated Si (Back)</b>	65.44	64.66
	65.03	64.37

**FIGURE 4:** CONTACT ANGLE MEASUREMENTS OF DEIONIZED WATER ON SI

properties such as wetting, i.e. hydrophilicity and hydrophobicity. An optical contact angle meter was used to determine the left and right contact angles for the front and back sides of an untreated silicon wafer and the front side of a silicon wafer treated with hydrofluoric acid.

**Figure 4** shows that for the front side of the untreated silicon wafer, the left angle and the right angles were less than 90 degrees, showing that the attractive forces to the surface exceeded surface tension and that the front side of the silicon wafer was hydrophilic.

For the back side of the untreated silicon, the left and right angles were also less than 90 degrees but higher than those of the untreated front side, revealing that the back

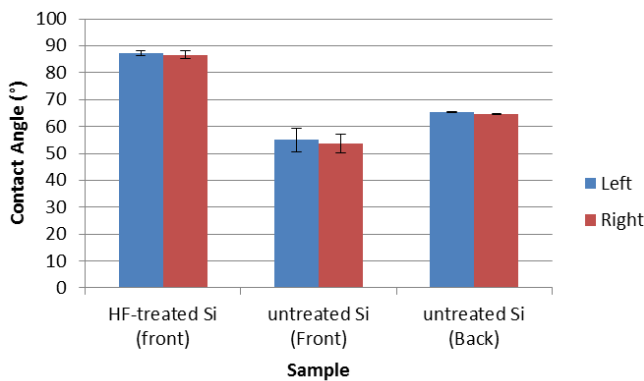


**FIGURE 5:** GRAPH OF AVERAGES OF CONTACT ANGLE DATA WITH ERROR BARS

side of the silicon had a greater degree of hydrophobicity. This observation can be attributed to the fact that the back side was rough, resulting in a capillary action effect that created greater contact angles. Nevertheless, we can conclude that the silicon wafer is generally hydrophilic.

To simulate a super-hydrophobic surface, the front side of the silicon wafer was treated with hydrofluoric acid. We assumed that the contact angles for this condition would exceed 90 degrees, since on a hydrophobic surface, the surface tension would exceed the attractive forces to the surface. As seen in **Figure 5**, the left and right contact angles greatly exceeded those of the untreated silicon wafer. However, they did not exceed 90 degrees, as expected by a hydrophobic surface. This error may have occurred because the silicon wafer was touched by human fingers, then wiped “clean” with a tissue. Contamination of the silicon wafer or the inability to sufficiently clean the surface of the silicon wafer with hydrofluoric acid immediately before measurements can create inaccurate results. Therefore, we conclude that silicon surfaces must be completely and immediately cleaned with hydrofluoric acid to represent the super-hydrophobic surface before measurements are taken.

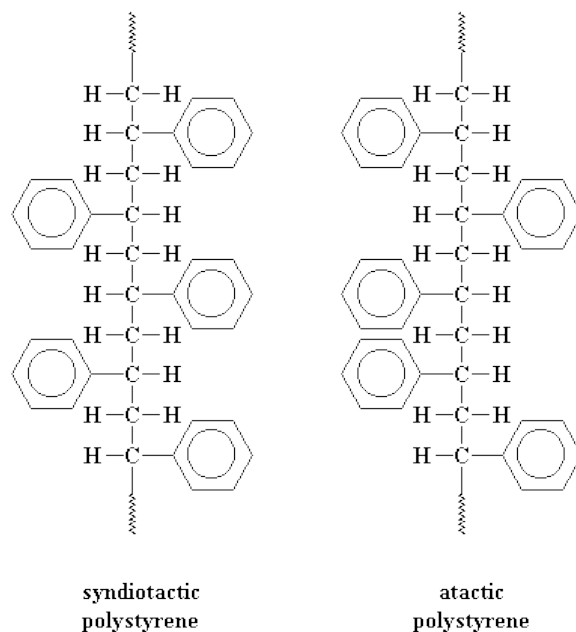
## B. POLYMER FTIR

Another key part of our experiment was the identification of the polymer beads, whose composition was similar to that of the Styrofoam® packing peanuts. The hot press compression method produced a thin, clear polymer film.

A caliper measured the thickness of the polymer film to be 0.155 mm. The

resulting mold was then placed in a FTIR machine for analysis. In Fourier Transform Infrared Spectroscopy, infrared radiation is passed through a sample and a resulting spectrum of absorbance v. wavenumbers ( $\text{cm}^{-1}$ ) is obtained. The spectrum of our polymer was displayed as an image on a computer screen. As each compound has a unique spectrum which is linked to its molecular structure, the sample of interest can be matched accordingly with a library database, thus giving the identity and structure of our polymer.

As shown in **Figure 6**, our FTIR image obtained a 79.59% match with the spectrum of poly(styrene) atactic. Poly(styrene) atactic is similar to regular polystyrene, but is randomly oriented in space, as exhibited by **Figure 7** ("Polystyrene"). It is apparent that the absorbance for certain wavenumbers was saturated and exaggerated, perhaps attributed to the thickness of our film. In the future, we can apply more pressure to the hot press so that the saturation will not occur,



Syndiotactic polystyrene has a regular structure, so it can pack into crystal structures. The irregular atactic polystyrene can't.

**FIGURE 7: IMAGE SHOWING DIFFERENCE BETWEEN ATACTIC AND ORDERED POLYSTYRENE ("POLYSTYRENE")**

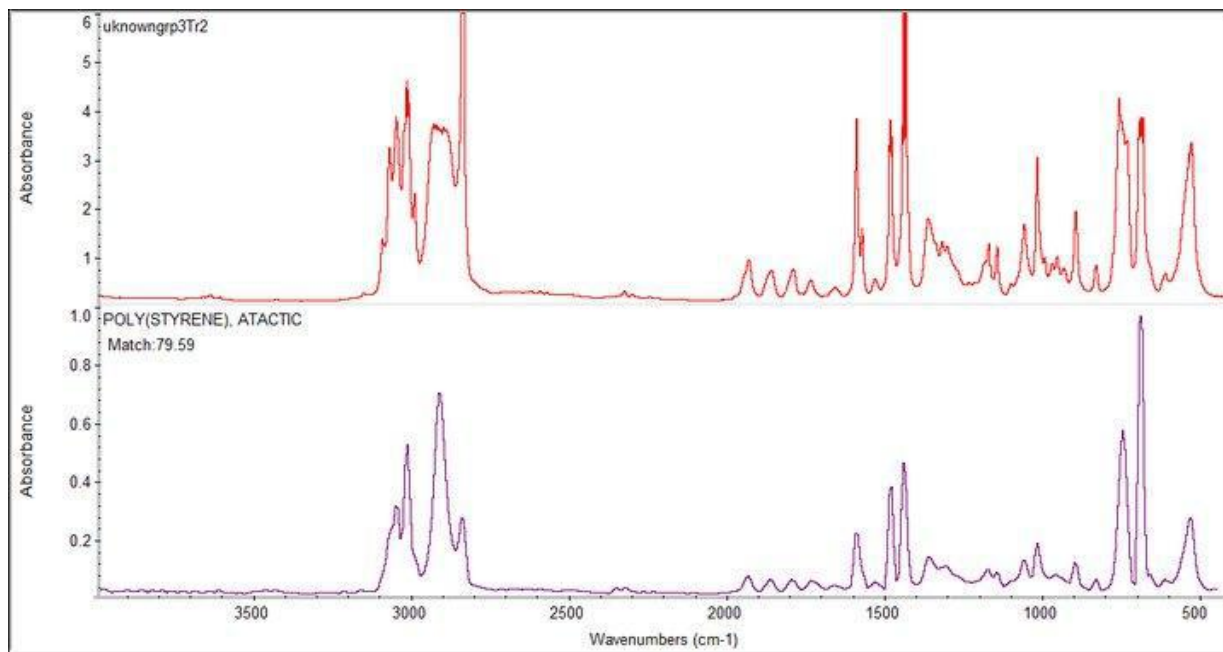


**FIGURE 6: FTIR SPECTRUM OF THE THIN-FILM, SHOWING 79.59% ACCURACY, SATURATION AND POLY(STYRENE), ATACTIC.**

Team:	Concentration (mg/mL):	Avg. Thickness (nm):	Error (nm):	ln of Thickness:	Error of ln:
1. Zohaib , Tom	5	27.5	1.19	3.31	0.123
2. Victoria, Alina	10	58.3	1.49	4.07	0.072
3. J.J., Drew, Josh	15	103	2.88	4.63	0.097
4. David, Hansen, Ani P.	20	1276	1.081	4.849	0.0293
5. Alissa, Japbani	25	1934	10.38	5.265	0.1517
6. Matt, Ani S.	30	2133	1.541	5.363	0.0204

giving us a thinner film and a more accurate

had a shiny bluish tint. An ellipsometer was

**FIGURE 8:** TABLE WITH RESULTS OF CONCENTRATION V. THIN-FILM THICKNESS WITH STANDARD OF THE MEAN OF LINEAR AND NATURAL LOG OF THICKNESS

result. Nevertheless, as our FTIR image had a relatively good match with the spectrum from the library database, we could conclude that the identity of polymer is poly(styrene) atactic.

utilized to measure the thickness of the polymer films on the silicon piece. The refractive index of the ellipsometer was set at 1.5894 for polystyrene and two thickness measurements in angstroms (Å) were measured for each silicon piece. The measurements are shown in **Figure 11**.

### C. ELLIPSOMETRY RESULTS:

Our group of three was assigned to prepare an approximate 20 mg/mL of packing peanut solution. A balance with an accuracy of up to 4 decimal places measured 0.0404 g of the packing peanut polymer, which was dissolved into approximately 2 mL of toluene. Thus, the concentration of the solution was actually 20.2 mg/mL.

Overall, the average value of the thickness, as seen in **Figure 8** and given by each individual thickness measurement divided by the number of measurements, was 1275.75 Å. The standard deviation for the thicknesses of our concentration was 37.44 nm. By dividing the standard deviation by the square root of the number of data entries, we were able to obtain the standard error of the mean, which was found to be 10.81, a relatively small value that attests to the consistency of our data. However, our data point at 25 mg/mL was off of the best fit line, indicating that the silicon, thin film, or polymer solution was contaminated at some point of the process.

After spin casting, the silicon pieces

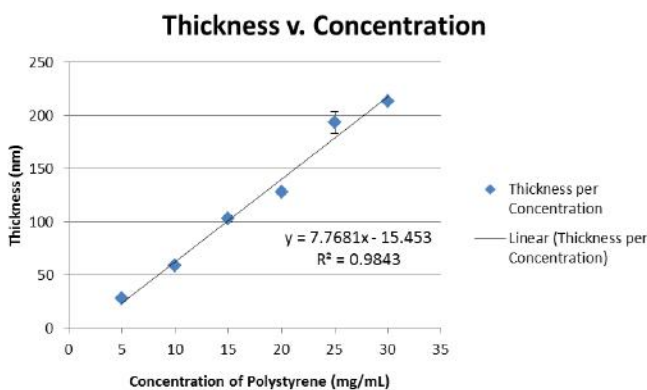


**FIGURE 9:** LINEAR THICKNESS V. CONCENTRATION GRAPH WITH BEST-FIT LINE AND ERROR BARS

As seen in **Figures 9 and 10**, the thickness data for our specific concentration fit relatively well on the thickness v. concentration for the linear plot and semi-logarithmic plot. Furthermore, as evidenced by the minimal standard deviation for our thickness measurements, our data points

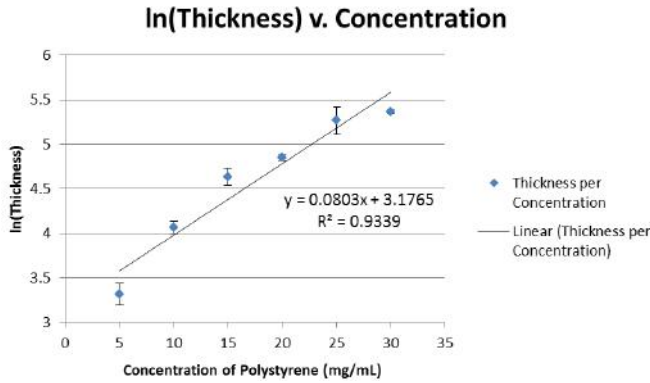


**FIGURE 10:** NATURAL LOG OF THICKNESS V. CONCENTRATION GRAPH WITH BEST-FIT LINE AND ERROR BARS

fluctuated to a small degree and our error bars (standard error) were not substantially large to skew the regression line for both plots. The value for the standard error of the natural log of our thickness measurements differed little from the other values taken by the other groups of 2 or 3 that had different concentrations.

From **Figures 9 and 10**, we found out that the linear plot had a higher R factor of 0.9843, as opposed to the smaller R value of 0.9339 for the semi-logarithmic plot.

### 3. DETERMINATION OF MOLECULAR WEIGHT

To determine the molecular weight, we used the formula in the spin casting experiment packet, which was given as:

$$\log(y) = 3.378 - 0.322 \log(x)$$

Conc.(mg/mL):	Thickness (Å):	Thickness (Å):
<b>5</b>	260	276
	318	337
	248	253
	250	260
	542	564
<b>10</b>	536	549
	634	602
	645	597
	1004	984
	836	937
<b>15</b>	1127	1100
	1097	1101
	916	1123
	961	1130
	1249	1229
<b>20</b>	1265	1269
	1320	1363
	1268	1310
	1264	1256
	1244	1272
<b>25</b>	1706	1665
	2333	2420
	1792	1684
	1923	1953
	2153	2127
<b>30</b>	2105	2171
	2149	2069
	2094	2202

To obtain the concentration at 300 nm or 3000 Å, we then used the regression equation for the linear plot of our data. The R value for our linear plot was higher than that of the R value for our semi-logarithmic plot, showing that our linear regression equation would serve as a better fit for figuring out the extrapolated value for concentration at a certain thickness. The equation for obtaining our concentration was:

$$y = 7.7681x - 15.453$$

We made use of our linear regression equation to extrapolate the value of concentration at 300 nm. We could then use the extrapolated value for concentration and plug it into the formula for the molecular weight, using the following steps:

- $y = 7.7681x - 15.453$
- $300 = 7.7681x - 15.453$
- $x = 40.608$

- $\log(y) = 3.378 - 0.322 \log(x)$
- $\log(40.608) = 3.378 - 0.322 \log(x)$
- $x = 313000 \text{ g/mol}$

The value for our molecular weight was quite expected since polymers are assumed to have a relatively high molecular weight. Thus, the molecular weight for our packing peanuts seemed to be a reasonable value.

---

#### IV. CONCLUSION

---

From the FTIR and its library database, the polymer similar to the packing peanuts was identified to be poly(styrene) atactic. Our analysis of the silicon wafer concluded that it was of [1,0,0] orientation and hydrophilic. Our group used spin casting to determine the molecular weight of a Styrofoam packing peanut. Solutions composed of the polymer dissolved in toluene were spun cast on cleaved silicon pieces. The specific concentration given to us was approximately 20 mg/mL and we were

able to obtain an average thickness of 127.575 nm. By extrapolating the concentration to 300 nm using the regression equation for our linear plot, we were able to obtain a concentration of 40.608 mg/mL. This value was then inserted into the equation for molecular weight, giving us the result of 31300 g/mol. From these results, we could conclude that the Styrofoam packing peanuts are made of substances of relatively high molecular mass.

---

#### V. REFERENCES

---

- "Contact Angle." Wafer Bumping. Web. 10 Jul 2011. <<http://www.wafer-bumping.com/documents/techno/polymers.html>>.
- Dunbar, A. D. F., et al. "A solution concentration dependent transition from self-stratification to lateral phase separation in spin-cast PS:d-PMMA thin films." *European Physical Journal E* 31.4 (2010): 369-375. *Academic search Complete*. Web. 10 July 2011. <<http://web.ebscohost.com/ehost/detail?sid=7a0861a3-4ba0-4dc7-93f8-66133e7c4477@sessionmgr12&vid=1&hid=15&>>.
- Gersappe, Dilip. Lecture on Properties of Polymers. Garcia MRSEC Summer Research Program. Stony Brook University, Engineering Building, Lecture Hall 143. 6 July 2011. Lecture.
- "Polystyrene." *Polymer Science Learning Center*. Department of Polymer Science, The University of Southern Mississippi, 2005. Web. 10 July 2011. <<http://pslc.ws/macrog/styrene.htm>>.

Schubert, D. W. " Spin coating as a method for polymer molecular weight determination." *Polymer Bulletin* 38.2 (1997): 177-184. *SpringerLink*. Web. 11 July 2011.  
<<http://www.springerlink.com/content/wukgr2lepdm0tadj/>>.

"Spin Casting." Nanomaterial Engineering Group. Web. 10 Jul 2011.  
<<http://www.nmeg.group.shef.ac.uk/index.php?page=spincast>>.